

## SOL-GEL-DERIVED MICROARRAY-BASED ASSAYS

**ADVANCES IN THE USE OF  
SOL-GEL-DERIVED MICROARRAYS  
AS AN ASSAY AND DETECTION PLATFORM**

By

JULIE M. LEBERT, B.Sc. (Honours)

A Thesis

Submitted to the School of Graduate Studies

in Partial Fulfillment of the Requirements

for the Degree

Master of Science

McMaster University

© Copyright by Julie M. Lebert, August 2009

MASTER OF SCIENCE (2009)

(Chemical Biology)

McMaster University

Hamilton, Ontario

TITLE: Advances in the Use of Sol-Gel-Derived Microarrays as an Assay and Detection Platform

AUTHOR: Julie M. Lebert, B.Sc. (Honours) (McMaster University)

SUPERVISOR: Dr. John D. Brennan

NUMBER OF PAGES: ix, 120

## Abstract

The use of sol-gel immobilization in the fabrication of microarrays is a relatively new approach that has shown potential to become a leading methodology in this field. However, there are a limited number of assay systems that have been reported using this method. Furthermore, methods to produce high-density sol-gel-derived microarrays have not been reported. Herein, two novel assays utilizing sol-gel-derived microarrays are presented. In the first case, the solid phase of sol-gel-derived microarrays was employed as a detection platform for monitoring the activity of glycogen synthase kinase 3- $\beta$  (GSK3 $\beta$ ) in solution using a phosphospecific stain. Using this assay format, the ability to detect hyperphosphorylated product over the pre-phosphorylated substrate was demonstrated and a  $z'$  value of 0.49 was obtained, indicating amenability to small molecule screening. Secondly, a fluorogenic assay for acetylcholinesterase (AChE) was developed that is compatible with sol-gel derived microarrays and standard imaging instrumentation. A thiol-reactive fluorogenic dye, typically used for detection of thiolated oligonucleotides, was successfully used to monitor AChE activity both in solution and in silica. Further, a functional sol-gel-derived AChE microarray was fabricated and activity on array was detected. We have also reported on the optimization of materials for the fabrication of high-density kinase microarrays using sol-gel immobilization. By employing a directed criteria-based screen, optimal materials were quickly and efficiently identified. Two materials, 1.5SS/1PVA/Glycerol and 0.25DGS, were identified as the optimal materials for fabrication of sol-gel-derived functional microarrays.

## Acknowledgements

I would like to thank my supervisor Dr. John Brennan for all of his input and advice. He has taught me so much about all aspects of research over the past 2 years and his passion for his work is something to be envied. To my committee members, Dr. Brian McCarry and Dr. Fred Capretta, I thank them for their insights and suggestions for my project(s); they helped me progress through the many obstacles I encountered. I would also like to extend my gratitude to my lab-mates (and step-lab-mates!) over the past 2 years for helpful discussions and lots of laughs. I would especially like to recognize Jessamyn Little; her enthusiasm and determination were a breathe of fresh air. I thank my parents for their encouragement and support throughout my degree, especially in the times when I needed it the most. They raised me to always do my best, to never give up and to occasionally let go; to them, I owe my successes and accomplishments. To David, I thank him for his love and his support, but most of all his patience. He has always seen my potential and has helped me to see it too.

## Table of Contents

<b>Chapter 1: Introduction</b>	<b>1</b>
1.1 High Throughput Screening of Small Molecules	1
1.2 Functional Protein Microarrays	1
1.3 Protein Immobilization	3
1.4 Sol-Gel Entrapment	6
1.5 Fabrication of Sol-Gel-Derived Microarrays	10
1.6 Materials Screening for Sol-Gel-Derived Microarray Fabrication	12
1.7 Small Molecule Screening Using Protein Microarrays	16
1.8 Kinases	18
1.9 Acetylcholinesterase	22
1.10 Thesis Overview	23
1.11 References	26
<b>Chapter 2: Sol-Gel-Derived Microarrays as a Solid-Phase Platform for Detection of GSK3<math>\beta</math> Activity</b>	<b>35</b>
2.1 Introduction	37
2.2 Experimental	40
2.2.1 Materials	40
2.2.2 Arraying Methods	42
2.2.3 Assay Procedures	43
2.3 Results and Discussion	46

2.4 Conclusion	54
2.5 References	56
<b>Chapter 3: Materials Screen for Fabrication of Sol-Gel-Derived High-Density Kinase Microarrays</b>	<b>60</b>
3.1 Introduction	62
3.2 Experimental	66
3.2.1 Materials	66
3.2.2 Procedures	68
3.3 Results and Discussion	73
3.4 Conclusion	86
3.5 References	87
3.6 Supplementary Information	91
<b>Chapter 4: Acetylcholinesterase Assay Using a Fluorogenic Thiol-Reactive Dye Compatible with Standard Microarray Scanner Technology</b>	<b>97</b>
4.1 Introduction	98
4.2 Experimental	101
4.2.1 Materials	101
4.2.2 Procedures	102
4.3 Results and Discussion	106

4.4 Conclusion	113
4.5 References	114
<b>Chapter 5: Conclusions</b>	<b>117</b>
5.1 References	120

## List of Tables and Figures

**Table 1.1** Selection of assays used for monitor kinase activity.

**Table 2.1** Inhibitor and substrate structures.

**Table 2.2** Optimization of GSK-3 $\beta$  concentration and assay incubation time

**Table 3.1** Kinase activity retention in monoliths of various sol-gel materials.

**Table 3.2** A summary of the sol-gel formulations screened and the results.

**Table 4.1** Activity of AChE in solution and entrapped in silica using thiol-reactive fluorogenic dye.

**Table 4.2** Activity of AChE in solution and entrapped in silica using the Ellman assay

**Figure 1.1** Comparison of methods of protein immobilization.

**Figure 1.2** Schematic representation of an enzyme entrapped in sol-gel-derived silica.

**Figure 1.3** General process for the sol-gel entrapment of biomolecules.

**Figure 1.4** Scheme of the contact pin-printing of microarrays.

**Figure 1.5** a) Image of sol-gel-derived microspots spaced 500  $\mu\text{m}$ . b) Fluorescent image comparing sol-gel-derived (columns 1 and 2) versus monolayer (columns 3 and 4) microarrays containing anti-fluorescein antibody loaded with fluorescein.

**Figure 2.1** GSK/GSM assay scheme.

**Figure 2.2** Comparison of direct covalent and sol-gel entrapment immobilization technique using a GSM peptide gradient.

**Figure 2.3** GSK3 $\beta$  assays with various substrates (as labeled in x-axis) in the absence (-) and presence (+) of heparin.

**Figure 2.4** Z' plot for GSK3 $\beta$  assay with GSM peptide.

**Figure 2.5** Substrate-selective inhibition of GSK with various inhibitors at 4  $\mu\text{M}$ .

**Figure 2.6** IC<sub>50</sub> curve of SB415286 using GSM/GSK3 $\beta$  assay.

**Figure 3.1** General method for fabrication of sol-gel-derived protein microarrays.

**Figure 3.2** Scheme of criteria-directed screen used to identify optimal materials for fabrication of high-density kinase microarrays

**Figure 3.3** Optical images of materials showing various failure modes of materials.

**Figure 3.4** A) Composite image of microarray consisting of 12,000 spots (60 samples x 200 spots/sample). B) Various modes of failure used to assess stain compatibility.

**Figure 3.5** Results of criteria-directed screen used to identify optimal materials for fabrication of high-density kinase microarray

**Figure 3.6**  $\beta$ -Casein (3.9 -500  $\mu\text{g/mL}$ ) printed in 1.5SS/1PVA/Glycerol on a SuperAmine slide.

**Figure 3.7** Assays of 4 kinases performed on a sol-gel based microarray in 1.5SS/1PVA printed on an amine-derivatized slide.

**Figure 3.8**  $\text{IC}_{50}$  assay performed on a p38 $\alpha$ /MBP microarray over-spotted with several concentrations of staurosporine at a constant ATP concentration.

**Figure 3.9** Kinase activity in 1.5SS/1PVA/Glycerol monoliths.

**Figure 4.1** Assay scheme for AChE activity detection using BODIPY<sup>®</sup> FL L-cystine.

**Figure 4.2** Fluorescence spectra of BODIPY FL L-Cystine in dimer and free forms.

**Figure 4.3** pH-dependence of ATCh autohydrolysis.

**Figure 4.4** Activity of AChE A) in solution and B) entrapped in silica monitored using BODIPY<sup>®</sup> FL L-cystine.

**Figure 4.5** Michaelis-Menten curves for AChE in A) solution and B) silica.

**Figure 4.6** Fabrication of sol-gel-derived AChE microarray with retention of AChE activity on array.

## **Chapter 1: Introduction**

Portions of this introduction were excerpted from Lebert, J.M.; Forsberg, E.M.; Brennan, J.D. 2008. Solid-phase assays for small molecules screening using sol-gel entrapped proteins. *Biochemistry and Cell Biology*, **2008**, *86*, 100-110. © 2008 NRC Canada or its licensors. Reproduced with permission.

### **1.1 High Throughput Screening of Small Molecules**

The advent of combinatorial chemistry and parallel synthesis allows for the rapid creation of vast libraries of small molecules that may find use as therapeutics. In initial phases of drug development, pharmaceutical companies typically screen small molecule libraries against the biological target of interest in order to identify potential drug leads. With small molecule libraries now reaching several million compounds, there has been an increased demand to improve the throughput and decrease the cost of the screening process. Assay miniaturization, particularly in the form of functional protein microarrays, represents a promising path to improve the high throughput screening (HTS) of such compounds.

### **1.2 Functional Protein Microarrays**

Microarrays consist of several hundred or thousand spatially ordered elements, typically 50-300  $\mu\text{m}$  in diameter, printed onto a surface, such as derivatized glass slides. Each microarray includes all necessary controls along with samples of interest, such that control and screening assays can be performed in a highly parallel fashion.<sup>1</sup> The

development of microarray technology in the 1990s primarily focused on DNA and in 1995, Schena *et al.* first reported on the use of the technology to assess gene expression.<sup>2</sup> The advancement of genome sequencing technologies and the relatively direct methods for immobilization of DNA<sup>3</sup> has resulted in DNA-based microarrays becoming a routine tool for biochemical research. While these microarrays provide vast amounts of data on the DNA or mRNA level, it can be difficult to make direct correlations between this data and the conditions at the proteome level.<sup>4, 5</sup> Additionally, it is not possible to use DNA microarrays directly as a screening platform for assaying of small molecules in a high throughput-screening environment since DNA is generally not a suitable target for small molecule therapeutics.

Following the success of DNA microarrays, protein arrays emerged as a system for the simultaneous detection of analytes<sup>6</sup> and in 2000, the first protein microarray was reported for the detection of protein-protein interactions.<sup>7</sup> Subsequently, high-density protein microarrays were fabricated for the elucidation of novel protein-protein interactions and profiling of substrate specificity.<sup>8, 9</sup> As an alternative approach, small molecule or peptide microarrays have been prepared and used to assess protein binding or modification to the bound substrates with detection by fluorescence<sup>10</sup> matrix-assisted laser desorption ionization mass spectrometry (MALDI-MS)<sup>11, 12</sup> or surface plasmon resonance (SPR).<sup>13</sup>

The above examples utilize immobilized proteins, peptides or small molecules as substrate microarrays for assessment of enzyme activity. There are far fewer examples of functional protein microarrays, where the enzyme, and possibly substrate, are

immobilized in microarray format and assayed directly on array. By immobilizing the enzyme directly, lower volumes can be used for assaying large numbers of compounds, thereby reducing assay cost. This is particularly advantageous for expensive low-abundance proteins. Additionally, the solid phase nature of microarray assays allows for reduction of reaction volumes, increased sample concentration, and accelerated reaction kinetics.<sup>14</sup> Additionally, selective dyes and stains can also be employed with solid-phase assays by using washing steps to reduce background noise and improve assay sensitivity.<sup>15</sup>

### **1.3 Protein Immobilization**

Microarrays are typically prepared using standard protein immobilization techniques that have been applied for other applications, such as biosensor development and affinity chromatography. Examples of technique commonly used for bioimmobilization include those based on: i) covalent attachment<sup>16</sup>; ii) affinity-based immobilization methods<sup>17</sup>; and iii) microencapsulation into activated hydrogels<sup>18, 19</sup> as shown in Figure 1.1.<sup>20</sup>

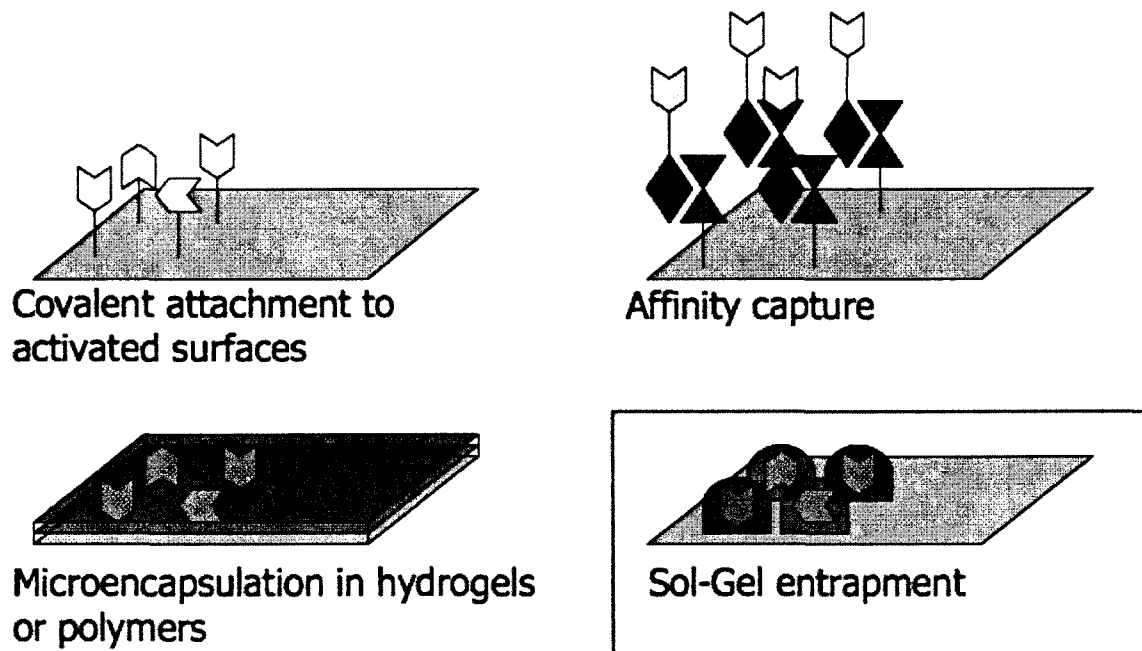


**Figure 1.1.** Comparison of methods of protein immobilization.<sup>20</sup>

Despite demonstrated success for each of these immobilization methods, each technique has specific drawbacks that limit its versatility and applicability to a wide variety of proteins and biomolecules. Both immobilization within hydrogels and covalent attachment methods rely on direct bonds formed between the surface and protein, which can compromise the structure and stability of the protein. Additionally, protein orientation is also frequently uncontrolled in these two approaches, which can result in lower sensitivity and increased biomolecule consumption due to the presence of protein with blocked active sites. Covalent attachment also suffers from dehydration problems, thus highly sensitive proteins may not be able to withstand the dehydration stresses. Affinity-based techniques rely on either labour intensive genetic manipulation of the protein of interest to insert a hexahistidine (His<sub>6</sub>) or glutathione S-transferase (GST) tag

for adhesion to nickel or glutathione supports, or modification of the protein structure by processes, such as biotinylation, for linking to streptavidin coated surfaces. For these techniques, protein conformational stability can be impaired due to direct modification to the protein structure.

A relatively new route to biomolecule immobilization involves the sol-gel process to entrap biologicals within a porous inorganic silicate matrix (Figures 1.2).<sup>21, 22, 23, 24, 25</sup> The sol-gel process refers to the formation of a three-dimensional network from a colloidal suspension of particles, typically 1 – 10 nm in diameter.<sup>26, 27</sup> This process is a low temperature polymerization that can occur in aqueous solutions under mild pH conditions. While various metal oxides can be used, such as TiO<sub>2</sub> and Al<sub>2</sub>O<sub>3</sub>, most research has focused on SiO<sub>2</sub>.<sup>26, 27, 28</sup> Protein entrapment within sol-gel-derived materials was first reported in 1955,<sup>29</sup> however the field did not gain significant attention until 1990 with Avnir's seminal paper reporting on the entrapment of alkaline phosphate in tetraalkoxysilane-derived silica with retention of 30% activity.<sup>30</sup> Since this time, the field has advanced significantly, with reports on the entrapment of a wide variety of biomolecules, including antibodies, soluble enzymes, membrane-bound receptors, DNA aptamers and even whole cells, in a diverse range of sol-gel-derived materials.<sup>24, 31</sup>

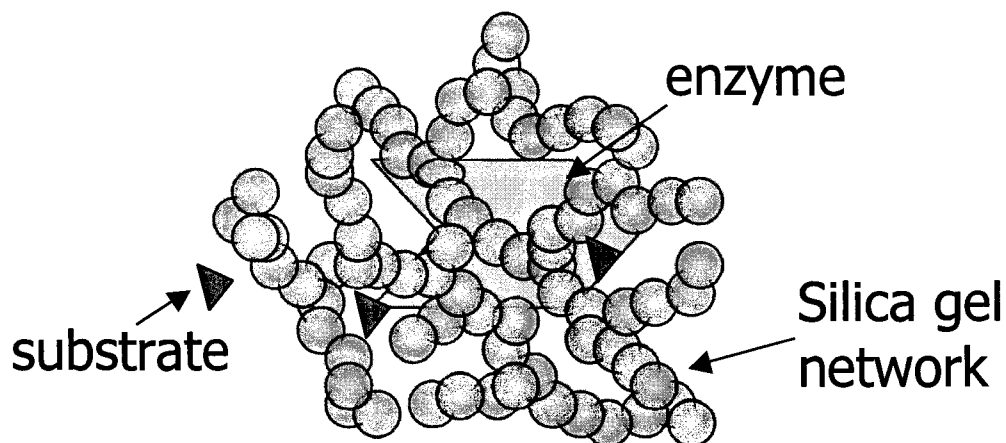


**Figure 1.2** Schematic representation of an enzyme entrapped in sol-gel-derived silica. Enzyme is accessible to small molecules and substrates, but it is unable to leach from the spot. Figure adapted from Pierre 2004.<sup>42</sup>

## 1.4 Sol-Gel Entrapment

Bioencapsulation in silica via the sol-gel process typically involves two steps (Figure 1.3). The first is the preparation of the silica precursor via hydrolysis to create a suspension of silica nanoparticles 1 – 10 nm in diameter called a “sol”. The subsequent step involves combining the “sol” solution with a buffered protein sample to induce polymerization. The buffer present in the biological sample neutralizes the pH and increases the ionic strength of the “sol”, resulting in rapid condensation and the formation of a loosely cross-linked silica matrix called a “gel”. This resulting gel is highly hydrated and porous, and thus allows small molecules to move freely in and out of the material, while retaining the larger biomolecule(s) of interest.

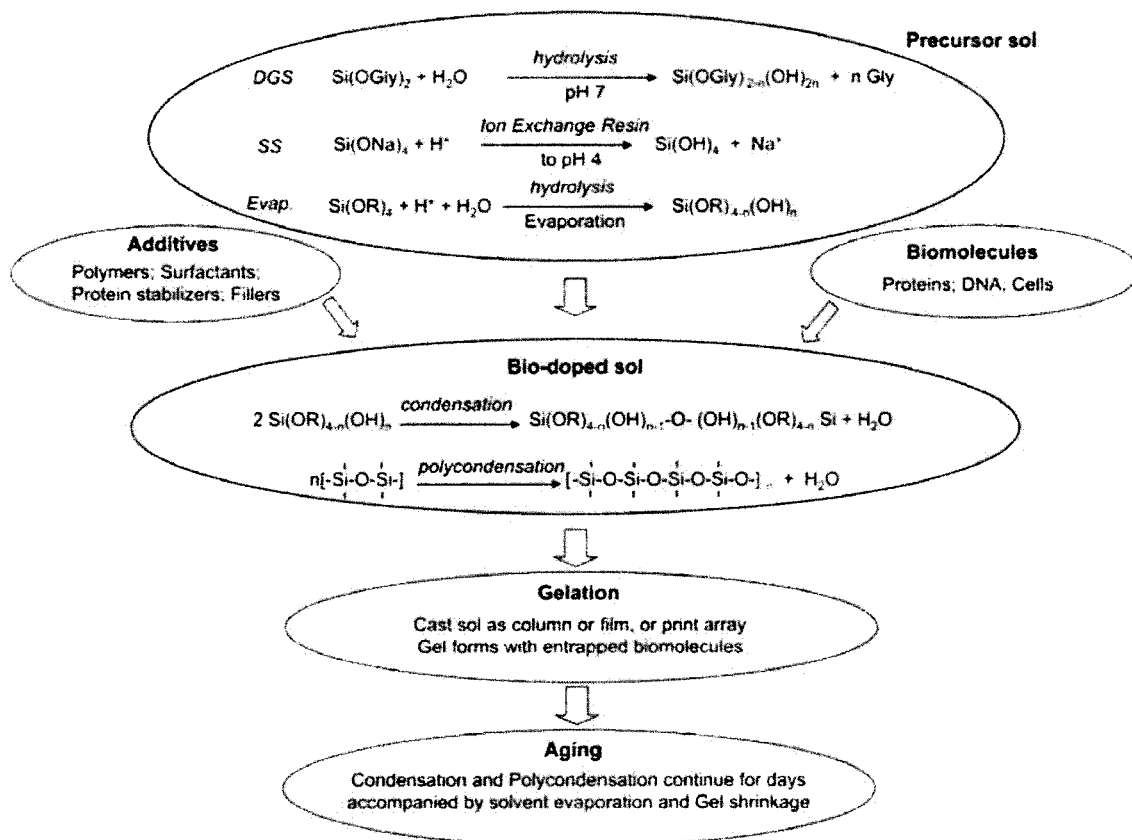


**Figure 1.3** General process for the sol-gel entrapment of biomolecules. Reproduced from Lebert *et al.* 2008.<sup>32</sup>

The sol solution is typically prepared by hydrolysis of tetraalkoxysilanes  $[\text{Si(OR)}_4]$  under acidic or basic catalysis; specifically, tetramethoxysilane (TMOS) and tetraethoxysilane (TEOS) are most often used. Upon hydrolysis, TMOS and TEOS release methanol and ethanol respectively. Although most proteins can tolerate small amounts of alcohol, it is detrimental to protein stability and becomes a greater issue when working with fragile or unstable proteins such as kinases and G-protein coupled receptors (GPCRs). Methods to remove the alcohol prior to encapsulation via evaporation have been developed,<sup>33</sup> however one can eliminate the presence of alcohols directly by using

bio-friendly silica precursors in place of the tetraalkoxysilanes. Examples of bio-friendly precursors include glycerated silanes,<sup>34, 35, 36</sup> which release the protein stabilizer glycerol as the hydrolysis by-product, and sodium silicate,<sup>37</sup> a pre-hydrolyzed precursor that, after  $\text{Na}^+$  to  $\text{H}^+$  cation exchange, can directly undergo condensation and polycondensation processes. An added benefit of using these precursors is that they can be both hydrolyzed and condensed at neutral pH, which is ideal for protein entrapment. Additionally, there are silane precursors with covalently tethered sugars, such as gluconamidyl triethoxysilane, that can also be incorporated into the sol solutions. While these precursors still release alcohol during the hydrolysis process, the sugar moiety can help stabilize the protein and retain water in the material.<sup>38</sup>

In the second step of the process, it is possible to include a variety of additives along with the buffered protein sample, in order to modify the final properties of the material. Examples of additives include: i) polymers, such as polyethylene glycol and polyvinyl alcohol; ii) protein stabilizers, such as glycerol and sugars; and iii) silanes additives, such as tethered sugar silanes, mentioned above, as well as other functional silanes. Similar to the type of silica precursor used, the type and amount of additives can have a drastic effect on the final properties of the material, including pore size and distribution and surface chemistry. Additives provide a versatile method to optimize and tune the material properties to retain maximal activity of the protein of interest while ensuring material compatibility for the desired application.

After combining the buffered protein sample and desired additives with the silica precursor solution, gelation is initiated and depending on the variables discussed above,

gelation can occur in seconds to hours or even days. Typical sol-gel immobilization protocols have gelation times less than 60 minutes. During the window of time between the mixing of protein and sol solutions and gelation, it is possible to cast the material in a variety of formats, such as columns, thin films and microarrays. Depending on the format desired, the required gel time and material properties vary. For instance, columns require a macroporous morphology (pore diameter >50 nm) to allow flow of eluent through the column; however for microarrays mesoporous materials with long gelation times are needed to prevent leaching and allow for printing. It is important to note that material properties are also affected by pH, ionic strength and the nature of the buffered solution containing the protein of interest, and possibly even by the protein itself.<sup>39</sup>

After gelation has occurred on the macroscopic scale, the resulting material continues to evolve in a process called aging or syneresis. Aging involves the continued condensation of free SiOH groups within the matrix, resulting in both shrinkage of the material itself and the pore sizes within the material. After gelation and aging, the matrix contains nano-scale pores, which allow for the diffusion of small molecules in and out of the material, while retaining the protein.

The sol-gel technique for protein immobilization offers several key advantages over the more traditional techniques. Firstly, as mentioned above, no modifications to the protein structure are needed for this immobilization strategy. As such, proteins in their native form can be used, reducing the potential of destabilizing the protein structure. Secondly, it has been shown that entrapment of enzymes can itself be stabilizing to pH and temperature, preventing denaturation.<sup>23, 31, 40, 41, 42</sup> Thirdly, all surfaces of the protein

should be accessible for interaction with the analyte and thus allosteric interactions may be detected.<sup>43</sup> Lastly, this technique has been successful with a large number of proteins from a wide variety of protein families, as noted in a number of recent reviews.<sup>23, 24, 42</sup> While these advantages have led a number of groups, including ours, to investigate this route for production of functional protein microarrays, the potential of this method has yet to be reached due to the limited number of assay systems that have been successfully applied to this format. Thus it is necessary to expand the number of assay systems amenable to sol-gel-derived microarrays before this technique can be used as a general research tool for screening.

## **1.5 Fabrication of Sol-Gel-Derived Microarrays**

The use of sol-gel technology for the fabrication of immobilized protein microarrays is a relatively new area as compared to arrays formed by more traditional immobilization techniques, such as covalent attachment to activated surfaces or affinity capture. This field has emerged over the past decade, with the first report of successful entrapment of a protein in a sol-gel-derived microarray format by Cho *et al.* in 2002.<sup>44</sup> In this pioneering work, glucose oxidase was entrapped in a TEOS-based xerogel array with retention of activity and the ability to simultaneously detect glucose and O<sub>2</sub> on array was demonstrated. Since this initial report, there have been a number of proteins successfully used in sol-gel-derived microarrays, including antibodies,<sup>45, 46</sup> kinases,<sup>47</sup> P450s,<sup>48</sup> horseradish peroxidase<sup>49</sup> and urease.<sup>49</sup> Sol-gel derived microarrays present several benefits over the traditional immobilization methods used for microarray fabrication,

including higher protein loading due to the 3-dimensional nature of the microspots,<sup>46</sup> and the ability to entrap multiple enzymes within a single array element, making coupled assays possible.<sup>49</sup>

There are a number of methods that can be used to prepare microarrays, however sol-gel-derived protein microarrays tend to be fabricated by either contact pin-printing (Figure 1.4),<sup>45, 50</sup> or non-contact printing, such as inkjet printing.<sup>48</sup> While many of the criteria needed for the pin-printing of microarrays are similar to those for ink-jet-based non-contact printing, only pin-printed microarrays will be discussed in detail, as this is the printing technique used throughout this thesis.

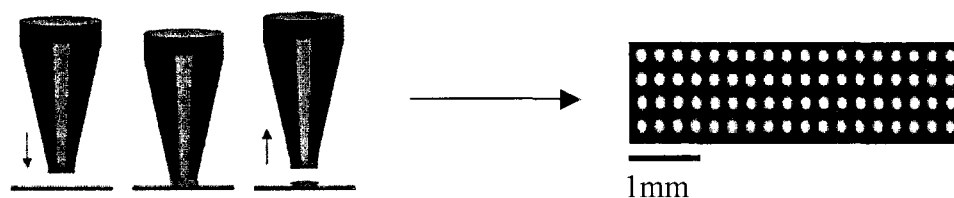


**Figure 1.4** Scheme of the contact pin-printing of microarrays. Figure obtained in part from Reference 50.

Contact pin-printing involves dipping a solid or capillary pin into a solution, followed by deposition of the solution onto a planar surface via contacting of the pin with the surface. This method has several features that make it highly amenable to printing sol-gel-derived microarrays, including the direct adaptability from printing standard spotting solutions to bio-doped sols, spot size variability simply by pin choice or printhead speed, and the potential for parallel printing using multiple pins simultaneously to enable efficient array fabrication. However, due to the nature of the sol-gel process, a number of criteria must be met in order to successfully print bio-doped sol-gel derived

microarrays: the sol must have a sufficiently long gelation time to prevent gelation of the material in the capillary of the pin and variable spot size/volume caused by changing viscosities during the gelation process; surface tension and viscosity must be such that the material can be deposited on the substrate surface; the spots must be uniform for quantitative analysis; and must also adhere to the substrate surface, and be resistant to cracking and leaching from washing steps. Additionally, the material must also retain of the bioactivity and accessibility of the protein by the analyte while preventing protein leaching. To simultaneously meet all of these criteria, it is best to screen a wide range of materials followed by optimization of those materials that pass the initial screen.

## **1.6 Materials Screening for Sol-Gel-Derived Microarray Fabrication**

In 2002, Cho *et al.* described the high throughput screening of sol-gel materials for either growth factor delivery or retention of native protein structure and activity.<sup>45</sup> In the first series of experiments, the group screened 900 bio-degradable polylactic acid-based materials for successful entrapment of keratinocyte growth factor (KGF) in microarray format with materials printed onto fused silica or glass microscope slides. By comparing the emission spectra of native and entrapment KGF, six formulations were identified that appeared to retain the KGF in its native structure over a period of one month. A second set of materials was also screened, where ~600 silica sol-gel compositions were analyzed for maximum retention of binding activity of anti-fluorescein antibody. Using TMOS as the silica precursor, compositions were prepared with various amounts of additives: aminopropyltriethoxysilane (APTES), Nafion,

polyethyleneimine (PEI, 70kDa), polyethyleneoxide (PEO, 100kDa), and dextran (25kDa). The formulations containing anti-fluorescein antibody were pin-printed onto cleaned plain glass slides and allowed to age a minimum of 3 days at 4 °C before analysis. While most (>80%) of the formulations demonstrated a detectable level of fluorescein binding, only a few materials gave maximum binding, including an unusual material composed of 95% TMOS, 4% APTES, 1% Nafion, which had a hydrolysis time of 10 h and a pH of 6.2 (20 mM Tris buffer). A complex composition like this would not have been predicted and thus demonstrates the benefits of material screening.

In 2003, Rupcich *et al.* looked at the effects of the slide surface chemistry, the nature of the sol-gel precursor, the type and concentration of buffer, the water-to-silane ratio, the pH of the sol and the presence of the protein stabilizer glycerol, on the quality of the resulting microarray.<sup>46</sup> Of the buffer conditions screened, 100 mM Tris at pH 8 kept the final sol pH above 5.5 and had gelation times sufficiently long for printing. Silica precursors, including tetraethylorthosilicate (TEOS), sodium silicate (SS), diglyceryl silane (DGS) and monosorbitol silane (MSS) were mixed in various buffer:silane ratios (1:1, 1.5:1, 2:1, 3:1) with 100 mM Tris (pH 8) and 0, 25 or 40% glycerol and tested for their gelation time and printability. These silica precursors were chosen to explore how bio-friendly precursors compare to traditional silica precursors that release alcohol during hydrolysis. Some sols with gelation times of <10 minutes were able to print 100 spots, however gelation times of >20 minutes were vital to prevent gelation of the sol in the pin. The spot quality was also compared between three surfaces, un-derivatized, aminopropyltriethoxysilane (APTES)-coated and 3-

glycidoxypropyltrimethoxysilane (GPS)-coated glass slides. It was found that the more hydrophobic surfaces, APTES and GPS-coated slides, were better for spot shape and uniformity. Bio-doped sols prepared using SS with no glycerol and printed onto APTES or GPS coated slides were best for reproducible spot formation. Interestingly the addition of glycerol tended to cause cracking after washing of the microarray spots. The three-dimensional sol-gel derived microspots were shown to immobilize > 50-fold more protein relative to the printing of proteins directly onto the slide surface (Figure 1.5).

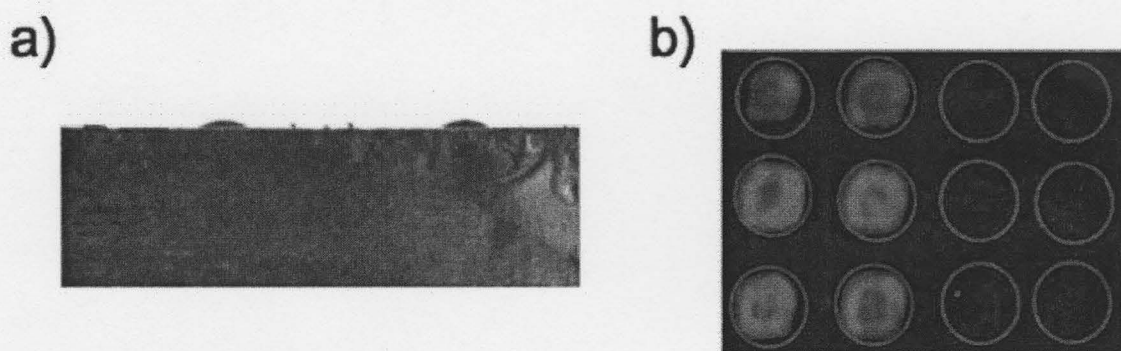


**Figure 1.5** a) Image of sol-gel-derived microspots spaced 500  $\mu\text{m}$ . b) Fluorescent image comparing sol-gel-derived (columns 1 and 2) versus monolayer (columns 3 and 4) microarrays containing anti-fluorescein antibody loaded with fluorescein. Images adapted from Rupcich *et al.* 2003.<sup>46</sup>

In 2006, Kim *et al.* took high throughput screening of sol-gel materials for microarrays to the next level by screening 100,000 formulations to identify materials that could entrap antibodies without leaching and yet allow binding of secondary proteins.<sup>51</sup> Formulations were prepared with 5-25% silica monomers [tetramethyl orthosilicate, methyltrimethoxysilane, tetraethyl orthosilicate, ethyltriethoxysilane, tetramethoxysilicate, methyltrimethoxysilicate, 3-aminotrimethoxysilane], 5-15% silica intermediates [polyglycerylsilicate, diglycerylsilicate], and additives [N-

triethoxysilylpropyl-O-poly(ethylene oxide) urethane, glycerol, poly(ethylene) glycol, PEG400, PEG 800]. All compositions were prepared in 10 mM HCl and then mixed with buffers with a range of concentrations (0 - 500 mM) and pHs (4-9) and containing various salts [potassium sulfate, ammonium phosphate, sodium phosphate]. Formulations were arrayed onto poly(methyl methacrylate) slides and screened against the following criteria: adhesion, spot morphology, gelation time, optical transparency and auto-fluorescence. The 700 materials that passed the first set of criteria were categorized based on their immobilization efficiency of Cy-3-labelled small molecules, protein or antibodies. Seven formulations were found to be suitable for protein immobilization. Bovine serum albumin (BSA) arrays were printed with each of these seven materials and assessed by incubating the array with Cy3-labelled anti-BSA antibody, washing, and imaging. Additionally, the seven materials were examined for nonspecific absorption, pore size and sensitivity. The best material identified for protein immobilization and detection using labeled antibody was 25.5% TMOS, 12.5% MTMS, 5% PEG8000.

While the above examples show the importance of materials optimization for fabrication of highly functional sol-gel-derived protein microarrays, there are no reports describing the fabrications of high-density sol-gel derived protein microarrays. In 2007, Tehan *et al.* reported on the use of quartz pins to print microspots on the order of 10  $\mu\text{m}$ .<sup>52</sup> With array elements of this size, it would be possible to fabricate super high-density microarrays with densities of 630 000 – 860 000 spots/cm<sup>2</sup>. Using these pins, their studies indicated that it was possible to print a variety of solutions and sols of varying hydrophobicity and to adjust spot size via silanization of the quartz pin. Although

it is necessary to have pins capable of printing high-density microarrays, it is equally imperative to find sol-gel compositions with suitable properties to allow for the printing of these arrays. The ability to print high-density microarray is essential for bringing this technology into the high throughput screening environment.

### **1.7 Small Molecule Screening Using Protein Microarrays**

The application of microarrays to small molecules screening has primarily focused on assaying for kinase inhibitors.<sup>12, 13</sup> However, rather than immobilizing the kinase, substrate microarrays were fabricated in order to assess the activity of soluble kinases via observation of changes in substrate structure upon exposure to kinases. A number of functional protein microarrays have been successfully fabricated to screen inhibitors on array, including microarrays of phosphatases and serine hydrolases,<sup>53</sup> cysteine proteases<sup>54</sup> and the integrin  $\alpha\beta3$ -vitronectin interaction<sup>55</sup>. Membrane-receptors, such as GPCRs, have also been arrayed and used to screen for inhibitors. In the past decade, Lahiri *et al.* have described the fabrication of GPCR microarrays for competitive binding assays<sup>56</sup> and function-based GPCR assays.<sup>57</sup> Receptor microarrays for competitive binding assays were prepared by printing phospholipid microsomes onto amniopropylsilane derivatized surfaces. These receptors retained their ability to bind fluorescent probes and, using competitive displacement of fluorescently labelled ligands, inhibitors were identified. Similarly, the group immobilized microsomes doped with GPCR onto glass slides. By using highly porous glass slides, ligands could access the N-terminus of the GPCR and the non-hydrolysable Eu(III)-labelled guanosine 5'-

triphosphate (GTP) analog could interact with G $\alpha$  subunit of the GPCR:G-protein complex. Using the binding of Eu-labelled GTP, small molecules with agonistic or antagonistic properties could be identified.

The ability to entrap membrane proteins within sol-gel materials<sup>58</sup> suggests that it should be possible to fabricate GPCR microarrays for nanovolume screening. Indeed, sol-gel derived microarrays have been utilized for the entrapment of a series of membrane-associated CYP450 enzymes and used for high-throughput analysis of drug metabolism by these enzymes.<sup>48</sup> In this work, CYP1A2, CYP2B6 and CYP3A4 were immobilized in sol-gel based microarrays and overprinted with ~ 30 nL of a substrate/drug of interest and incubated. The microarrays were then overlaid with a second cell-coated slide, and a live/dead stain was subsequently applied to the cell-based slide to determine which drug metabolites were cytotoxic. It was clearly shown that the CYP containing arrays could convert the non-toxic pro-drug cyclophosphamide into the cytotoxic chemotherapeutic 4-hydroxycyclophosphamide, as indicated by site specific cell death on the overlaid cancer cell slide. They further showed the versatility of the microarray platform (termed the MetaChip<sup>TM</sup>) by assaying several different drugs against the CYP isoforms, with all compounds exhibiting activities and inhibition constants close to those in solution.

Two protein families of particular interest for inhibitor screening are kinases and esterases. Kinases are currently the second most widely studied target in pharmaceutical companies due to their involvement in a great number of diseases. Choline esterases, particularly acetylcholinesterase, have regained attention due their involvement in Alzheimer's disease and other nervous system diseases. Because of this broad interest,

our efforts have focused on developing functional protein microarrays for these two classes of proteins.

## **1.8 Kinases**

Kinases play an essential and complex role in cellular metabolism and signalling pathways. These enzymes transmit cellular signals along a pathway by transferring phosphate groups from ATP to a substrate protein or molecule. Phosphorylation is believed to be one of the most common covalent post-translational modifications - in fact, one-third of eukaryotic gene products are predicted to undergo phosphorylation at some stage of their lifecycle.<sup>59</sup> Fittingly, there are over 500 protein kinases in the human proteome, which perform these phosphorylation events.<sup>60</sup> The improper regulation of kinase activity has been implicated in a number of diseases, including cancer,<sup>61</sup> inflammation,<sup>62, 63, 64</sup> and diabetes,<sup>65, 66</sup> and as such, it is not surprising that kinases have become the second most targeted family of proteins by pharmaceutical companies.<sup>67</sup>

Among the kinases, glycogen synthase kinase-3 (GSK-3) is of significant interest to both academic and pharmaceutical driven research, as it plays an intricate and central role in basic cellular metabolism. Originally, GSK-3 was identified through its ability to inactivate glycogen synthase via phosphorylation, and thereby regulate glycogen metabolism.<sup>68,69</sup> However, over the past two decades, it has been found that this kinase has a multitude of putative substrates and is essential for many cellular functions including cytoskeletal regulation,<sup>70</sup> apoptosis,<sup>71</sup> and transcription factor regulation<sup>72</sup>. Additionally, GSK-3 has been implicated in a number of pathological conditions such as

schizophrenia,<sup>73</sup> heart disease,<sup>74</sup> non-insulin-dependent diabetes mellitus,<sup>75</sup> cancer<sup>76</sup> and Alzheimer's disease.<sup>77</sup>

There are a variety of methods used to monitor kinase activity; a summary of frequently used assays is described in Table 1.1. Although all of these methods have utility, there are also disadvantages associated with each, as described in the table. Many of these assays require expensive reagents, such as synthetic substrates or expensive antibodies, as well many formats are not compatible with sol-gel-derived microarrays. Furthermore, due to the unique preference of GSK-3 for pre-phosphorylated, or 'primed', substrates, these methods are not ideal to monitor GSK-3 activity.<sup>78</sup>

**Table 1.1** Selection of assays used for monitor kinase activity. Adapted in part from Reference 67.

<b>Method</b>	<b>Technique</b>	<b>Disadvantages</b>
<i>Luciferase Coupled Assay</i> <sup>79</sup>	Luminescence signal generated from luciferase-luciferin reaction with un-reacted ATP	Requires high turnover of ATP due to high sensitivity of ATP detection
<i>Homogenous time-resolved fluorescence (HTRF) based assays</i> <sup>80</sup>	Labelled antibodies bring Eu-fluorophore FRET pair in close proximity	Relies on the availability of expensive antibodies specific for the substrates.
<i>Scintillation proximity assay (SPA)</i> <sup>80</sup>	Streptavidin-coated scintillant beads bind to biotinylated peptides Using ATP <sup>33</sup> , emission of beta particles in close proximity to scintillant beads result in emission of light	Uses radioactive ATP
<i>Fluorescence polarization (FP) assays</i> <sup>81,82</sup>	Antiphospho-antibody binds to fluorophore-labelled substrate peptide to slow depolarization of light	Requires both labelled peptide and antibody specific for system

<b>Method</b>	<b>Technique</b>	<b>Disadvantages</b>
<i>IMAP assay</i> <sup>83, 84</sup>	Fluorescence polarization assay Phosphorylated peptides bind trivalent metal ion coated beads to increase mass	Require large turnover Protein substrates cannot be used
<i>NADH coupled Assay</i> <sup>85</sup>	Absorbance decrease assay monitors consumption of NADH (340nm)	Signal decrease assay Requires secondary screening to ensure inhibitor specific to kinase (off-target hits)
<i>IQ</i> <sup>86</sup>	Fluorophore-labelled peptide is quenched upon phosphorylation by proprietary quencher	Signal decrease assay Sensitive to compound interference
<i>MS</i> <sup>87</sup>	Changes in mass due to phosphorylation monitored	Limited to MS-compatible assay conditions
<i>Radioactivity</i> <sup>88</sup>	Radioactive ATP is used to monitor generation of phosphorylated product	Use of radioactivity
<i>Amplified luminescence proximity homogenous assay (ALPHA)</i> <sup>89</sup>	In close proximity donor-acceptor beads generate light.	Relies on antibodies and biotin-streptavidin Very sensitive to compound interference
<i>Z'-Lyte</i> <sup>90</sup>	Phosphorylation inhibits cleavage of a peptide which is dually labelled with a FRET pair	Requires availability of double-labelled peptide Requires presence of a cleavage sight in peptide sequence

In 2003, Martin *et al.* reported on the adaptation of a phospho-selective stain, typically used for phosphoprotein identification in gels, for quantitative detection of phosphoproteins and phosphopeptides in microarray format.<sup>91</sup> Pro-Q® Diamond™ stain by Invitrogen is a rhodamine-based dye that binds selectively to phosphorylated residues via a Fe<sup>3+</sup> bridge. Pro-Q® Diamond™ stain was found to be compatible with both

covalently immobilized and hydro-gel-based protein/peptide microarrays by Martin *et al.* The authors were also able to demonstrate the use of immobilized peptide arrays and the Pro-Q<sup>®</sup> Diamond<sup>™</sup> stain to monitor kinase activity.

The compatibility of Pro-Q<sup>®</sup> Diamond<sup>™</sup> with sol-gel-derived silica microarrays was later confirmed by the Brennan group using Protein Kinase A (PKA) and kemptide as a model kinase:substrate system.<sup>47</sup> In this paper, Rupcich *et al.* reported on the fabrication of a functional sol-gel-derived kinase microarray as a platform for nanovolume screening of inhibitors. The kinase microarray was based on the co-immobilization of the substrate, kemptide, and the model kinase, PKA ( $\alpha$ -catalytic subunit), within a single array element using sodium silicate as the silica precursor. Nano-litre volumes of known PKA inhibitors, H7 and H89, at various concentrations were overprinted on top of the individual array elements, followed by overprinting of ATP. After a set incubation period, the entire array was washed and stained with Pro-Q<sup>®</sup> Diamond<sup>™</sup> dye. Using a fluorescence slide scanner to image the array, the IC<sub>50</sub> values of these inhibitors were determined using less than 40 nL of inhibitor solution per curve and were found to be comparable to literature values. However, all arrays used in this study had <100 array elements, and thus high density microarrays were not demonstrated.

## 1.9 Acetylcholinesterase

Functioning in the synaptic cleft, acetylcholinesterase (AChE) catalyzes the deactivation of neurotransmitter acetylcholine via hydrolysis to choline and acetate. This enzyme has regained attention recently for its association with Alzheimer's disease (AD).

In fact, several drugs that inhibit AChE are currently available on the market for treatment of AD, including galanthamine,<sup>92</sup> donepezil,<sup>93</sup> and rivastigmine.<sup>94</sup>

Acetylcholinesterase has historically been assayed using the Ellman assay. This well-known assay utilizes a substrate analog, acetylthiocholine, and monitors reaction of the product thiocholine with 5,5'-dithiobis(2-nitrobenzoic acid) (DTNB). This reaction results in formation of 5-thio-2-nitrobenzoate (TNB<sup>-</sup>), which absorbs at 412nm. Although this assay has been shown to be robust, because it relies on absorbance measurements, this assay is not amenable to the microarray format.

A number of fluorogenic assays for AChE are available, which involve either direct monitoring using fluorogenic substrate mimics or indirect monitoring using coupled assays or a pH-sensitive dye. Examples of fluorogenic substrates include 1-naphthylacetate<sup>95</sup> and 1-methyl-7-acetoxy-quinolinium iodide.<sup>96</sup> However, these compounds require excitation in the near-UV or blue-violet visible region and thus are not amenable to standard microarray scanners that use 532 and 633 nm lasers for excitation. Coupled assays for AChE include Amplex Red<sup>®</sup> Acetylcholine/Acetylcholinesterase Assay from Invitrogen<sup>97</sup> which couples choline generation to H<sub>2</sub>O<sub>2</sub> production via choline oxidase catalysis. Horseradish peroxidase in turn reacts with peroxide and the Amplex Red reagent to generate a fluorescence signal. While compatible with array scanners, this coupled assay requires secondary assays to assess off-target inhibition. Additionally, reports on utilizing the pH change produced from generation of acetate to induce changes in fluorescence intensity have been used.<sup>98,99</sup> In fact, Tsai and Doong reported on the generation of functional AChE

microarrays using the pH-sensitive dye fluorescein isothiocyanate (FITC)-dextran which was referenced to the intensity of the pH-insensitive dye tetramethylrhodamine isothiocyanate (TRITC)-dextran.<sup>100</sup> While this method is ratiometric, it is very sensitive to environmental changes and interferences from the nature of the compounds to be screened and requires tight control over buffer capacity and assay conditions. These problems could be eliminated by utilization of a non-pH sensitive dye system.

## **1.10 Thesis Overview**

Sol-gel immobilization as an approach to functional protein microarray fabrication has shown potential to become a leading methodology in this field. However, there remain a number of challenges with employing this approach that must be addressed. Firstly, the number of assay systems reported in literature using this approach is low and thus this number must be increased in order to fully demonstrate the potential of the technique. Secondly, a sol-gel composition universally amenable to protein microarray technology or even a single protein class has yet to be identified. For instance, it has been shown that functional PKA microarrays can be fabricated in SS,<sup>47</sup> however it is not known if this precursor and entrapment method is amenable to all kinases or potentially all soluble proteins. Thirdly, methods to produce high-density sol-gel-derived microarrays have not been reported. The scale-up of this technology is required in order to move into the HTS environment. Given the potential of sol-gel derived microarrays, this thesis will report on our efforts in evaluating new assay systems amenable to this technology and the development of methods to fabricate high-density sol-gel-derived

microarrays. Particular attention will be paid to the development of methods for the fabrication of such devices for use with kinases and esterases.

Chapter 2 will describe results utilizing sol-gel-derived microarrays as a solid phase platform for detection of GSK3 $\beta$  activity. Assays using GSK3 $\beta$  were conducted in solution, followed by entrapment in a sol-gel-derived microarray format. This solid-phase format enabled the use of a fluorescent phospho-specific stain to monitor the degree of phosphorylation within each sample microspot. Using this solution-based method, it was possible to monitor inhibition of the reaction to generate IC<sub>50</sub> curves.

Chapter 3 of this thesis will discuss overcoming the challenges of producing functional kinase microarrays using sol-gel entrapment and the generation of high-density sol-gel-derived microarrays. While sol-gel immobilization to fabricate functional kinase protein microarrays has shown promise as discussed above,<sup>47</sup> several issues must be addressed. Firstly, initial studies with other kinases have concluded that the immobilization procedure used for PKA is not generic to all kinases. Secondly, the sol-gel composition employed in the original kinase array paper cannot be implemented to fabricate high-density microarrays due to the relatively short gelation time of the precursor solution. In this chapter, the results of a directed materials screen to optimize of sol-gel compositions that allow for both robust high-density microarray fabrication and retention of activity for a wide number of kinases will be presented. Factors examined in the screen were buffer type, concentration and pH, silica precursor and concentration, ormosil additives, small molecule additives and slide surface chemistry. The materials the

were amenable to high-density array fabrication were then tested for retention of kinase activity for a selection of therapeutically relevant kinase targets

Chapter 4 will present our work toward developing functional sol-gel-derived acetylcholinesterase microarrays using a fluorogenic thiol-reactive dye. This fluorogenic dye is compatible with standard DNA microarray scanners and was assessed for its ability to monitor AChE activity both in solution and in silica using micro-well plate assays. This is the first report of this dye being used to monitor the activity of AChE. Using SS, a functional sol-gel-derived AChE microarray was fabricated and shown to retain AChE activity on array.

Finally, Chapter 5 will provide conclusions on this body of work and propose directions for future research in this area.

## 1.11 References

1. Angenendt, P.; Larch, H.; Kreutzberger, J.; Glokler, J. Subnanoliter enzymatic assays on microarrays. *Proteomics*. **2005**, *5*, 420-425.
2. Schena, M.; Shalon, D.; David, R.W.; Brown, P.O. Quantitative monitoring of gene expression patterns with a complementary DNA microarray. *Science*. **1995**, *270*, 467-470.
3. Kimmel, A.; Oliver, B., eds. DNA Microarrays: Array Platforms & Wet-Bench Protocols, Volume 410 (Methods In Enzymology). Academic Press, San Diego, CA., **2006**.
4. Anderson, L.; Seilhamer, J. A comparison of selected mRNA and protein abundances in human liver. *Electrophoresis*. **1997**, *18*, 533-537.
5. Griffin, T.J.; Gygi, S.P.; Ideker, T.; Rist, B.; Eng, J.; Hood, L.; Aebersold, R. Complementary profiling of gene expression at the transcriptome and proteome levels in *Saccharomyces cerevisiae*. *Molecular & Cellular Proteomics*. **2002**, *1*, 323-333.
6. Rowe, C.A.; Scruggs, S.B.; Feldstein, M.J.; Golden, J.P.; Ligler, F.S. An array immunosensor for simultaneous detection of clinical analytes. *Analytical Chemistry*. **1999**, *71*, 433-439.
7. MacBeath, G.; Schreiber, S.L. Printing protein as microarrays for high-throughput function determination. *Science*. **2000**, *289*, 1760-1763.
8. Zhu, H.; Bilgin, M.; Bangham, R.; Hall, D.; Casamayor, A.; Bertone, P.; Lan, N.; Jansen, R.; Bidlingmaier, S.; Houfek, T.; Mitchell, T.; Miller, P.; Dean, R.A.; Gerstein, M.; Snyder, M. Global analysis of protein activities using proteome chips. *Science*. **2001**, *293*, 2101-2105.
9. Ptacek, J.; Devgan, D.; Michaud, G.; Zhu, H.; Zhu, X.; Fasolo, J.; Guo, H.; Jona, G.; Breitreutz, A.; Sopko, R.; McCartney, R.R.; Schimdt, M.S.; Rachidi, N.; Lee, S-J.; Mah, A.S.; Meng, L.; Stark, M.J.R.; Stern, D.F.; De Virgilio, C.; Tyers, M.; Andrews, B.; Gersteins, M. Schewewitzer, B.; Predki, P.F.; Snyder, M. Global analysis of protein phosphorylation in yeast. *Nature*. **2005**, *438*, 679-684.
10. Koehler, A.N.; Shamji, A.F.; Schreiber, S.L. Discovery of an inhibitor of a transcription factor using small molecules microarrays and diversity-oriented synthesis. *Journal of the American Chemical Society*. **2003**, *125*, 8420-8421.

11. Min, D.-H.; Tang, W.-J.; Mrksich, M. Chemical screening by mass spectrometry to identify inhibitors of anthrax lethal factor. *Nature*. **2004**, *22*, 717-723.
12. Min, D.-H.; Su, J.; Mrksich, M. Profiling kinase activities by using a peptide chip and mass spectrometry. *Angewandte Chemie International Edition*. **2004**, *43*, 5973-5977.
13. Houseman, B.T.; Huh, J.H.; Kron, S.J.; Mrksich, M. Peptide chips for the quantitative evaluation of protein kinase activity. *Nature Biotechnology*. **2002**, *20*, 270-274.
14. Rupcich, N.; Brennan, J.D. Fabrication of sol-gel-derived protein microarrays for diagnostics and screening. *In Functional protein microarrays in drug discovery. Edited by P.F. Predki*. **2007**, CRC Press, Boca Raton, FL, 73-97.
15. Martin, K.; Steinberg, T.H.; Cooley, L.A.; Gee, K.R.; Beechem, J.M.; Patton, W.F. Quantitative analysis of protein phosphorylation status and protein kinase activity on microarrays using a novel fluorescent phosphorylation sensor dye. *Proteomics*. **2003**, *3*, 1244-1255.
16. Weetall, H.H. Preparation of immobilized proteins covalently coupled through silane coupling agents to inorganic supports. *Applied Biochemistry and Biotechnology*. **1993**, *41*, 157-188.
17. Camarero, J.A. New developments for the site-specific attachment of protein to surfaces. *Biophysical Reviews and Letters*. **2006**, *1*, 1-28.
18. O'Driscoll, K.F. Techniques of enzyme entrapment in gels. *Methods in Enzymology*. **1976**, *44*, 169-183.
19. Scouten, W.H. A survey of enzyme coupling techniques. *Methods in Enzymology*. **1987**, *135*, 30-65.
20. Snyder, M.; Zhu, H. Protein chip technology. *Current Opinion in Chemical Biology*. **2003**, *7*, 55-63.
21. Braun, S.; Rappoport, S.; Zusman, R.; Avnir, D.; Ottolenghi, M. Biochemically active sol-gel glasses: the trapping of enzymes. *Materials Letters*. **1990**, *10*, 1-5.
22. Ellerby, L.M.; Nishida, C.R.; Nishida, F.; Yamanaka, S.A.; Dunn, B.; Valentine, J.S.; Zink, J.I. Encapsulation of protein in transparent porous silicate prepared by the sol-gel method. *Science*. **1992**, *255*, 1113-1115.

23. Jin, W.; Brennan, J.D. Properties and applications of proteins encapsulated within sol-gel derived materials. *Analytica Chimica Acta*. **2002**, *461*, 1-36.
24. Avnir, D.; Coradin, T.; Livage, J. Recent bio-applications of sol-gel materials. *Journal of Materials Chemistry*. **2006**, *16*, 1013-1030.
25. Brennan, J.D. Biofriendly sol-gel processing for entrapment of soluble and membrane-bound proteins: toward novel solid-phase assays for high-throughput screening. *Accounts of Chemical Research*. **2007**, *40*, 827-835.
26. Hench, L.L.; West, J.K. The sol-gel process. *Chemical Reviews*. **1990**, *90*, 33-72.
27. Brinker, C.J.; Scherer, G.W. Sol-gel science: the physics and chemistry of sol-gel processing. **1990**. Academic Press, San Deigo, CA.
28. Anderson, D.M.; Leaming, G.F.; Sposito, G. Volume of changes of thixotropic, sodium bentonite suspension during sol-gel-sel transition. *Science*. **1963**, *141*, 104-1041.
29. Dickey, F.H. Specific adsorption. *Journal of Physical Chemistry*. **1955**, *58*, 695-707.
30. Braun, S.; Rappoport, S.; Zusman, R.; Avnir, D.; Ottolenghi, M. Biochemically active sol-gel glasses: the trapping of enzymes. *Materials Letters*. **1990**, *10*, 1-5.
31. Gill, I. Bio-doped nanocomposite polymers: sol-gel bioencapsulates. *Chemistry of Materials*. **2001**, *13*, 3404-3421.
32. Lebert, J.M; Forsberg, E.M.; Brennan, J.D. Solid-phase assays for small molecule screening using sol-gel entrapped proteins. *Biochemistry and Cell Biology*. **2008**, *86*, 100-110.
33. Ferrer, M.L.; del Monte, F.; Levy, D. A novel and simple alcohol-free sol-gel route for encapsulation of labile proteins. *Chemistry of Materials*. **2002**, *14*, 3619-3621.
34. Gill, I.; Ballesteros, A. Encapsulation of biologicals within silicate, siloxane, and hybrid sol-gel polymers: an efficient and generic approach. *Journal of the American Chemical Society*. **1998**, *120*, 8587-8598.
35. Brook, M.A.; Chen, Y.; Guo, K.; Zhang, Z.; Brennan, J.D. Sugar-modified silanes: precursors for silica monoliths. *Journal of Materials Chemistry*. **2004**, *14*, 1469-1479.

36. Brook, M.A.; Chen, Y.; Guo, K.; Zhang, Z.; Jin, W.; Deisingh, A.; Cruz-Aguado, J.; Brennan, J.D. Proteins entrapped in silica monoliths prepared from glyceroxysilanes. *Journal of Sol-Gel Science and Technology*. **2004**, *31*, 343-348.
37. Bhatia, R.B.; Brinker, C.J.; Gupta, A.K.; Singh, A.K. Aqueous Sol-Gel Process for Protein Encapsulation. *Chemistry of Materials*. **2000**, *12*, 2434-2441.
38. Cruz-Aguado, J.A.; Chen, Y.; Zhang, Z.; Brook, M.A.; Brennan, J.D. Entrapment of Src protein tyrosine kinase in sugar-modified silica. *Analytical Chemistry*. **2004**, *76*, 4182-4188.
39. Besanger, T.R.; Hodgson, R.J.; Green, J.R.A.; Brennan, J.D. Immobilized enzyme reactor chromatography: optimization of protein retention and enzyme activity in monolithic silica stationary phases. *Analytica Chimica Acta*. **2006**, *564*, 106-115.
40. Bottcher, H. Bioactive sol-gel coatings. *Journal fur Praktische Chemie*. **2002**, *342*, 427-436.
41. Livage, J.; Coradin, T.; Roux, C. Encapsulation of biomolecules in silica gels. *Journal of Physics: Condensed Matter*. **2001**, *13*, R673-R691.
42. Pierre, A.C. The sol-gel encapsulation of enzymes. *Biocatalysis and Biotransformations*. **2004**, *22*, 145-170.
43. Flora, K.; Brennan, J.D. Fluorometric detection of Ca<sup>2+</sup> based on an induced change in the conformation of sol-gel entrapped parvalbumin. *Analytical Chemistry*. **1998**, *70*, 4595-4513.
44. Cho, E.J.; Bright, F.V. Pin-printed biosensor arrays for simultaneous detection of glucose and O<sub>2</sub>. *Analytical Chemistry*. **2002**, *74*, 6177-6184.
45. Cho, E.J.; Tao, Z.; Tang, Y.; Tehan, E.C.; Bright, F.V.; Hicks, W.L.; Gardella, J.A.; Hard, R. Tools to rapidly produce and screen biodegradable polymers and sol-gel-derived xerogel formulations. *Applied Spectroscopy*. **2002**, *56*, 1385-1389.
46. Rupcich, N.; Goldstein, A.; Brennan, J.D. Optimization of sol-gel formulations and surface treatments for the development of pin-printed protein microarrays. *Chemistry of Materials*. **2003**, *15*, 1803-1811.
47. Rupcich, N.; Green, J.; Brennan, J.D. Nanovolume kinase inhibition assay using a sol-gel derived multi-component microarray. *Analytical Chemistry*. **2005**, *77*, 8013-3019.

48. Lee, M.Y.; Park, C.B; Dordick, J.S.; Clark, D.S. Metabolizing enzyme toxicology assay chip (MetaChip) for high-throughput microscale toxicity analyses. *Proc. Natl. Acad. Sci. U.S.A.* **2005**, *102*, 983-987.
49. Rupcich, N.; Brennan, J.D. Coupled enzyme reaction microarrays based on pin-printing of sol-gel biomaterials. *Analytica Chimica Acta.* **2003**, *500*, 3-12.
50. Stealth Pins. *ArrayIt*<sup>®</sup>. <<www.arrayit.com>>.
51. Kim, S.; Kim, Y.; Kim, P.; Ha, J.; Kim, K.; Sohn, M.; Yoo, J.-S.; Lee, J.; Kwon, J.-A.; Lee, K.N. Improved sensitivity and physical properties of sol-gel protein chips using large-scale material screening and selection. *Analytical Chemistry.* **2006**, *78*, 7392-7396.
52. Tehran, E.C.; Higbee, D.J.; Wood, T.D.; Bright, F.V. Tailored quartz pins for high-density microsensor array fabrication. *Analytical Chemistry.* **2007**, *79*, 5429-5434.
53. Chen, G.Y.; Uttamchandani, M.; Zhu, Q.; Wang, G.; Yao, S.Q. Developing a strategy for activity-based detection of enzymes in a protein microarrays. *ChemBioChem.* **2003**, *4*, 336-339.
54. Uttamchandani, M.; Liu, K.; Panickerb, R.C.; Yao, S.Q. Activity-based fingerprinting and inhibitor discovery of cysteine proteases in a microarray. *Chemical Communications.* **2007**, *15*, 1518-1520.
55. Lee, Y.; Kang, D.-K.; Chang, S.-I.; Han, M.H.; Kang, I.-C. High-throughput screening of novel peptide inhibitors of an integrin receptor from the hexapeptide library by using a protein microarray chip. *Journal of Biomolecular Screening.* **2004**, *9*, 687-694.
56. Fang, Y.; Frutos, A.G.; Lahiri, J. Membrane protein microarrays. *Journal of the American Chemical Society.* **2002**, *124*, 2394-2395.
57. Hong, Y.; Webb, B.L.; Su, H.; Mozdy, E.J.; Fang, Y.; Wu, Q.; Lui, L.; Beck, J.; Ferrie, A.M.; Raghavan, S.; Mauro, J.; Carre, A.; Mueller, D.; Lai, F.; Rasnow, B.; Johnson, M.; Min, H.; Salon, J.; Lahiri, J. Functional GPCR microarrays. *Journal of the American Chemical Society.* **2005**, *127*, 15350-15351.
58. Besanger, T.R.; Easewarmothly, B.; Brennan, J.D. Entrapment of highly active membrane-bound receptors in macroporous sol-gel derived silica. *Analytical Chemistry.* **2004**, *76*, 6470-6475.

59. Ahn, N.G.; Resing, K.A. Toward the phosphoproteome. *Nature Biotechnology*. **2001**, *19*, 317-318.
60. Manning, G.; Whyte, D.B.; Martinez, R.; Hunter, T.; Sudarsnam, S. The protein kinase complement of the human genome. *Science*. **2002**, *298*, 1912-1934.
61. Dancey, J.; Sausville, E.A. Issues and progress with protein kinase inhibitors for cancer treatment. *Nat. Rev. Drug Discovery*. **2003**, *2*, 296-313.
62. Schieven, G.L. The biology of p38 kinase: a central role in inflammation. *Current Topics in Medicinal Chemistry*. **2005**, *5*, 921-928.
63. Rossi, A.G; Sawatzky, D.A.; Walker, A.; Ward, C.; Sheldrake, T.A.; Riley, N.A.; Caldicott, A.; Martinez-Losa, M.; Walker, T.R.; Duffin, R.; Gray, M.; Crescenzi, E.; Martin, M.C.; Brady, H.J.; Savill, J.S.; Dransfield, I.; Haslett, C. Cyclin-dependent kinase inhibitors enhance the resolution of inflammation by promoting inflammatory cell apoptosis. *Nature Medicine*. **2006**, *12*, 1056-1064.
64. Jope, R.S.; Yuskaitis, C.J.; Beurel, E. Glycogen synthase kinase-3 (GSK3): inflammation, diseases and therapeutics. *Neurochemistry Research*. **2007**, *32*, 577-595.
65. Zdychova, J.; and Komers, R. Emerging role of Akt kinase/Protein kinase B signaling in pathophysiology of diabetes and its complications. *Physiological Research*. **2005**, *54*, 1-16.
66. Henriksen, E.J.; Dokken, B.B. Role of glycogen synthase kinase-3 in insulin resistance and type 2 diabetes. *Current Drug Targets*. **2006**, *7*, 1435-1441.
67. Van Ahsen, O.; Bomer, U. High-Throughput Screening for kinase inhibitors. *ChemBioChem*. **2005**, *6*, 481-490.
68. Embi, N.; Rylatt, D.B.; Cohen, P. Glycogen synthase kinase-3 from rabbit skeletal muscle. Separation from cyclic-AMP-dependent protein kinase and phosphorylase kinase. *European Journal of Biochemistry*. **1980**, *170*, 519-527.
69. Woodgett, J.R.; Cohen, P. Mutlisite phosphorylation of glycogen synthase: molecular basis for the substrate specificity of glycogen synthase kinase-3 and casein kinase-II(glycogen synthase kinase-5). *Biochimica Biophysica Acta*. **1984**, *788*, 339-347.

70. Hanger, D.P.; Hughes, K.; Woodgett, J.R.; Brion, J.P., Anderton, B.H. Glycogen synthase kinase-3 induces Alzheimer's disease-like phosphorylation of tau: generation of paired helix filament epitopes and neuronal localization of the kinase. *Neuroscience Letters*. **1992**, *147*, 58-62.
71. Pap, M.; Cooper, G.M. Glycogen synthase kinase-3 in the phosphatidylinositol 3-kinase/Akt cell survival pathway. *Journal of Biological Chemistry*. **1998**, *273*, 19929-19932.
72. Grimes, C.A.; Jope, R.S. The multifaceted roles of glycogen synthase kinase 3 $\beta$  in cellular signaling. *Progress in Neurobiology*. **2001**, *65*, 391-426.
73. Kozlovsky, N.; Belmaker, R.H.; Agam, G. GSK-3 and the neurodevelopmental hypothesis of schizophrenia. *European Neuropsychopharmacology*. **2002**, *12*, 13-25.
74. Murphy, E. Inhibit GSK-3 $\beta$  or there's heartbreak dead ahead. *Journal of Clinical Investigations*. **2004**, *113*, 1526-1528.
75. Eldar-Finkelman, H. Glycogen synthase kinase 3: an emerging therapeutic target. *Trends in Molecular Medicine*. **2002**, *8*, 126-132.
76. Manoukian, A.S.; Woodgett, J.R. Role of glycogen synthase kinase-3 in cancer: regulation by Wnts and other signaling pathways. *Advanced Cancer Research*. **2002**, *84*, 203-229.
77. Pei, J.-J.; Tanaka, T.; Rung, Y.-C.; Braak, E.; Iqbal, K. Grundke-Iqbal, I. Distribution, levels, and activity of glycogen synthase kinase-3 in the Alzheimer disease brain. *Journal of neuropathology and experimental neurology*. **1997**, *56*, 70-78.
78. Fiol, C.J.; Mahrenholz, A.M.; Wang, Y.; Roeske, R.W.; Roach, P.J. Formation of protein kinase recognition sites by covalent modification of the substrate. *The Journal of Biological Chemistry*. **1987**, *262*, 14042-14048.
79. Kupcho, K.; Somberg, R.; Bulleit, B.; Goueli, S.A. A homogeneous, nonradioactive high-throughput fluorogenic protein kinase assay. *Analytical Biochemistry*. **2003**, *317*, 210-217.
80. Park, Y.W.; Cummings, R.T; Wu, L.; Zheng, S.; Cameron, P.M.; Woods, A.; Ziller, D.M.; Marcy, A.I.; Hermes, J.D. Homogeneous proximity tyrosine kinase assays: scintillation proximity assay versus homogeneous time-resolved fluorescence. *Anal. Biochem*. **1999**, *269*, 94-104.

81. Fowler, A.; Swift, D.; Longman, E.; Acornley, A.; Hemsley, P.; Murray, D.; Unitt, J.; Dale, I.; Sullivan, E.; Coldwell, M. An evaluation of fluorescence polarization and lifetime discriminated polarization for high throughput screening of serine/threonine kinases. *Analytical Chemistry*. **2002**, *308*, 223-231.
82. Turek-Etienne, T.C.; Lei, M.; Terracciano, J.S.; Langsdorf, E.F.; Bryant, R.W.; Hart, R.F.; Horan, A.C. Use of red-shifted dyes in a fluorescence polarization AKT kinase assay for detection of biological activity in natural product extracts. *Journal of Biomolecular Screening*. **2004**, *9*, 53-61.
83. Beasley, J.R.; Dunn, D.A.; Walker, T.L.; Parlato, S.M.; Lehrach, J.M.; Auld, D.S. Evaluation of compound interference in immobilized metal ion affinity-based fluorescence polarization detection with a four million member compound collection. *Assay and Drug Development Technology*. **2003**, *1*, 455-459.
84. Loomans, E.M.G.; van Doornmalen, A.M.; Wat, J.W.Y.; Zaman, G.J.R. High-throughput screening with immobilized metal ion affinity-based fluorescence polarization detection, a homogeneous assay for protein kinases. *Assay and Drug Development Technology*. **2003**, *1*, 445-453.
85. Kiiianitsa, K.; Solinger, J.A.; Heyer, W-D. NADH-coupled microplate photometric assay for kinetic studies of ATP-hydrolyzing enzymes with low and high specific activities. *Analytical Biochemistry*. **2003**, *321*, 266-271.
86. McCauley, T.J.; Stanaitis, M.L.; Savage, M.D.; Onken, J.; Milis, S.Z. IQ<sup>TM</sup> Technology: Development of a universal, homogeneous method for high-throughput screening of kinase and phosphatases activity. *Journal of the Association for Laboratory Automation*, **2003**, *8(2)*, 36-40.
87. Partserniak, I.; Werstuck, G.; Capretta, A.; Brennan, J.D. An ESI-MS/MS method for screening of small-molecules mixtures against glycogen synthase kinase-3 $\beta$  (GSK3 $\beta$ ). *ChemBioChem*, **2008**, *9*, 1065-1073.
88. Witt, J.J.; Roskoski, R. Rapid protein kinase assay using phosphocellulose-paper absorption. *Analytical Biochemistry*. **1975**, *66*, 253-258.
89. Li, Y.; Cummings, R.T.; Cunningham, B.R.; Chen, Y.; Zhou, G. Homogeneous assays for adenosine 5'-monophosphate-activated protein kinase. *Analytical Biochemistry*. **2003**, *321*, 151-156.
90. Z'-Lyte<sup>TM</sup> Kinase Assay Kits. *Invitrogen*. <<www.invitrogen.com>>.

91. Matrin, K.; Steinberg, T.H.; Cooley, L.A.; Gee, K.R.; Beechem, J.M.; Patton, W.F. Quantitative analysis of protein phosphorylation status and protein kinase activity on microarrays using a novel fluorescent phosphorylation sensor dye. *Proteomics*. **2003**, *3*, 1244-1255.
92. Scott, L.J.; Goa, K.L. Galantamine: A review of its use in Alzheimer's disease. *Drugs*. **2000**, *60*(5), 1095-1122.
93. Rogers, S.L.; Farlow, M.R.; Doody, R.S.; Moh, R.; Friedhoff, L.T. A 24-week, double-blind, placebo-controlled trial of donepezil in patients with Alzheimer's disease. *Neurology*. **1998**, *50*(1), 136-145.
94. Rosler, M.; Anand, R.; Cicin-Sain, A.; Gauthier, S.; Agid, Y.; Dal-Bianco, R.; Stahelin, H.B.; Hartman, R.; Gharabawl, M. Efficacy and safety of revistigmine in patients with Alzheimer's disease: international randomized controlled trial. *BMJ*. **1999**, *318*, 633-639.
95. Siegel, G.J.; Lehrer, G.M.; Silides, D. The kinetics of cholinesterases measured fluorometrically. *The Journal of Histochemistry and Cytochemistry*. **1966**, *14*(6), 473-478.
96. Prince, A.K. Spectrophotometric study of the acetylcholinesterase-catalyzed hydrolysis of 1-methyl-acetoxyquinolinium iodides. *Archives of Biochemistry and Biophysics*. **1966**, *113*, 195-204.
97. Amplex® Red Acetylcholine/Acetylcholinesterase Assay Kit (A12217). *Invitrogen*. <<<http://probes.invitrogen.com/media/pis/mp12217.pdf>>>.
98. Ozturk, G.; Alp, S.; Timur, S. A fluorescent biosensor based on acetylcholinesterase and 5-oxazolone derivative immobilized in polyvinylchloride (PVC) matrix. *Journal of Molecular Catalysis B: Enzymology*. **2007**, *47*, 111-116.
99. Dong, R.-A.; Tsai, H.-C. Immobilization and characterization of sol-gel-encapsulated acetylcholinesterase fiber-optic biosensor. *Analytica Chimica Acta*. **2001**, *434*, 239-246.
100. Tsai, H.-C.; Doong, R.-A. Simultaneous determination of pH, urea, acetylcholine and heavy metals using array-based enzymatic optical biosensor. *Biosensors and Bioelectronics*, **2005**, *20*, 1796-1804.

## **Chapter 2**

# **Sol-Gel-Derived Microarrays as a Solid-Phase Platform for Detection of GSK-3 $\beta$ Activity**

In the following chapter, I was responsible for all experimental design, data analysis, interpretation and presentation. I wrote the first draft of the manuscript and Dr. Brennan provided editorial input to generate the final draft.

## **Chapter 2: Sol-Gel-Derived Microarrays as a Solid-Phase Platform for Detection of GSK-3 $\beta$ Activity**

### **Abstract**

A solution-based glycogen synthase kinase 3 $\beta$  (GSK-3 $\beta$ ) assay was developed, utilizing sol-gel entrapment for generation of a microarray-based solid phase platform that allowed for detection of phosphorylated substrates using a fluorescent stain. Solution assay mixtures were immobilized in silica in microarray format via pin-printing of the sol and biomolecule mixture. Using Pro-Q<sup>®</sup> Diamond<sup>™</sup> stain, a phospho-residue specific dye, the extent of phosphorylation in each microarray element was analyzed. GSK-3 $\beta$  has a preference for pre-phosphorylated, or primed, substrates, and therefore the ability to detect hyperphosphorylation was demonstrated using a gradient of GSM peptide, a primed substrate for GSK-3 $\beta$ . After assaying four different GSK-3 $\beta$  substrates, GSM peptide was found to be the optimal substrate to monitor GSK-3 $\beta$  activity using the microarray format based on signal-to-background and cost/availability considerations. This assay was found to be amenable to small molecule screening, with a z' value of ~0.5. Three different GSK-3 $\beta$  inhibitors, with varying potency and modes of action, were tested with this system. The known ATP-competitive and non-competitive inhibitors were correctly identified and showed a level of inhibition corresponding to their potency. The ATP-competitive inhibitor, SB415286, was chosen for further characterization and it was shown that the microarray assay could be used to generate an IC<sub>50</sub> value.

## 2.1 Introduction

Phosphorylation is a ubiquitous post-translational protein modification that plays a key role in the regulation of many cellular processes.<sup>1</sup> The improper regulation of phosphorylation by kinases has been associated with a wide range of diseases and as such kinases have become the second most targeted family of proteins for drug development.<sup>2</sup> A particularly interesting kinase is glycogen synthase kinase 3 (GSK-3), which is involved in many central cellular functions including cell cycle progression,<sup>3, 4</sup> apoptosis,<sup>5</sup> and transcription factor regulation<sup>6</sup>. It has also been implicated in various pathological conditions including schizophrenia,<sup>7</sup> heart disease,<sup>8</sup> non-insulin-dependent diabetes mellitus,<sup>9</sup> cancer<sup>10</sup> and Alzheimer's disease.<sup>11</sup> The association of GSK-3 in Alzheimer's disease is attributed to its role in the hyperphosphorylation of tau protein.<sup>12</sup> Using antisense treatment and phosphatidylinositol(3,4,5)triphosphate (PtdIns(3,4,5)P<sub>3</sub>) inhibition studies, Takashima *et al.* were able to establish that the  $\beta$ -isomer of GSK-3 (GSK-3 $\beta$ ) was the key isomer responsible for the hyperphosphorylation of tau.<sup>13</sup> As such, it is of both therapeutic, as well as academic, interest to identify inhibitors of GSK-3 $\beta$ .

There are a wide variety of methods currently used to screen small molecule libraries in high throughput to identify kinase inhibitors. The most prevalent of these are the scintillation proximity assay (SPA),<sup>14</sup> homogeneous time-resolved fluorescence (HTRF) assay,<sup>14</sup> fluorescence polarization (FP) assay,<sup>15, 16</sup> and amplified luminescence proximity homogeneous assay (ALPHA).<sup>17, 18</sup> While each method has its strengths, there are also disadvantages associated with each: SPA requires the use of radioactive ATP<sup>33</sup>; HTRF and FP assays require expensive labelled antibodies; while ALPHA screens are

very sensitive to interferences.<sup>18</sup> Additionally, the methods are not ideal for GSK-3 $\beta$ , due to the unique preference of GSK-3 $\beta$  for pre-phosphorylated, or 'primed' substrates. GSK-3 $\beta$  has a recognition sequence of S-X-X-X-pS, where pS is a phosphoserine,<sup>19</sup> and most of the assays described above are unable to distinguish between the primed substrate and hyperphosphorylated product.

In 2005, a mass spectrometry-based assay for GSK-3 $\beta$  activity was reported by Bowley *et al.*<sup>20</sup> This method involved the covalent attachment of the substrate peptides to a gold-plated surface, followed by incubation of the plate with GSK-3 $\beta$  and necessary cofactors. To detect the generated product, surface enhanced laser desorption/ionization time of flight mass spectrometry (SELDI-TOF-MS) was used. This format allowed for rapid, non-radioactive-based assaying of GSK-3 $\beta$  activity. However, this method is not amenable to the large protein substrates of GSK-3 $\beta$  and the mode of MS used is known to be only semi-quantitative in nature.

Partserniak *et al.* also published a MS-based assay for GSK-3 $\beta$  in 2008.<sup>21</sup> This article reported a solution-based GSK-3 $\beta$  assay with the substrate phosphopeptide, GSM, using ESI-MS to detect levels of pGSM relative to GSM. Levels of ammonium acetate buffer and magnesium ion were screened for maximal GSK-3 $\beta$  activity while maintaining a high MS signal. Using this method, a screen of 100 compounds in mixtures of 10 compounds each was performed and samples spiked with known inhibitors were correctly identified. This method however is limited to MS-compatible assay conditions and is not easily amenable to protein substrates of GSK-3 $\beta$ .

A relatively novel method to monitor kinase activity involves the use of a phospho-specific stain, Pro-Q<sup>®</sup> Diamond<sup>™</sup> from Invitrogen, in conjunction with microarrays as a solid phase support. In 2003, Martin *et al.* reported on the adaptation of this stain, which is typically used for phosphoprotein identification in gels, for quantitative detection of both phosphoproteins and phosphopeptides on covalently immobilized and hydrogel-based protein/peptide microarrays.<sup>22</sup> Kinase activity could also be monitored using the substrate microarrays and the phospho-specific stain.<sup>22</sup> The compatibility of this dye with sol-gel-derived silica microarrays was later confirmed by the Brennan group using protein kinase A (PKA) and kemptide as a model kinase system.<sup>23</sup>

Herein, we investigate the application of Pro-Q<sup>®</sup> Diamond<sup>™</sup> stain with sol-gel-derived microarrays as a solid phase platform for the monitoring of GSK-3 $\beta$  activity and inhibition in solution. By carrying out reactions in solution, then entrapping the final reaction mixture in silica in microarray format, the required solid phase support is generated. The inexpensive Pro-Q<sup>®</sup> Diamond<sup>™</sup> stain can then be employed for end-point detection to assess the degree of phosphorylation in each microspot (Figure 2.1). Sol-gel-derived microarrays are a particularly attractive solid phase platform for this assay format due to their high loading capacity and sensitivity relative to monolayer immobilization techniques.<sup>24</sup> Additionally, this assay format does not rely on expensive antibodies or labelled substrates, nor does it require specific buffer conditions to be compatible with the detection mode. Furthermore, the type of substrate is not limited with this kinase assay - both peptide and protein substrates can theoretically be employed. Lastly and

most importantly, this method is shown to be quantitative and compatible with primed substrates.

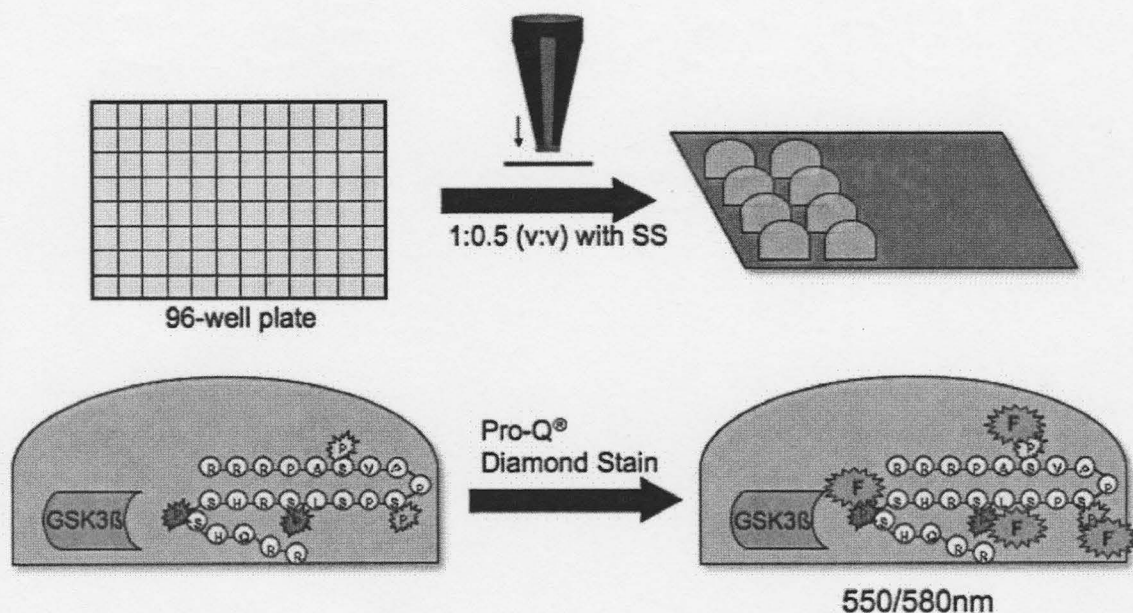


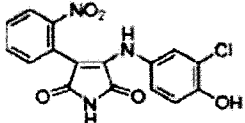
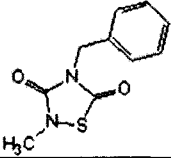
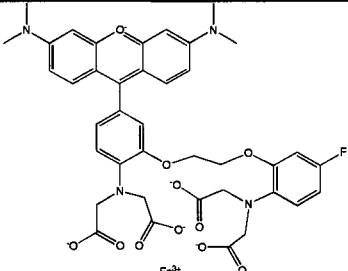
**Figure 2.1** GSK-3 $\beta$ /GSM assay scheme. Solution-run assays are printed as sol-gel-derived microarrays, then stained with Pro-Q<sup>®</sup> Diamond<sup>™</sup> stain and imaged fluorescently.

## 2.2 Experimental

**2.2.1 Materials.** The structure of GSK-3 $\beta$  substrates and inhibitors, as well as Pro-Q<sup>®</sup> Diamond<sup>™</sup> stain are shown in Table 2.1.  $\beta$ -casein, bovine serum albumin (BSA), adenosine triphosphate Mg(II) salt, MgCl<sub>2</sub>, sodium silicate, Dowex 50x8-100 cation exchange resin and SB415286 were obtained from Sigma (Oakville, ON). Glycogen synthase kinase 3 $\beta$  and CREB peptide were purchased from New England Biolabs. FRATtide, GSK Inhibitor I and Tau protein was obtained from EMD Biosciences (Mississauga, ON).  $\beta$ -Catenin was purchased from Millipore (Etobicoke, ON).

SuperAldehyde<sup>TM</sup> derivatized glass microscope slides were purchased from ArrayIt (Sunnyvale, CA). Pro-Q<sup>®</sup> Diamond<sup>TM</sup> phosphorylation dye and destaining solution were purchased from Invitrogen (Burlington, ON). Water was purified with a Milli-Q Synthesis A10 water purification system. All other chemicals and solvents used were of analytical grade, and were used without further purification.

**Table 2.1** Inhibitor and substrate structures.

Inhibitor/Substrate	Structure	Comments
β-catenin	112kDa protein (GST tagged)	Not primed Complex with axin enhances phosphorylation <sup>25</sup>
CREB peptide	KRREILSRRPS(p)YRK (14-mer)	Primed One site for phosphorylation
Tau protein	60 kDa protein (His <sub>6</sub> Tag)	Not primed Nine phosphorylation sites Heparin enhances phosphorylation <sup>26</sup>
GSM peptide	RRRPASVPPSPSLSRHS (pS)HQRR (22-mer)	Primed 3 phosphorylation sites
SB41286		ATP-competitive IC <sub>50</sub> 78 nM (K <sub>i</sub> 33.1 nM) <sup>27</sup>
GSK Inhibitor I (TDZD-8)		Non-ATP competitive IC <sub>50</sub> 2 μM (K <sub>i</sub> ~ 0.5 μM) <sup>28</sup>
FRATtide	SQPETRTGDDDPHRLQLQL VLSGNLIKEAVRRLHSRRL Q (39-mer)	Prevents binding of un-primed substrates <sup>29</sup>
Pro-Q <sup>®</sup> Diamond <sup>TM</sup> Stain		Selectively stains phosphate groups Ex/Em: 500/580 nm

### 2.2.2 Arraying Methods.

*Sodium silicate preparation.* The sodium silicate precursor solution (SS) was prepared by diluting 2.9 g of sodium silicate in 10 mL of ddH<sub>2</sub>O and immediately adding 5 g of the Dowex resin. The mixture was stirred for 30 seconds and then vacuum filtered through a Buckner funnel. The filtrate was then further filtered through a 0.45 µM membrane syringe filter to remove any particulates in the solution. The solution was made fresh daily and kept on ice until use.

*Spotting solution preparation.* Spotting solutions were formed by combining the buffered assay sample solutions (25 µL) in a 1:0.5 (v:v) ratio with SS to a final volume of 37.5 µL in a 96-well plate. These solutions were mixed immediately before printing to reduce any risks of gelation of the sample in the printing pin. The mixtures typically required at least 30 min to gel, allowing samples to be printed as often as required.

*Microarray Pin-Printing and Slide Aging.* A Virtek Chipwriter Pro (Virtek Engineering Sciences Inc., Toronto, ON) robotic pin-spotter equipped with a SMP3 stealth microspotting pin (250 nL uptake, 0.6 nL delivery, Telechem Inc., Sunnyvale, CA) was used to print 100 µm diameter spots onto aldehyde-derivatized glass microscope slides from 96-well plates using a printhead speed of 10 mm.s<sup>-1</sup>. The time required to uptake and print a single sample (with 15-20 replicates) is approximately 3 minutes, including the time required for washing, sonicating and drying the pin following spotting. Printing was performed at room temperature with humidity at ~80%. Arrays were allowed to age at 30° C overnight at high humidity prior to staining and imaging.

*Pro-Q Staining/Destaining.* Aged arrays were stained with Pro-Q® Diamond™ stain for 45 min with shaking. The slides were then destained twice for 10 min with shaking using the commercial destaining solution from Invitrogen. Lastly, the slides were washed with ddH<sub>2</sub>O for 10 min with shaking and spun dry using a high-speed slide centrifuge (max. speed ~6000 rpm) (Telechem International).

*Fluorescence Imaging.* Fluorescence images of the microarrays were taken with a ScanArray Express (Packard Biosciences). Excitation was performed with the 548 nm laser at 90% laser power and emission at 580 nm was monitored with 50% gain. For experiments involving internal controls, the 647 nm laser was used for excitation and emission was monitored at 668 nm.

*Image Analysis.* The microspot intensities were quantified using ArrayPro Analyzer software (MediaCybernetics). The corrected spot signal intensities were calculated by subtracting the local background from the total integrated signal. In each case, the average signal intensity of the replicate spots is reported with errors representing 1 standard deviation. Outliers were identified using the Q test and not included in the average.

### **2.2.3 Assay Procedures.**

*GSM Gradient.* A dilution series of GSM peptide (0 – 400 μM) in 50 mM Tris, pH 7.5, 10 mM MgCl<sub>2</sub> was printed 1) directly onto a SuperAldehyde slide and 2) mixed 1:0.5 (v:v) with SS and printed onto a SuperAldehyde slide. Both arrays were imaged and analyzed with the method described above.

*GSK-3 $\beta$  Optimization.* GSK-3 $\beta$  (10 units/ $\mu$ L or 5 units/ $\mu$ L) was mixed with GSM (50  $\mu$ M) and ATP (250  $\mu$ M) in 50 mM Tris pH 7.5, 10 mM MgCl<sub>2</sub> (25  $\mu$ L total volume) and the mixture was incubated for 2, 4 and 6 hours on a plate shaker at room temperature. As the negative control, the assay was run with all components except ATP. Following incubation, the samples were then mixed 1:0.5 (v:v) with SS and printed in arrays of 5 replicates per sample on a SuperAldehyde slide and analyzed as noted above.

*GSK-3 $\beta$  Assay Proof of Concept.* GSK-3 $\beta$  (10 units/ $\mu$ L) was mixed with one of  $\beta$ -Catenin (1  $\mu$ M)/CREB (50  $\mu$ M)/Tau (2  $\mu$ M)/GSM (50  $\mu$ M), as well as ATP (250  $\mu$ M) in 50 mM Tris pH 7.5, 10 mM MgCl<sub>2</sub> with or without 50  $\mu$ g/mL heparin (25  $\mu$ L total volume) and the mixture was incubated for 2 hours on a plate shaker at room temperature. As negative controls, the assays were run with all components (including heparin) except ATP. The samples were then mixed 1:0.5 (v:v) with SS and printed in arrays of 5 replicates per sample on a SuperAldehyde slide and analyzed as noted above.

*GSK-3 $\beta$ /GSM z' Plot.* Assays were run using GSK-3 $\beta$  (10 units/ $\mu$ L), GSM (100  $\mu$ M), ATP (100  $\mu$ M) in 100 mM Tris, pH 7.5, 10 mM MgCl<sub>2</sub>. Five assays were performed in parallel and incubated for 2.5 hours at room temperature on a plate shaker. As the negative control (NC) for the plot, assays were run without ATP. Each sample was used to generate 50 microspots and therefore in total 250 microspots were printed. This array was analyzed and used to generate a z' plot. To reduce variation due to differential spot volumes, only the last 25 spots were used for each sample to generate the z' plot. The z' value was calculated using Equation [1] provided below.

$$z' = 1 - \frac{3\sigma_s + 3\sigma_c}{|\mu_s - \mu_c|} \quad [1]$$

*Inhibition Assays.* Solutions containing GSK-3 $\beta$  (10 units/ $\mu$ L), GSM (50  $\mu$ M), ATP (50  $\mu$ M), and one of SB415285 (A)/GSK-3 $\beta$  Inhibitor I (B)/FRATtide (C) at 4  $\mu$ M in 50 mM Tris, pH 7.5, 10 mM MgCl<sub>2</sub> were incubated for 2 hr incubation with shaking at room temperature. Inhibitor stocks solution were 10 mM in DMSO (1  $\mu$ L in 25  $\mu$ L assay). Positive control (PC) samples utilized the assay conditions above with the addition of DMSO only; the negative control (NC) consisted of the same assay components as the positive control but without ATP. Solutions were printed onto an aldehyde-derivatized slide and processed as described above.

*GSK-3 $\beta$ /GSM IC<sub>50</sub> Determination.* To assess the IC<sub>50</sub> value of the known inhibitor, SB415286, the following assay conditions were used: GSK-3 $\beta$  (10 units/ $\mu$ L), GSM (50  $\mu$ M), ATP (50 $\mu$ M) and SB415286 (0-100  $\mu$ M) in 50 mM Tris, pH 7.5, 10 mM MgCl<sub>2</sub> with a 25  $\mu$ L total volume assay with a final concentration of 4% v/v DMSO (1 $\mu$ L in 25 $\mu$ L assay). GSK-3 $\beta$  was incubated with inhibitor for 10 min prior to addition of ATP to the assay mixture and incubation for 2 hrs at room temperature on a plate shaker. Samples were then mixed with SS and printed onto a SuperAldehyde slide. Arrays were prepared, imaged and analyzed using the method described above. The resulting IC<sub>50</sub> curve was plotted as RFU vs. log[SB415286] and fit to Hill-Slope model.<sup>30</sup>

## 2.3 Results and Discussion

*GSM gradient analysis.* Because GSK-3 $\beta$  has a preference for primed substrates, it was necessary to demonstrate the ability to detect hyperphosphorylation over and above the signal generated by the pre-phosphorylated substrate. Additionally, it was important to establish the quantitative nature of phosphorylation detection with the Pro-Q<sup>®</sup> Diamond<sup>™</sup> stain and the value of using sol-gel entrapment versus standard covalent attachment methods for microarray fabrication. These goals were achieved by printing gradients (5 – 400  $\mu$ M) of primed GSM peptide on aldehyde-derivatized slides by direct covalent immobilization and via sol-gel entrapment, allowing of the comparison between the two techniques and assessment of sensitivity to phosphoresidue concentration (Figure 2.2).

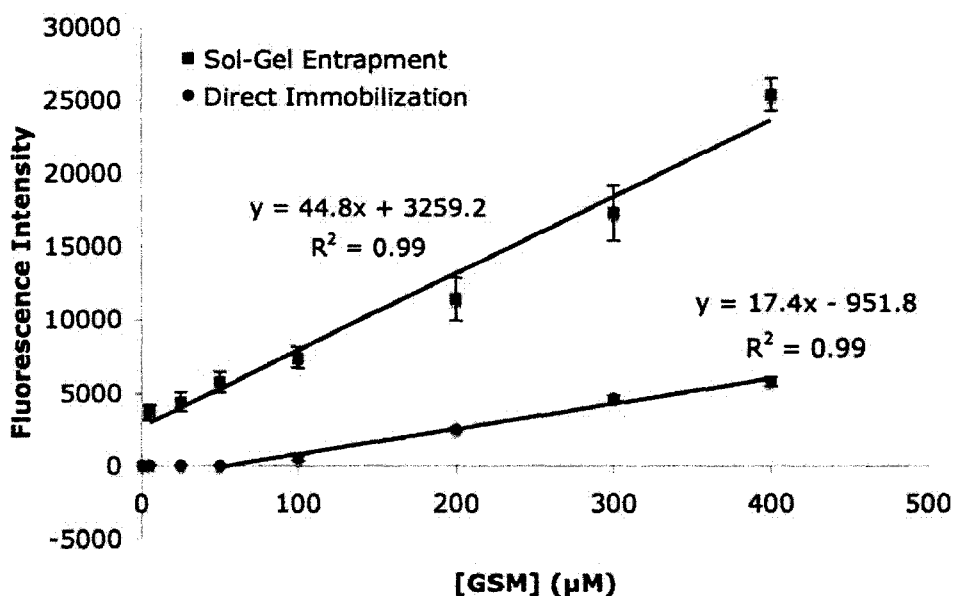


**Figure 2.2** Comparison of covalent immobilization and sol-gel entrapment techniques using a GSM peptide gradient printed onto an aldehyde-derivatized slides.

The results shown in Figure 2.2 indicate direct immobilization onto aldehyde-derivatized slides provided a linear trend ( $R^2=0.99$ ), however concentrations below 50  $\mu\text{M}$  were not detected above background. When using sol-gel entrapment, a 2.5-fold improvement in sensitivity and >5 fold higher overall signal levels were observed compared to direct immobilization. Furthermore, the gradient showed impressive linearity ( $R^2=0.99$ ) from 5  $\mu\text{M}$  to 400  $\mu\text{M}$ , although this method shows a higher background level. From this gradient, the optimal concentration of GSM for assaying is inferred to be 50 – 200  $\mu\text{M}$ , assuming a 2 - 4 fold increase in phosphorylated residues. The sol-gel-based data shows the inherently higher loading capacity of sol-gel-derived microarrays compared to monolayer protein immobilization techniques.<sup>24</sup> While previous work in our group reported a signal increase of 100-fold between monolayer and sol-gel immobilized anti-fluorescein antibody,<sup>24</sup> a ~5-fold increase in signal was observed between the covalently immobilized and sol-gel entrapped GSM sample (200 – 400  $\mu\text{M}$ ). This lower enhancement may be due to issues with leaching of GSM from the sol-gel microarray elements, low accessibility of dye to phosphate groups, or higher efficiency of covalent immobilization for peptides relative to antibodies. Even so, the sol-gel immobilized GSM microarray shows superior signal-to-background relative to the covalent immobilized microarray, allowing for a reduction in the concentrations of reagents used.

*GSM-3 $\beta$  Optimization.* Solution-based assay conditions were optimized for GSK-3 $\beta$  concentration and incubation time to maximize signal-to-background ratios for subsequent experiments. GSK-3 $\beta$  is known to be a slow enzyme and as such incubation

times of 2, 4 and 6 hours were examined at two levels of GSK-3 $\beta$  (5 and 10 units/ $\mu$ L) (Table 2.2). It was found that the higher concentration of GSK-3 $\beta$  (10 units/ $\mu$ L) gave better signal-to-background ratios at all time points relative to the lower concentration (5 units/ $\mu$ L). While signal-to-background values increased with increasing assay time, a 2-hour incubation time was chosen for further studies due to fact that the improvement was not substantial enough to justify the longer incubation time.

**Table 2.2** Optimization of GSK-3 $\beta$  concentration and assay incubation time. Assays were performed with 50 $\mu$ M GSM and 250  $\mu$ M ATP.

<b>GSK3<math>\beta</math> (units/<math>\mu</math>L)</b>	<b>Incubation time (h)</b>	<b>PC/NC</b>
5	2	2.3
5	4	2.6
5	6	3.0
10	2	3.3
10	4	3.4
10	6	3.7

*GSK-3 $\beta$  assay proof of concept.* Following the PKA sol-gel-derived microarray-based assay reported by our group,<sup>23</sup> initial studies focused on the entrapment of GSK-3 $\beta$  prior to assaying. These efforts, however, were unsuccessful, and thus we pursued solution-based studies using the sol-gel-derived microarray as a solid phase platform for phosphorylation detection with Pro-Q<sup>®</sup> Diamond<sup>™</sup> phosphospecific stain.

GSK-3 $\beta$  has over 40 putative substrates ranging in size, number of phosphorylation sites and primed status.<sup>31</sup> As such, four substrates were chosen for consideration with the microarray-based GSK-3 $\beta$  assay based on availability, potential degree of phosphorylation, involvement in key pathways, primed or unprimed status, as well as the nature of the substrate (protein or peptide). The four different substrates

examined were  $\beta$ -catenin, tau protein, CREB peptide, and GSM peptide (Figure 2.3).  $\beta$ -Catenin and tau are both unprimed protein substrates with three<sup>32</sup> and nine<sup>33</sup> potential sites for phosphorylation, respectively. Two primed synthetic peptides were also examined; CREB (14-mer) and GSM (22-mer) peptides have one<sup>34</sup> and three<sup>35</sup> additional phosphorylation sites, respectively. Theoretically, both the unprimed and primed substrates should be compatible with the microarray assay format; detection of phosphorylation of unprimed substrates was demonstrated previously with the PKA/kemptide system and, as discussed above, it should also be possible to detect hyperphosphorylation of a primed substrate.

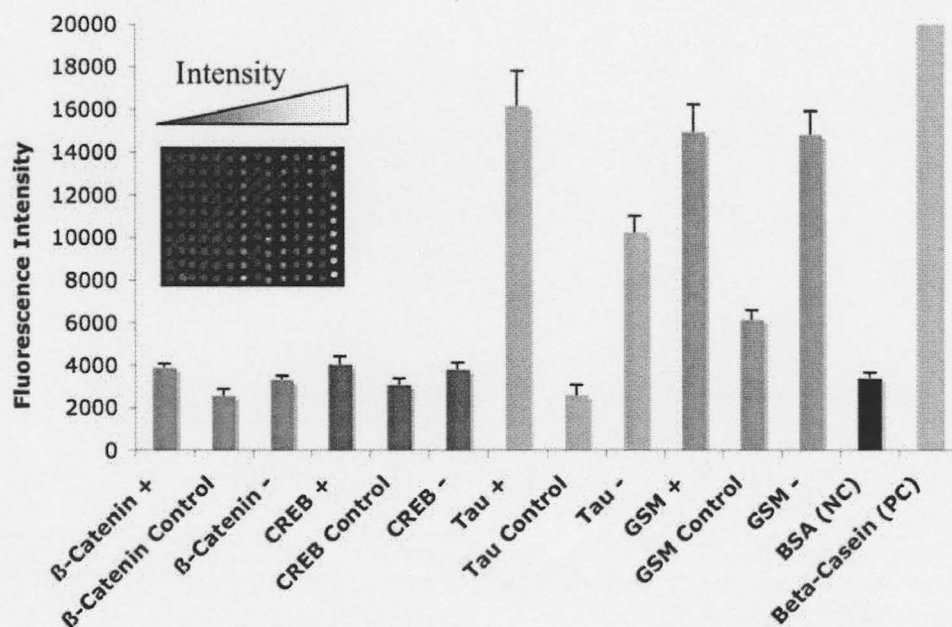


**Figure 2.3** GSK-3 $\beta$  assays with various substrates (as labelled in x-axis) in the absence (-) and presence (+) of heparin. Control samples contain GSK-3 $\beta$ , substrate and heparin, but no ATP. Note: microarray image is false coloured and edited for clarity. Columns in microarray are in the same sample order as presented in the chart.

Based on the results, two of the four substrates, GSM and tau, were identified as potential substrates for use with this assay format. The other two substrates, which did not show a significant signal increase over background, were  $\beta$ -catenin and CREB peptide. The lack of signal from  $\beta$ -catenin was not surprising as phosphorylation of this protein generally requires formation of a complex involving  $\beta$ -catenin, GSK-3 $\beta$  and axin.<sup>25</sup> The lack of signal increase for the CREB peptide may be attributed to leaching, as this peptide is relatively small (12-mer), or low binding efficiency of the phosphospecific dye.

Both tau protein and GSM peptide gave substantial signal increases over the negative controls. GSM phosphorylation gave a 2.4-fold signal increase over the negative control, which was not affected by the presence of heparin. For tau protein, a 4-fold enhancement of signal over background was observed. This increase could be improved to 6-fold through the utilization of heparin, a known potentiator of tau phosphorylation by GSK-3 $\beta$ .<sup>26</sup> Unfortunately, these impressive results for tau protein were counterbalanced by a comparatively high cost, and issues with short shelf life and poor stability of the tau protein. For these reasons, GSM was the substrate of choice for further investigation of this assay format.

*Assessment of Assay Quality for HTS.* In high throughput screening, it is vital to have a robust and reproducible assay with a large separation between positive and negative control signals. A large separation with highly reproducible positive and negative control values provides a 'hit' window where inhibitors from the screening can be identified confidently. The quality of this 'hit' window and thus the suitability of this assay to high

throughput screening is often described by a  $z'$  value (or Z-factor).<sup>36</sup> As a general rule, a  $z'$  value  $>0.5$  represents an excellent assay for high throughput screening.<sup>36</sup>

A  $z'$  plot was generated for this assay to assess its applicability to high throughput screening. To construct the plot, five positive control (PC) assays and five corresponding negative control (NC) assays were run in parallel and printed as microarrays of 50 spots/sample. Due to spot variation in the first 25 spots resulting from decreasing array element size, only the final 25 microspots were used to generate the  $z'$  plot (Figure 2.4). From this plot, the  $z'$  value was calculated using equation [1] and found to be 0.48 ( $\sim 0.5$ ), showing that the assay is of the minimum quality required for small molecule screening and inhibitor identification. This value may be improved with the use of an internal standard to correct for spot size/volume variations, the major contributing factor to the lower  $z'$  value.

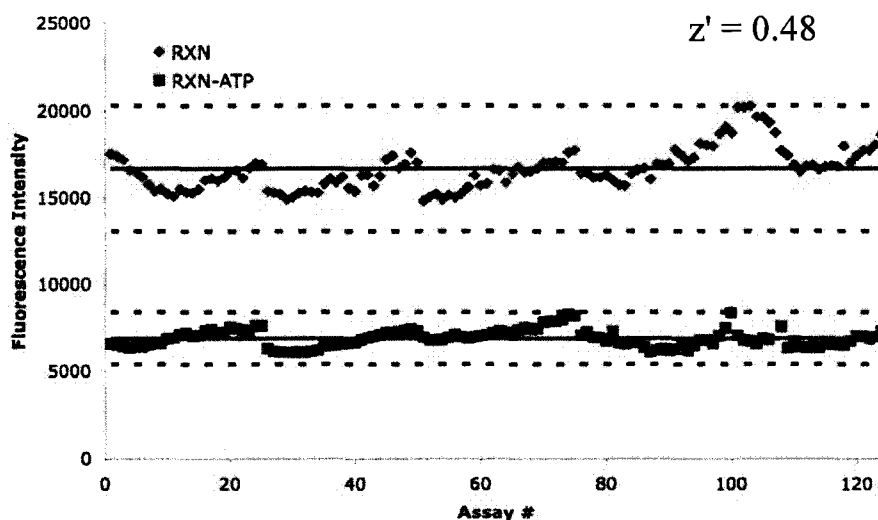


**Figure 2.4**  $z'$  plot for GSK-3 $\beta$  assay with GSM peptide. Negative control is the assay without ATP (RXN-ATP), positive control is the assay with ATP (RXN). The solid lines represent the average of the positive and negative control assays. The dashed lines are  $\pm 3$  standard deviations from the average.

*Inhibition Assays.*

The ability to identify potent GSK-3 $\beta$  inhibitors using the microarray-based assay was investigated using three known GSK-3 $\beta$  inhibitors with different modes of action were chosen for study: A) SB415286, an ATP-competitive inhibitor;<sup>27</sup> B) GSK-3 $\beta$  Inhibitor I, a non-ATP competitive inhibitor;<sup>28</sup> and C) FRATtide, a peptidic unprimed site inhibitor.<sup>29</sup> GSK-3 $\beta$  was incubated with each inhibitor at a concentration of 4  $\mu$ M, which is within the typical screening range. As seen in Figure 2.5 below, inhibition was observed for both inhibitor A and inhibitor B relative to the positive control. For inhibitor A, 70% inhibition was obtained compared to inhibitor B with 28% inhibition and inhibitor C with no inhibition. The larger degree of inhibition for inhibitor A was expected due to its greater potency ( $K_i = 33.1$  nM<sup>27</sup>) relative to inhibitor B ( $K_i = \sim 500$  nM<sup>28</sup>). Additionally, the lack of inhibition by inhibitor C was expected as FRATtide blocks phosphorylation of unprimed substrates and GSM is pre-phosphorylated.<sup>29</sup>

Using this assay format, the known inhibitors of GSK-3 $\beta$  were correctly identified, further demonstrating the applicability of this assay for small molecule screening. Efforts are currently underway to perform a 1000 compound screen consisting of a subset of the Canadian Compound Collection (obtained from McMaster University HTS Lab) using this assay. Mixtures of 20 compounds will be used to increase the throughput of the assay with deconvolution of any mixtures that show GSK-3 $\beta$  inhibition in order to identify inhibitors.

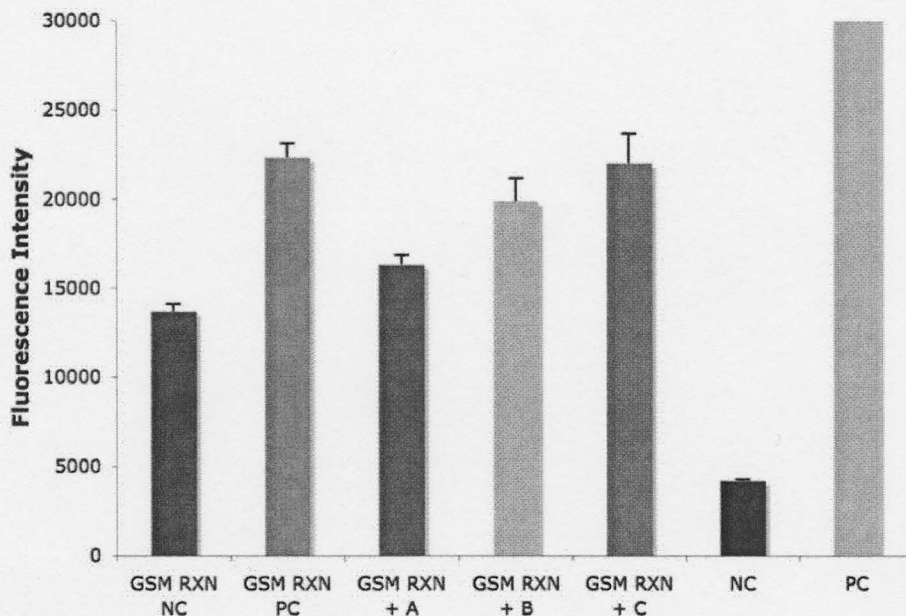


**Figure 2.5** Substrate-selective inhibition of GSK-3 $\beta$  with various inhibitors at a concentration of 4  $\mu$ M. A = SB415286, B = GSK-3 $\beta$  Inhibitor I, C = FRATtide, NC = negative control (BSA), PC = positive control ( $\beta$ -Casein), RXN NCs (no ATP), RXN PCs. Note: the PC ( $\beta$ -casein) signal is above the scale of graph ( $\sim$ 54,000 RFU).

*IC<sub>50</sub> Analysis.* To further assess the quantitative nature of the microarray assay, a dose-response curve for the known inhibitor, SB415286, which showed highest inhibition in preliminary inhibition assays, was generated to assess the IC<sub>50</sub> value. The dose-response curve followed the expected trend and was successfully fit to a Hill-Slope model (Figure 2.6).<sup>30</sup> Using equation [2] below, the  $K_i$  value was derived from the IC<sub>50</sub> plots<sup>37</sup>

$$K_i = \frac{IC_{50}}{\left(\frac{[S]}{K_M} + 1\right)} \quad [2]$$

where [S] is the substrate concentration and  $K_M$  is the Michaelis constant for the enzyme and the ATP substrate. The  $K_i$  for this inhibitors was determined to be 360 nM, which is roughly 10-fold greater than the literature value of 33.1 nM.<sup>27</sup> The difference in  $K_i$  values

may be attributed to differences in assay incubation time or degradation of the inhibitor stock. Additionally, the small difference in the measurements around the inflection point can significantly change the  $IC_{50}$  value. Nonetheless, it was shown that this assay format is able to generate an  $IC_{50}$  curve to assess the relative potency of potential inhibitors identified during small molecule screening.

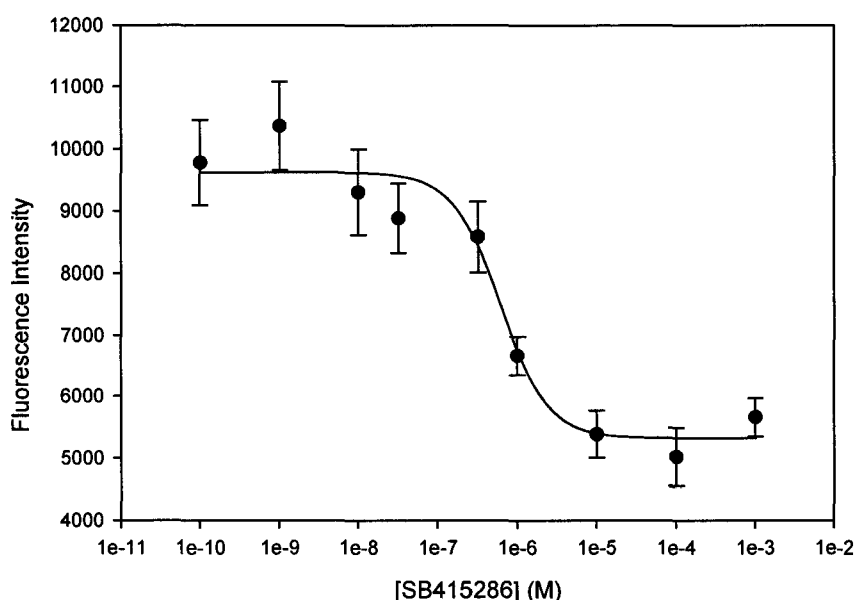


**Figure 2.6**  $IC_{50}$  curve of SB415286 using GSM/GSK3 $\beta$  assay. Assay was run with GSM and ATP at 50  $\mu$ M.

## 2.4 Conclusion

Our results demonstrate that sol-gel-derived microarrays are a promising solid phase platform for the detection of solution-based GSK-3 $\beta$  activity using Pro-Q<sup>®</sup> Diamond<sup>™</sup> phosphospecific stain. Sol-gel based microarrays provide a higher loading capacity and greater sensitivity than microarrays based on covalent immobilization of assay components. Additionally, the ability to discern primed substrates relative to

multiply phosphorylated products is easily achieved using sol-gel-derived microarrays. Using the microarray assay format, four substrates were examined and GSM peptide was identified as the optimal substrate for this assay. The suitability of this assay for an HTS environment was evaluated using a z' plot. The z' value found was ~0.5 indicating that the assay quality is acceptable for single point screening in an HTS environment. Using three GSK-3 $\beta$  inhibitors with varying modes of action, the potent ATP-competitive inhibitor, SB415286, was successfully identified using this assay. Inhibition of GSK-3 $\beta$  by SB415286 was further explored through the generation of an IC<sub>50</sub> curve, showing the ability of this assay to characterize inhibitor efficacy. Overall, the use of sol-gel-derived microarrays and Pro-Q<sup>®</sup> Diamond<sup>™</sup> phosphospecific stain to monitor kinase activity presents a very promising kinase assay format. This assay benefits from the ease of solution based assays and the use of an inexpensive end point detection reagent. Additionally, no modification to the kinase or substrate is required and both protein and peptide substrates can be employed, making this assay an appealing approach for almost any kinase/substrate pair.

## 2.5 References

1. Ahn, N.G.; Resing, K.A. Toward the phosphoproteome. *Nature Biotechnology*. **2001**, *19*, 317-318.
2. Van Ahsen, O.; Bomer, U. High-throughput screening for kinase inhibitors. *ChemBioChem*. **2005**, *6*, 481-490.
3. Diehl, J.A.; Cheng, M.; Roussel, M.F.; Sherr, C.J. Glycogen synthase kinase-3 $\beta$  regulates cyclin D1 proteolysis and subcellular localization. *Genes & Development*. **1998**, *12*, 3499-3511.
4. Watcharasit, P.; Bijur, G.N.; Dong, L.; Zhu, J.; Chen, X.; Jope, R.S. Glycogen synthase kinase-3 $\beta$  (GSK3 $\beta$ ) binds to and promotes the actions of p50\*. *Journal of Biological Chemistry*. **2003**, *278*, 48872-48879.
5. Pap, M.; Cooper, G.M. Glycogen synthase kinase-3 in the phosphatidylinositol 3-kinase/Akt cell survival pathway. *Journal of Biological Chemistry*. **1998**, *273*, 19929-19932.
6. Grimes, C.A.; Jope, R.S. The multifaceted roles of glycogen synthase kinase 3 $\beta$  in cellular signaling. *Progress in Neurobiology*. **2001**, *65*, 391-426.
7. Kozlovsky, N.; Belmaker, R.H.; Agam, G. GSK-3 and the neurodevelopmental hypothesis of schizophrenia. *European Neuropsychopharmacology*. **2002**, *12*, 13-25.
8. Murphy, E. Inhibit GSK-3 $\beta$  or there's heartbreak dead ahead. *Journal of Clinical Investigation*. **2004**, *113*, 1526-1528.
9. Eldar-Finkelman, H. Glycogen synthase kinase 3: an emerging therapeutic target. *Trends Molecular Medicine*. **2002**, *8*, 126-132.
10. Manoukian, A.S.; Woodgett, J.R. Role of glycogen synthase kinase-3 in cancer: regulation by Wnts and other signaling pathways. *Advances in Cancer Research*. **2002**, *84*, 203-229.
11. Avila, J.; Hernandez, F. GSK-3 inhibitors for Alzheimer's disease. *Expert Reviews in Neurotherapy*. **2007**, *11*, 1527-1533.
12. Hanger, D.P.; Hughes, K.; Woodgett, J.R.; Brion, J.P., Anderton, B.H. Glycogen synthase kinase-3 induces Alzheimer's disease-like phosphorylation of tau:

- generation of paired helical filament epitopes and neuronal localization of the kinase. *Neuroscience Letters*. **1992**, *147*, 58-62.
13. Takasimer, A.; Nogushi, K.; Sato, K.; Hosino, T.; Imahori, K. Tau protein kinase I is essential for amyloid beta-protein-induced neurotoxicity. *Proceedings of the National Academy of Science USA*. **1993**, *90*, 263-271.
  14. Park, Y.W.; Cummings, R.T; Wu, L.; Zheng, S.; Cameron, P.M.; Woods, A.; Zller, D.M.; Marcy, A.I.; Hermes, J.D. Homogeneous proximity tyrosine kinase assays: scintillation proximity assay versus homogeneous time-resolved fluorescence. *Analytical Biochemistry*. **1999**, *269*, 94-104.
  15. Fowler, A.; Swift, D.; Longman, E.; Acornley, A.; Hemsley, P.; Murray, D.; Unitt, J.; Dale, I.; Sullivan, E.; Coldwell, M. An evaluation of fluorescence polarization and lifetime discriminated polarization for high throughput screening of serine/threonine kinases. *Analytical Chemistry*. **2002**, *308*, 223-231.
  16. Turek-Etienne, T.C.; Lei, M.; Terracciano, J.S.; Langsdorf, E.F.; Bryant, R.W.; Hart, R.F.; Horan, A.C. Use of red-shifted dyes in a fluorescence polarization AKT kinase assay for detection of biological activity in natural product extracts. *Journal of Biomolecular Screening*. **2004**, *9*, 53-61.
  17. Li, Y.; Cummings, R.T.; Cunningham, B.R.; Chen, Y.; Zhou, G. Homogeneous assays for adenosine 5'-monophosphate-activated protein kinase. *Anal. Biochem*. **2003**, *321*, 151-156.
  18. Van Ahsen, O.; Bomer, U. High-Throughput Screening for kinase inhibitors. *ChemBioChem*. **2005**, *6*, 481-490.
  19. Fiol, C.J.; Mahrenholz, A.M.; Wang, Y.; Roeske, R.W.; Roach, P.J. Formation of protein kinase recognition sites by covalent modification of the substrate. *The Journal of Biological Chemistry*. **1987**, *262*, 14042-14048.
  20. Bowley, E.; Mulvihill, E.; Howard, J.C.; Pak, B.J.; Gsn, B.S.; O'Gorman, D.B. A novel mass spectrometry-based assay for GSK-3 $\beta$  activity. *BMC Biochemistry*. **2005**, *6*, 29-37.
  21. Partserniak, I.; Werstuck, G.; Capretta, A.; Brennan, J.D. An ESI-MS/MS method for screening of small-molecule mixtures against glycogen synthase kinase-3 $\beta$  (GSK-3 $\beta$ ). *ChemBioChem*. **2008**, *9*, 1065-1073.
  22. Matrin, K.; Steinberg, T.H.; Cooley, L.A.; Gee, K.R.; Beechem, J.M.; Patton, W.F. Quantitative analysis of protein phosphorylation status and protein kinase

- activity on microarrays using a novel fluorescent phosphorylation sensor dye. *Proteomics*. **2003**, *3*, 1244-1255.
23. Rupcich, N.; Green, J.R.A.; Brennan, J.D. Nanovolume kinase inhibition assay using a sol-gel-derived multicomponent microarray. *Analytical Chemistry*. **2005**, *77*, 8013-8019.
  24. Rupcich, N.; Goldstein, A.; Brennan, J.D. Optimization of sol-gel formulations and surface treatments for the development of pin-printed protein microarrays. *Chemistry of Materials*. **2003**, *15*, 1803-1811.
  25. Ikeda, S.; Kishida, S.; Yamamoto, H.; Murai, H.; Koyama, S.; Kikuchi, A. Axin, a negative regulator of the Wnt signaling pathway, forms a complex with GSK-3 $\beta$  and  $\beta$ -catenin and promotes GSK-3 $\beta$  dependent phosphorylation of  $\beta$ -catenin. *The EMBO Journal*. **1998**, *17*, 1371-1384.
  26. Song, J-S.; Yang, S-D. Tau protein kinase I/GSK-3 $\beta$ /kinase FA in heparin phosphorylates tau on Ser199, Thr231, Ser235, Ser262, Ser369, and Ser400 sites phosphorylated in Alzheimer disease brain. *Journal of Protein Chemistry*. **1995**, *14*, 95-105.
  27. Coghlan, M.P.; Culbert, A.A.; Cross, D.A.E.; Corcoran, S.L.; Yates, J.W.; Pearce, N.J.; Rausch, O.L.; Murphy, G.J.; Carter, P.S.; Cox, L.R.; Mills, D.; Brown, M.J.; Haigh, D.; Ward, R.W.; Smith, D.G.; Murray, K.J.; Reith, A.D.; Holder, J.C. Selective small molecule inhibitors of glycogen synthase kinase-3 modulate glycogen metabolism and gene transcription. *Chemistry and Biology*. **2000**, *7*, 793-803.
  28. Martinez, A.; Alonso, M.; Castro, A.; Perez, C.; Moreno, F.J. First non-ATP competitive glycogen synthase kinase 3  $\beta$  (GSK-3 $\beta$ ) inhibitors: thiadiazolidinones (TDZD) as potential drugs for the treatment of Alzheimer's disease. *Journal of Medicinal Chemistry*. **2002**, *45*, 1292-1299.
  29. Thomas, G. A GSK3-binding peptide from FRAT1 selectively inhibits the GSK3-catalyzed phosphorylation of axin and  $\beta$ -catenin. *FEBS Letters*. **1999**, *458*, 247-251.
  30. Assay Operation for SAR Support in Assay Guidance Manual Version 5.0. *Eli Lilly and Company and NIH Chemical Genomic Center*. **2008**.  
<<[www.ncgc.nih.gov/guidance/section3.html](http://www.ncgc.nih.gov/guidance/section3.html)>>.
  31. Doble, B.W.; Woodgett, J.R. GSK-3: tricks of the trade for a multi-tasking kinase. *Journal of Cell Science*. **2003**, *116*, 1175-1186.

32. Hagen, T.; Vida-Puig, A. Characterisation of the phosphorylation of  $\beta$ -catenin at the GSK-3 priming site Ser45. *Biochemical and Biophysical Research Communications*. **2002**, *294*, 324-328.
33. Ishiguro, K.; Takamatsu, K.; Tomizawa, K.; Omori, A.; Takahashi, M.; Arioka, M.; Uchida, T.; Imahori, K. Tau protein kinase I converts normal tau protein into A68-like component of paired helical filaments. *The Journal of Biological Chemistry*. **1992**, *267*, 10897-10901.
34. Wang, Q.M.; Roach, P.J.; Fiol, C.J. Use of a synthetic peptide as a selective substrate for glycogen synthase kinase 3. *Analytical Biochemistry*. **1994**, *220*, 397-402.
35. Ryves, W.J.; Fryer, L.; Dale, T.; Harwood, A.J. Assay for glycogen synthase kinase 3 (GSK-3) for use in crude cell extracts. *Analytical Biochemistry*. **1998**, *264*, 124-127.
36. Zhang, J-H.; Chung, T.D.Y.; Oldenburg, K.R. A simple statistical parameter for use in the evaluation and validation of high throughput screening assays. *Journal of Biomolecular Screening*. **1999**, *4*, 67-73.
37. Cheng, Y.; Prusoff, W.H. Relationship between the inhibition constant ( $K_1$ ) and the concentration of inhibitor which causes 50 per cent ( $I_{50}$ ) of an enzymatic reactions. *Biochemical Pharmacology*. **1973**, *22*, 3099-3108.

## **Chapter 3**

### **Materials Screen for Fabrication of Sol-Gel-Derived High-Density Kinase Microarrays**

As primary author, I was responsible for the experimental design, analysis, interpretation and presentation in Figures 3.1-3.6 and Supplementary Information. Jessamyn Little, a summer student under my direct supervision, assisted me with microarray fabrication for Figure 3.6. The experimental work of Dr. Xin Ge is presented in Figures 3.7 and 3.8. Dr. John Brennan provided editorial input to generate the final draft of the chapter.

## **Chapter 3: Materials Screen for Fabrication of Sol-Gel-Derived High-Density Kinase Microarrays**

### **Abstract**

Protein microarrays based on pin-printing of sol-gel entrapped biomolecules have emerged as a potential tool to accelerate drug screening and discovery. However, the ability to print high-density arrays of multiple proteins using this technology has yet to be demonstrated, primarily owing to difficulties associated with pin-printing of biocompatible sol-gel derived silica materials. In this study, we have performed a criteria-based directed screen of sol-gel based materials to identify compositions that are suitable for fabrication of high-density kinase microarrays. Materials were assessed for: 1) gelation time; 2) printability - the number of spots that could be printed and spot uniformity; and 3) adhesion to the slide surface; 4) resistance to cracking; and 5) compatibility with stain. Using an optimized buffer type, concentration and pH, variables examined were silica precursor and concentration, polymer additives and concentration, silane additives, small molecule additives and slide surface chemistry. Of the 69 sol-gel/surface combinations found to be compatible with high-density microarray fabrication, two materials were shown to retain activity of 3 of the 4 kinases studied in sol-gel-derived monoliths.

### 3.1 Introduction

The complex inter-play of phosphorylation and dephosphorylation events is involved in countless signaling pathways and cellular processes.<sup>1</sup> These phosphorylation events are performed by a class of proteins called kinases, which catalyze the transfer of a phosphate group from ATP to a substrate. While only a fraction of the 500 plus human protein kinases have been characterized,<sup>2</sup> research already has revealed that improper regulation of kinase activity is associated with numerous diseases such as cancer,<sup>3</sup> inflammation<sup>4</sup> and diabetes.<sup>5</sup> Consequently, kinases have become the second most targeted family of proteins for drug discovery, following G-protein coupled receptors (GPCRs).<sup>6</sup>

There exist a variety of homogenous assays for kinase activity that can be used in high-throughput screening for inhibitor identification.<sup>7</sup> However, recent requirements for increased assay throughput and decreased reagent volumes have led to the development of protein and peptide substrate microarrays for detection of kinase activity.<sup>8, 9</sup> Using peptide and protein microarrays, kinases can be rapidly characterized for their sequence recognition and activity.<sup>10, 11, 12, 13, 14, 15, 16</sup> While these arrays can quickly and efficiently assess the interactions between the kinase and each of the substrate microarray components, there are few reports of functional kinase microarrays, where the kinase is immobilized and can be used for nanovolume assays.<sup>17</sup>

An emerging functional protein array platform involves the pin-printing and immobilization of proteins onto a solid support using silica sol-gel entrapment (Figure 3.1).<sup>17</sup> Protein solutions are first mixed with silica-based sols, then pin-printed onto a

functionalized microscope slide, which is followed by gelation of the sol to entrap the protein in a spot that is on the order of 100  $\mu\text{m}$  in diameter. Advantages of this method include the applicability of sol-gel immobilization to a wide variety of proteins,<sup>18, 19, 20</sup> the ability to use native proteins and to tune the silica matrix with various precursors and additives to optimize the activity of that protein,<sup>21</sup> high protein loading,<sup>22</sup> and the ability to co-entrap multiple protein components in a single array element.<sup>17, 23, 24</sup> Our group has successfully demonstrated the use of this approach for monitoring kinase activity and inhibition with the co-entrapment of protein kinase A and its peptide substrate kemptide.<sup>17</sup> In this paper, a fluorescent phosphospecific stain, Pro-Q<sup>®</sup> Diamond<sup>™</sup> from Invitrogen,<sup>25</sup> was employed for end-point detection of degree of phosphorylation within each micro-assay.

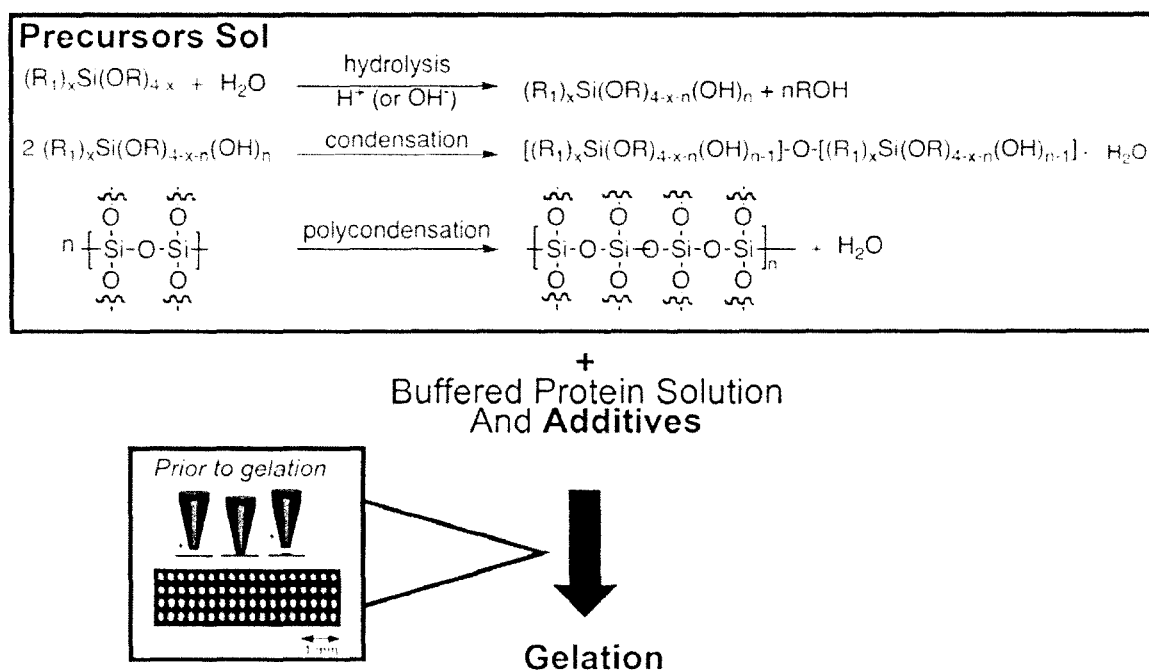


**Figure 3.1** General method for fabrication of sol-gel-derived protein microarrays.

While sol-gel based kinase arrays show promise for high-throughput screening to identify kinase inhibitors, there are significant issues that remain to be addressed regarding the material used to fabricate such arrays before these can be routinely and generically implemented. Firstly, the sol-gel composite material needs to have a long gelation time to allow for fabrication of high-density microarrays. Most materials used have relatively short gelation times (<30 min), which lead to non-uniform printing (since viscosity changes with time as the solution gels) and the potential for gelation in the spotting pin. Secondly, the material must have good adhesion to the substrate and should not crack when exposed to assay solutions. Thirdly, the material must be amenable to staining and destaining with phosphospecific dyes (such as Pro-Q<sup>®</sup> Diamond) as incompatibility with the stain, such as high non-specific binding, can lead to poor signal-to-background levels. Lastly, the material must be able to retain the activity of a range of kinases.

In order to meet the material requirements listed above for printing high-density sol-gel-derived functional protein microarrays, it is necessary to screen a range of sol-gel compositions and additives to identify optimal materials. There are numerous variables that can affect the materials properties, including buffer type, concentration and pH, the nature and concentration of silica precursors, presence of silane and/or polymer additives, slide surface chemistry, and small molecule additives. To assess these parameters, one can either perform a large-scale screen to assess all possible combinations or a smaller screen based on systematic hierarchical fulfilment of selected criteria. While there are advantages to screening a wide range of variables in a comprehensive manner – such as

the 100,000 composition screen performed by Kim *et al.* to identify optimal materials for protein-protein interactions on sol-gel-derived microarrays<sup>26</sup> – this approach is both time-consuming and costly. Instead, by using a small directed screen based on the systematic fulfilment of various criteria in a step-wise manner, the number of materials screened can be greatly reduced and should theoretically result in findings similar to an undirected approach (Figure 3.2).

To this end, we have screened materials based on two biocompatible silica precursors (diglycylsilane (DGS) or sodium silicate(SS)) at two concentrations, three polymer additives at two concentrations, six organosilane additives and five small molecule additives produced at a single buffer composition which was optimized to produce long gelation times and entrap protein at neutral pH, with all materials printed onto four slides with different surface chemistry. Materials were selected for further study and optimization based on: 1) gelation times; 2) the number of spots that could be printed; 3) spot uniformity; 4) adhesion to slide surface; 5) resistance to cracking; and 6) compatibility with the stain. Variables were screened in a hierarchical manner against criteria in the following order, i) silane precursor and concentration and polymer additive and concentration, ii) silane additives, and iii) small molecule additives. Compositions that passed the minimum material property requirements were then assayed for kinase activity against four kinase targets. This multi-step screening, involving primary screening of gel times, secondary screening of material properties in microarray format and tertiary screening for assay compatibility, allowed for rapid identification of materials that were suitable for fabrication of high-density microarrays, and demonstrates

that small, directed material screening studies have potential for efficient optimization of materials for specific applications.

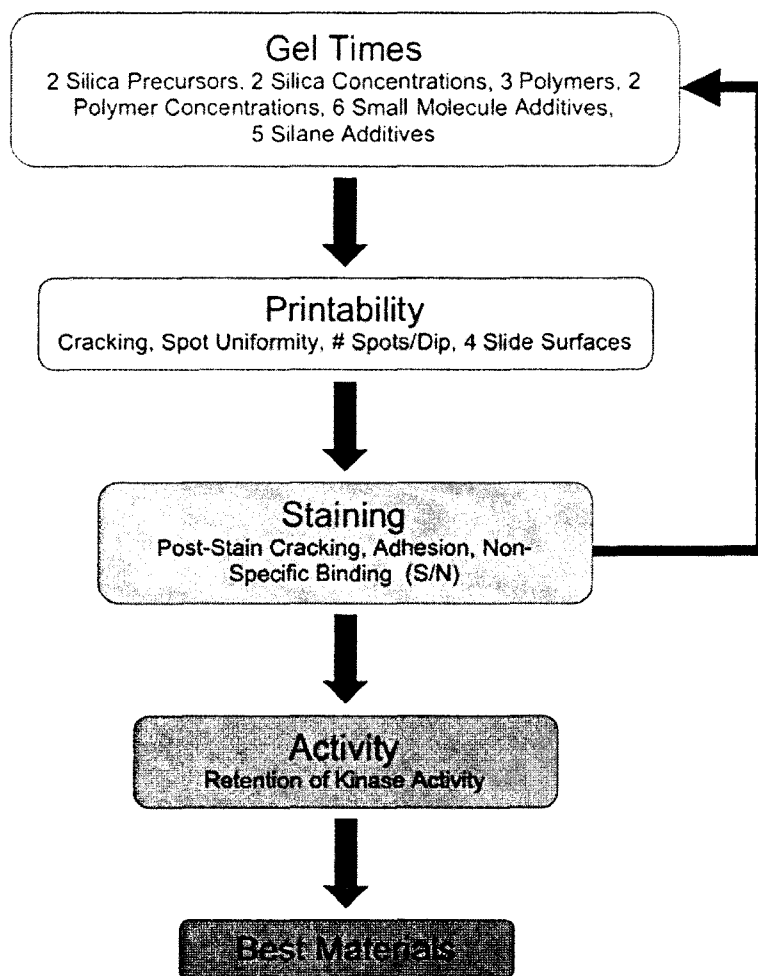


**Figure 3.2** Scheme of criteria-directed screen used to identify optimal materials for fabrication of high-density kinase microarrays.

## 3.2 Experimental

### 3.2.1 Chemicals.

Sodium silicate (27 wt% SiO<sub>2</sub>, 10 wt% NaOH) was purchased from Fisher (Ottawa, ON).

Diglycerylsilane (DGS) was prepared as described previously from

tetramethylorthosilicate (TMOS) (SigmaAldrich) and anhydrous glycerol (SigmaAldrich).<sup>27</sup> Bis[(3-methyldimethoxysilyl)propyl]-polypropylene oxide (Bis-PEG), N-(3-triethoxysilylpropyl) gluconamide (GLS), aminopropyl triethoxysilane (APTES), bis-(triethoxysilyl) ethane (Bis-TEOS), phenyldimethylsilane (PhDMS) and carboxyethyl silanetriol (Si-COOH) were purchased from Gelest (Morrisville, PA). Glycerol, sorbitol, trehalose, N $\epsilon$ -acetyl-lysine, Triton<sup>®</sup> X-100, magnesium chloride hexahydrate, manganese(II) chloride tetrahydrate, adenosine 5'-triphosphate disodium salt (ATP),  $\beta$ -nicotinamide adenine dinucleotide reduced dipotassium salt hydrate (NADH), phospho(enol)pyruvate monosodium salt (PEP), polyvinyl alcohol (PVA, MW=9000), polyethylene imine (PEI, MW=1300), polyethylene glycol (PEG, MW=600),  $\beta$ -casein, bovine serum albumin (BSA), pyruvate kinase from rabbit muscle (PK), D-lactatic dehydrogenase from *Lactobacillus leichmanii* (LDH), poly(Glu<sub>4</sub>Tyr) and Dowex 50x8-100 strongly acidic cation exchange resin, were obtained from Sigma-Aldrich (Oakville, ON). The kinases p38 $\alpha$ /SAPK2a (p38 $\alpha$ ), mitogen-activated protein kinase 2/Erk2 (MAPK2), epidermal growth factor receptor (EGFR), glycogen synthase kinase 3 $\beta$  (GSK-3 $\beta$ ), the substrate myelin basic protein (MBP, substrate for p38 $\alpha$  and MAPK2), and the general kinase inhibitor staurosporine were donated by Millipore (Billerica, MA). GSM (substrate for GSK-3 $\beta$ ) was purchased from Millipore. Pro-Q<sup>®</sup> Diamond<sup>™</sup> phosphospecific staining and destaining solutions were purchased from Invitrogen (Burlington, ON). SuperAldehyde<sup>®</sup>, SuperEpoxy<sup>®</sup> and SuperAmine<sup>®</sup> derivatized microscope slides were purchased from ArrayIt (Sunnyvale, CA). Poly(methyl methacrylate) (PMMA) slides were obtained from Exakt Technologies (Oklahoma City,

OK). Water was purified with Milli-Q Synthesis A10 water purification system. All other chemicals and solvents were of analytical grade and were used without further purification.

### 3.2.2 Procedures.

*Preparation of Materials for Screening:* Two biocompatible precursors (sodium silicate and DGS), 3 polymers (PEI, PEG, PVA), 6 silanes (GLS, MTMS, MDSPPPO, APTES and Si-COOH) and 8 additives (N $\epsilon$ -acetyl lysine, glycerol, sorbitol, trehalose, Triton<sup>®</sup> X-100) were chosen as material components to perform screening. Organosilanes were hydrolyzed by sonication in water for 20 min prior to addition to sol solutions. Additives were prepared as aqueous solutions and used directly for preparing spotting solutions. Silica precursor solutions containing sodium silicate and diglycerylsilane were prepared as described below.

Sodium silicate (SS) was prepared as follows: 2.59 g of sodium silicate was diluted with 10 ml of distilled, deionized water, and mixed with 5.5 g of Dowex strong acid cation-exchange resin. The mixture was immediately stirred for 1 min to lower the pH to a value of ~4.0. The mixture was filtered through Whatman #1 filter paper and then through a 0.2  $\mu$ m membrane syringe filter to remove any particulates. This sol (3SS) was used directly or diluted 1:1 (1.5SS) with ddH<sub>2</sub>O prior to use.

DGS sols were prepared by dissolving 0.5 g of DGS in 1 mL of ddH<sub>2</sub>O followed by sonication in ice water for 15 min to promote hydrolysis. The resulting sol was filtered through a 0.2  $\mu$ m membrane syringe filter to remove any particulates. The resulting sol

(0.5DGS) was used as is or diluted 1:1 (0.25DGS) with H<sub>2</sub>O to alter the water-to-silicon ratio in the final materials.

All sols were prepared by mixing the silane precursor solution with an equal volume of a buffered solution (Tris or HEPES buffer at 25 or 50 mM, pH 7.0 – 8.2) containing the organosilane, polymer and small molecule additives at 2x the final concentration of reagents desired in the final sol. The final pH was near neutral (6.8-7.2) in most cases, depending on the specific composition. The final composition formed is designated by the following nomenclature: using 0.25DGS/0.5PVA/GLS/Trehalose as an example, the first term denotes the silica precursor and concentration, the second term denotes the polymer additive and final concentration (% w/v), the remaining terms represent the silane additive and small molecule additive. Silanes were added to a final concentration of 1 % (w/v) and small molecules were added to 125 mM, except for glycerol at 2.5 % (v/v) and Triton<sup>®</sup> X-100 at 62.5 μM. All compositions were prepared to a final volume of 100 μL for gel time analysis and printing of microarrays.

*Gel Times:* All sol compositions were assessed for gel time prior to printing. In order to print high-density microarrays, it is necessary to have very long gelation times to ensure uniform spots and prevent gelation within the pin. The gel times of the 100 μL sol –gel formulations were determined by measuring the time between addition of the sol and when the monolith would no longer flow upon tilting the vial.

*Microarray Printing:* Only those compositions with gelation times >2.5 hours were examined for printability. The silica sol spotting solutions containing various additives were spotted using a Virtek Chipwriter Pro<sup>®</sup> contact pin-printer equipped with a

Telechem SMP3 stealth quill pin (250 nL uptake; 0.7 nL delivery; 200 spots/loading, 100  $\mu\text{m}$  spot diameter) (ArrayIt). Virtek Chipwriter Pro software was used to control all the parameters associated with microarraying, such as sample position, spot position and pattern, and inter-element spacing (usually set to 250  $\mu\text{m}$ ). Microspots were printed onto glass microscope slides modified with aldehyde, amine, or epoxy groups or plastic slides made of PMMA. Printing was done at room temperature ( $23 \pm 2$  °C) at ~80% relative humidity to slow evaporation of water from the spots. Completion of an array of 200 spots ( $20 \times 5$ ) took about 12 minutes to perform, including pin wash and dry cycles, when using a printhead speed of  $10 \text{ mm}\cdot\text{s}^{-1}$ .

*Optical Imaging of Microarrays:* Following printing, the arrays were aged for at least 24 hours prior to obtaining optical images of microarrays using an Olympus BX50 brightfield/fluorescence microscope equipped with mercury lamp and a Roper Scientific Coolsnap Fx CCD camera. At this stage, microarrays were assessed for the number of spots printed, spot uniformity, transparency, and cracking. Array were again optically imaged after staining with Pro-Q<sup>®</sup> Diamond<sup>™</sup> stain (see below) to examine for cracking and spot adhesion after the staining process.

*Staining Microarrays with Pro-Q<sup>®</sup> Diamond<sup>™</sup>:* Microarrays were stained for 45 minutes with Pro-Q<sup>®</sup> Diamond<sup>™</sup> stain by immersing the slide in the dye solution with gentle shaking. Excess dye was removed, then the slides were destained by incubating the slide in the commercial Pro-Q<sup>®</sup> Diamond<sup>™</sup> destaining solution twice for 10 minutes each. Slides were removed from the solution and spun dry using a micro-centrifuge (maximum speed ~6000 rpm) (Telechem).

*Fluorescence Imaging of Microarrays:* The stained slides were imaged using a ScanArray Express Microarray Scanner (Packard Biosciences) with laser excitation at 543nm, 90% laser power and 50% gain. The fluorescence intensities of the resulting images were quantified using Array Pro Analyzer (MediaCybernetics). Signal values were calculated by subtracting local background from each spot. In each case, the signal average of the replicates is reported with error bars representing 1 standard deviation.

*Kinase Activity in Monoliths.* Kinases (0.1  $\mu\text{g}$ ) and substrates were entrapped in the various sol-gel formulations to generate 50  $\mu\text{L}$  monoliths in UV-transparent,  $\frac{1}{2}$  area 96-well plates. The following kinase/substrate combinations were used: p38 $\alpha$ /MBP, MAPK2/MBP, EGFR/p(E<sub>4</sub>Y), and GSK-3 $\beta$ /GSM. MBP and p(E<sub>4</sub>Y) were entrapped at 0.25 mg/mL, GSM was entrapped at 25  $\mu\text{M}$ . For p38 $\alpha$ /MAPK2/GSK-3 $\beta$  monoliths, Mg<sup>2+</sup> was included in the formulation at a final concentration of 1 mM. For EGFR, Mn<sup>2+</sup> at 1 mM was included in the sol mixture. The monoliths were allowed to age overnight at 4 °C. To test the kinase for retention of activity, a NADH-coupled assay was used.<sup>28</sup> Above the monoliths, 50  $\mu\text{L}$  of the following solution was pipetted: 10 U/mL LDH, 5 U/mL PK, 2 mM PEP, 500  $\mu\text{M}$  NADH, 500  $\mu\text{M}$  ATP in 25 mM HEPES, pH 7.5 buffer. Absorbance at 340 nm was monitored for 1 hour on an Infinite<sup>®</sup> M1000 platereader (Tecan) with reads every 1 minute and shaking between each read. The temperature was maintained at 25 °C. Data was analyzed by comparing the slopes of the positive control (PC), containing active kinase and all necessary assay components, and negative control (NC), containing denatured kinase in place of the active kinase. Slopes were determined using the linear response region of the assay.

*Linear Response of Signal in 1.5SS/1PVA/Glycerol Microarrays.* Using the material 1.5SS/1PVA/Glycerol, a gradient (3.9  $\mu\text{g/mL}$  – 500  $\mu\text{g/mL}$ ) of  $\beta$ -Casein, a phosphoprotein with 5 phosphoserine residues, was printed onto a SuperAmine slide. The  $\beta$ -casein solutions were prepared at steps of 2-fold dilutions in 25 mM HEPES, pH 8.0. The microarray was then analyzed as described above.

*Functional Kinase Microarrays:* The 1.5SS/1PVA material printed on an amine-derivatized slide surface was selected for further studies involving kinase assays. Sols were prepared by adding components in the order of water, PVA, NaOH, Tris·HCL (25 mM), sodium silicate, substrates and enzymes to achieve a final pH of 7.0-7.5. For a typical reaction volume of 25  $\mu\text{L}$ , 1-2 U of kinases were added, and the final concentrations substrates were set as: were 27  $\mu\text{M}$  MBP; 5 mg/ml pE4Y; 37.5  $\mu\text{M}$  GSM. The arrays were printed using the following kinase/substrate combinations: p38 $\alpha$ //MBP; MAPK2/MBP; EGFR/poly(E4Y); GSK-3 $\beta$ /GSM. After aging for 30 minutes, printed microspots were then exposed to ATP and inhibitor solutions by over-printing using the array printer to place the solutions directly over individual array elements or over-spotting of larger volumes of solution over the entire array at once. Preliminary assays utilized concentrations of the ATP and inhibitor staurosporine of 100  $\mu\text{M}$  in 50 mM Tris·HCL, pH 7.5 containing 10 mM  $\text{MgCl}_2$ . For  $\text{IC}_{50}$  measurements, the concentrations of staurosporine were varied over the range of 1 nM to 100  $\mu\text{M}$  using 100 mM ATP. Assays were performed in the microarray chamber with ~80% relative humidity. Following the designated reaction period, usually 2 hours, the arrays were stained and destained and imaged as described above.

### 3.3 Results and Discussion

*Selection of Precursors, Silanes and Additives and Screening Approach.* There are essentially an endless number of combinations of silica precursors, additives and processing conditions that can be screened for their ability to fabricate high-density sol-gel derived kinase microarrays. Therefore, it was necessary to select a set of variables for consideration in the screen in order to minimize the number of possible formulations. To this end, we specifically selected two bio-friendly precursors, six organosilanes with varying polarity and functionality, three polymers with different functionality, and five small molecules that would either help stabilize the kinases or aid in pin-printing. This “directed” screening approach provided a more focused method with a relatively high chance for successful identification of useful compositions.

The selected silica precursors for this screen were DGS and SS. Both of these precursors have both been used for successful entrapment of sensitive proteins with retention of activity.<sup>17, 29</sup> Additionally these precursors can be processed under aqueous conditions with no evolution of alcohol, a known destabilizer of protein structure.<sup>30</sup> Six organosilanes were selected to alter the polarity and surface charge of the silica material. Among these were GLS, which has previously been shown to improve kinase activity,<sup>31</sup> and a bifunctional PEG-modified silane (Bis-PEG), which was selected to assess whether it was possible to modify the polarity without reducing crosslink density. Three polymers (PEG, PVA, PEI) with varying functionality were selected to alter sol viscosity, surface tension, silica porosity and protein stability. Five small molecules were also studied; four of which (glycerol,<sup>32</sup> sorbitol,<sup>33</sup> trehalose<sup>34</sup> and N $\epsilon$ -acetyl lysine) are known to be

stabilizing toward proteins, acting as osmolytes to control the degree of hydration and ultimately the thermal stability of entrapped proteins. The final small molecule, Triton<sup>®</sup> X-100, is a nonionic detergent that was included to modify surface tension and aid in printing. Finally, we examined four different slide surface chemistries, which were expected to influence adhesion and cracking of the array elements.

Together, screening for the optimal buffer composition (discussed below) and all precursor and additive variables, would lead to ~20,000 potential compositions for testing on each type of substrate surface if a non-directed screen were employed. However, by using a directed screen where variables are evaluated on the systematic hierarchical fulfilment of selected criteria, it is possible to assess the factors using a much smaller number of experiments (refer to Figure 3.2). Assessing each set of criteria in a step-wise fashion, many variables can be eliminated quickly and the materials showing promise are carried forward in the optimization process in a feedback loop approach.

*Gelation Time Studies.* Prior to screening the various additives, the buffer type, concentration and pH were optimized for long gelation times and entrapment at neutral pH. Two buffers, Tris-HCl and HEPES, were examined at 25 and 50 mM ionic strengths and pH levels of 7.0 – 8.2. It was found that 25 mM HEPES buffer at pH 8.0 satisfied the gelation requirement (>2.5 hours) when mixed 1:1 (v/v) with SS or DGS at the two silica concentrations screened and results in entrapment at neutral pH (6.8-7.2).

Using the optimal buffer composition, gelation times for all the compositions were assessed prior to printing onto the slide surfaces. At this stage, it was determined that compositions containing amines, PEI and APTES, resulted in rapid gelation. These

additives were therefore eliminated from further studies. Additionally, compositions prepared using the higher concentration of DGS (0.5 g/mL) also produced gelation times under 2.5 hours and thus were not carried forward on in the study. Several additives, Bis-PEG, Bis-TEOS and PhDMS, were also eliminated immediately due to insolubility or immiscibility issues. In total, 135 gelation times, representing 540 possible sol/slide surface formulations (135 x 4 slide surfaces), were measured. Of the 135 gelation times, 106 had sufficiently long gelation times (>2.5 hours) to assess for printability.

*Printability Studies.* Those materials with gel times greater than 2.5 hours were printed onto amine, aldehyde and epoxy-derivatized slides and PMMA slides. The microarrays were allowed to age at 4 °C for a minimum of 24 hours, then imaged by optical microscopy to assess for number of spots printed, cracking, uniformity, phase separation and spreading. Figure 3.3 shows examples of the failure modes observed for different materials (note that only a small portion of the full 4 x 50 array is shown).

At this stage of the screen, many materials were eliminated due to the various failure modes described. Of the 81 SS-based compositions screened, 28 were eliminated at this point with the most common failure modes being poor spot deposition and poor spot uniformity. SS-based materials containing high silica content (3SS) and GLS appeared to have a higher failure rate. This issue with materials of higher silica content is not surprising as the higher silica concentrations had shorter gelation times and thus are more likely to undergo greater viscosity changes during the printing process. The trend observed for SS compositions containing GLS was not expected, but may be due to interaction between GLS and the silica nanoparticles. Additionally all SS-based materials

containing  $N_\epsilon$ -acetyl lysine exhibited cracking, suggesting that this amino acid derivative compromised the materials resistance to hydration stress. DGS-based composition all had excellent printability except those printed onto the PMMA slides. Poor printability on PMMA was also observed for many SS-based materials and thus the PMMA slide was removed from consideration. No significant difference was observed between the derivatized glass slides at this stage. In total, 192 sol/slide surface formulations tested for printability and 155 were carried forward and tested for compatibility with the staining process.

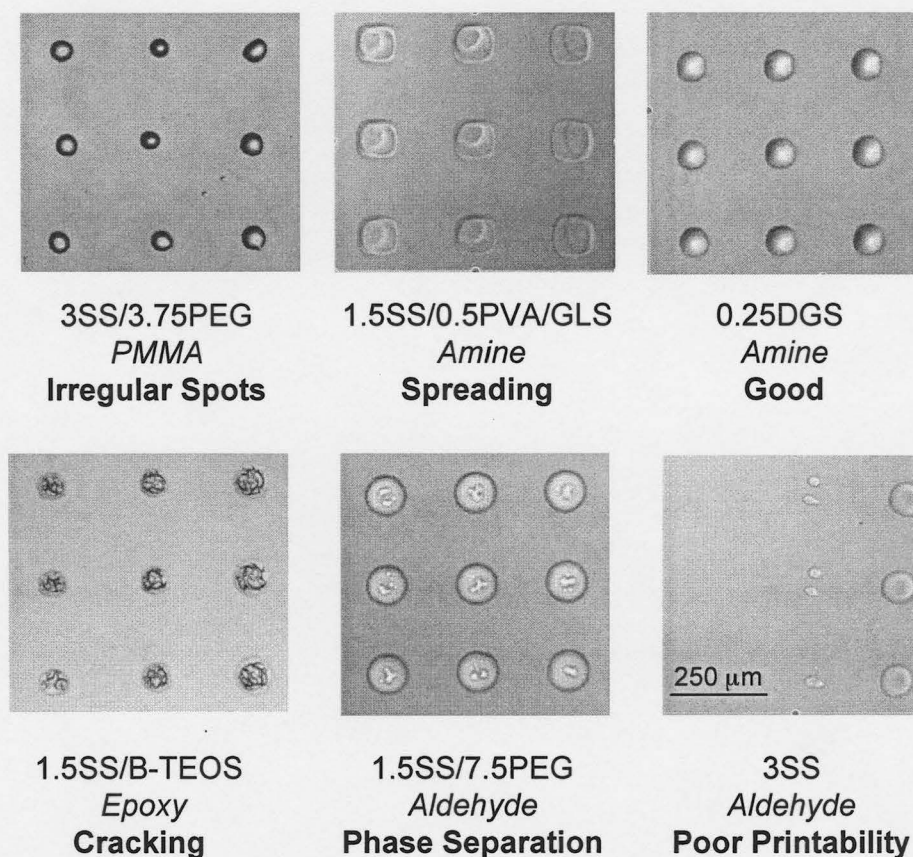


**Figure 3.3** Optical images of materials showing various failure modes of materials.

*Staining Compatibility Studies:* The 155 material /slide surface formulations that were found to be have acceptable printability were examined for compatibility with Pro-Q® Diamond™, a fluorescent phosphospecific stain. Two samples of each material were printed, one without protein and one with  $\beta$ -casein (0.125  $\mu\text{g/mL}$ ), a phosphoprotein containing 5 phosphoserine residues. Following staining, the S/B ratios between the two samples were evaluated to assess compatibility with the stain and non-specific binding of the dye to the material. Figure 3.4A shows an example of amine-derivatized slide that was analyzed, where 12,000 spots were printed consisting of positive and negative controls for 30 different sol materials with 200 spots/sample. Figure 3.4B shows examples of failure modes at this stage of the screening: low staining, high background, poor adhesion and cracking during the staining process. Post-staining cracking was a common problem in the materials screened, especially in DGS-based materials that included the silane additive GLS, where 15 of 36 materials containing GLS exhibited cracking. Cracking is a result of hydration stress, or pressure, on the material as water exits and enters the matrix.<sup>35</sup> If the material network is weaker than the hydration stress put on it, cracking will occur. PEG-modified materials were also observed to have post-staining cracking and/or poor S/N ratios and thus no materials containing PEG were carried forward. SS-derived materials containing both PVA and GLS also had a higher frequency of cracking (6 of 15 formulations). Adhesion issues were uncommon, however compositions containing silane Si-COOH exhibited poor adhesion, especially with the epoxy-derivatized slide surface. One of the trends identified for promising formulations was that the majority of the materials exhibiting both good printing and compatibility

with the staining contained PVA. In fact, 49 of the 69 optimal sol/slide surface compositions contained PVA at 0.5 or 1 % w/v. All three derivatized-glass surfaces were well represented in 69 materials.

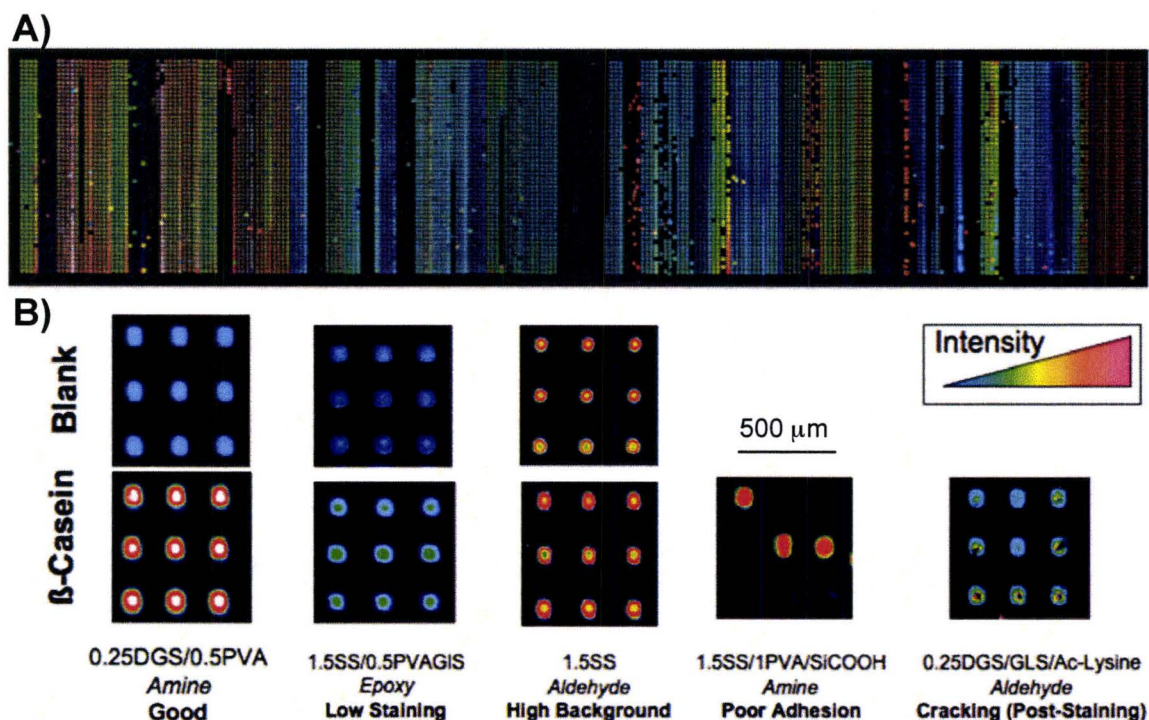


**Figure 3.4** A) Composite image of microarray consisting of 12,000 spots (60 samples x 200 spots/sample). B) Various modes of failure used to assess stain compatibility.

A summary of the total materials screened over the first three stages is provided in Figure 3.5. By using a directed criteria-based screen, the number of possible sol-gel compositions was rapidly decreased from ~20,000 for 4 different surfaces to 69 potential formulations, inclusive of slide surface. In total, 135 material gel times were analyzed representing 540 (135 x 4 slide surfaces) formulations. Of these, 192 sol/slide surface formulations were assessed for printability criteria, including number of spots printed per

dip, cracking, spot uniformity and spreading. At this stage, 37 materials were eliminated due to various printability issues and the remaining 155 were assessed for staining compatibility. Of the 155 materials screened, 86 did not exhibit the necessary material properties to be considered for kinase activity studies. Most frequently cracking due to the staining process was the failure mode. A table of results for all the materials and criteria screened is included as Supplementary Information.

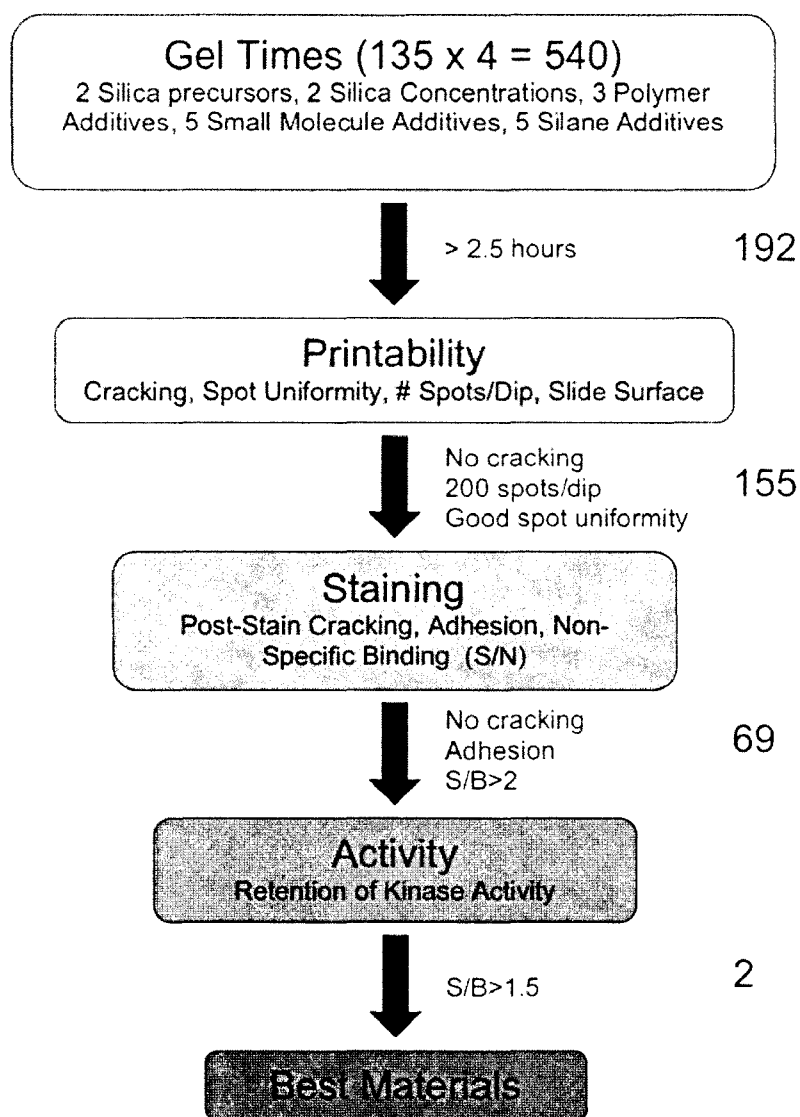


**Figure 3.5** Results of criteria-directed screen used to identify optimal materials for fabrication of high-density kinase microarrays.

*Kinase Activity in Monoliths.* Four kinases were studied for retention of activity in sol-gel materials: p38 $\alpha$ , MAPK2, EGFR and GSK-3 $\beta$ . These kinases were selected based on their therapeutic relevance: kinases p38 $\alpha$  and MAPK2 were chosen owing to their importance as targets for cancer therapy;<sup>36,37</sup> EGFR is a membrane-associated kinase that is over-expressed in tumor cells, and thus provides a useful demonstration of the extension of the microarray technology to membrane-associated kinases;<sup>38</sup> GSK-3 $\beta$  is an important target from treatment of several diseases, including Diabetes and Alzheimer's Disease.<sup>39</sup> Kinase activity was assessed in a selection of materials, which represented a range of the 69 final compositions, by entrapping the kinases in silica monoliths in a 96-well plate using the following kinase:substrate pairs, p38 $\alpha$ :MBP, MAPK2:MBP, EGFR:pE<sub>4</sub>Y, and GSK-3 $\beta$ :GSM. Monoliths were used to perform an initial kinase activity screen because this removed hydration issues that may be encountered during the printing process and also allowed for studying the materials left from printing. Kinases were assayed using a coupled NADH assay; absorbance at 340 nm was monitored over a 1-hour period in the plates and the rate of absorbance decrease was compared between the positive and negative controls (negative control contained denatured kinase) to determine those materials, which retained kinase activity. A summary of the materials screened and results is included in Table 3.1. No material was identified that retained the activity of all four kinases. However, several kinases seemed to retain activity in materials containing GLS, a trend previously observed for Src tyrosine kinase.<sup>31</sup> Additionally, two materials, 1.5SS/1PVA/Glycerol and 0.25DGS, were shown to retain

activity of three of the four kinases. The first material, 1.5SS/1PVA/Glycerol, was chosen for further investigation as it showed more promising kinase activity levels than 0.25DGS. The graph of absorbance at 340 nm over time for each of the kinases in 1.5SS/1PVA/Glycerol is included in the Supplementary Information (Figure 3.9).

**Table 3.1** Kinase activity retention in monoliths of various sol-gel materials. \* indicates a PC/NC ratio >1.5, \*\* indicates a PC/NC > 3.

Silica Precursor	[Silica]	Polymer	Silane	Small Molecule	p38 $\alpha$	MAPK2	EGFR	GSK-3B
SS	1.5	0.5PVA	GLS		**			
SS	1.5	0.5PVA	-	-			*	*
SS	1.5	1PVA	-	-				
SS	1.5	1PVA	-	Sorb				**
SS	1.5	1PVA	-	Glycerol	**		**	**
SS	1.5	1PVA	-	Triton				
SS	1.5	1PVA	GLS					
DGS	0.25	-	-	-	*	*		*
DGS	0.25	-	-	Sorb				
DGS	0.25	-	-	Ac-Lysine		*		
DGS	0.25	-	-	Glycerol				
DGS	0.25	-	-	Triton				
DGS	0.25	-	SiCOOH	-				
DGS	0.25	-	GLS	-	*	*		
DGS	0.25	-	GLS	Sorb		*		
DGS	0.25	1PVA	-	-				
DGS	0.25	1PVA	-	Sorb				
DGS	0.25	1PVA	-	Trehalose				
DGS	0.25	1PVA	-	Ac-Lysine				
DGS	0.25	1PVA	-	Glycerol				
DGS	0.25	1PVA	-	Triton				
DGS	0.25	-	GLS	Trehalose				
DGS	0.25	-	GLS	Ac-Lysine				*
DGS	0.25	-	GLS	Glycerol				
DGS	0.25	-	GLS	Triton	**			
DGS	0.25	0.5PVA	-	-				
DGS	0.25	0.5PVA	-	Sorb				
DGS	0.25	0.5PVA	-	Trehalose				
DGS	0.25	0.5PVA	-	Glycerol	*			

*Linear Response of Dye in 1.5SS/1PVA/Glycerol.* Prior to testing kinase activity on microarray, it was important to demonstrate the quantitative nature of this assay format. For this purpose, a  $\beta$ -casein gradient was prepared by printing varying concentrations of  $\beta$ -casein onto an amine-derivatized slide as an array using 1.5SS/1PVA/Glycerol (Figure

3.6). The fluorescence signal intensity from samples ranging from 3.9  $\mu\text{g/mL}$  to 500  $\mu\text{g/mL}$  were analyzed and the trend was shown to have excellent linearity ( $R^2 = 0.997$ ). While relatively large errors were observed for the highest concentrations, the errors associated with the lower, more biologically relevant, concentrations are much less significant.

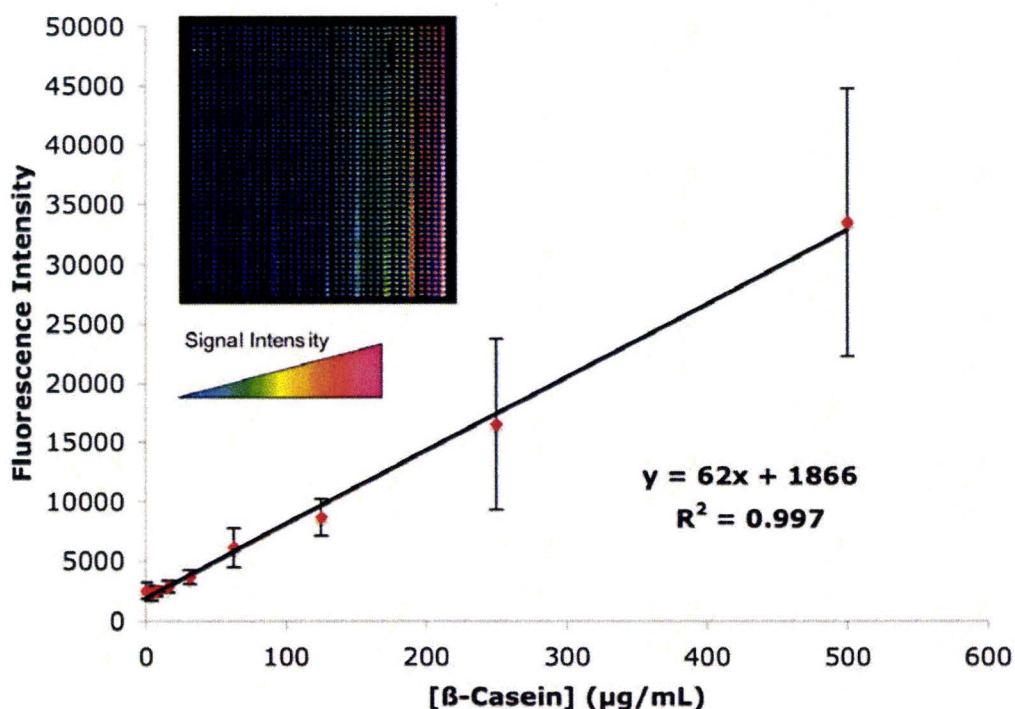


**Figure 3.6**  $\beta$ -Casein gradient (3.9 -500  $\mu\text{g/mL}$ ) printed in 1.5SS/1PVA/Glycerol on a SuperAmine slide. Microarray shows GSM gradient increasing from left to right. Each sample was printed in 200 (4 x 50) replicate spots.

*Functional Kinase Microarrays.* The kinases, GSK-3 $\beta$ , EGFR, MAPK2, p38 $\alpha$ , were entrapped with their respective substrates, GSM, pE<sub>4</sub>Y, and MBP, in 1.5SS/1PVA/Glycerol by printing the kinase:sol mixture onto an amine-derivatized slide. The microarray was aged overnight, after which ATP was spotted over top of the array

and allowed to incubate for 2.5 hours. While activity of the kinases on array could not be confirmed from the results, previous work by a member of our group demonstrated retention of kinase activity in a similar material, 1.5SS/1PVA prepared in Tris buffer and printed onto an amine-derivatized slide. The kinase:substrate pairs above were entrapped in the material and allowed to age 30 minutes, after which a 100  $\mu$ M ATP solution (in 50mM Tris-HCl and 10mM MgCl<sub>2</sub>) with and without 100  $\mu$ M staurosporine) was overprinted on the microarrays using the microarrayer (0.6 nL per assay), with one array element left untreated as a negative control. Reactions were run at 30 °C for 2 hours at 80% relative humidity followed by washing, staining and destaining. Figure 5A shows the scanned image of the resulting microarray while Figure 5B shows quantitative data of the signal-to-background ratios (S/B) for each array, where S/B is defined as the signal of the positive control (ATP reaction, middle row) to the negative control (no ATP present, top row). The results demonstrate that all four kinases remained active in the silica-based microarray (middle row) and that the kinases were all sensitive to the presence of the inhibitor staurosporine (bottom row). The S/B ratios for the four kinases were 4.5 (p38 $\alpha$ ), 3.7 (MAPK), 1.9 (EGFR) and 4.0 (GSK-3 $\beta$ ). The somewhat lower S/B for EGFR may reflect a decreased activity for the membrane-associated kinase relative to the soluble kinases.

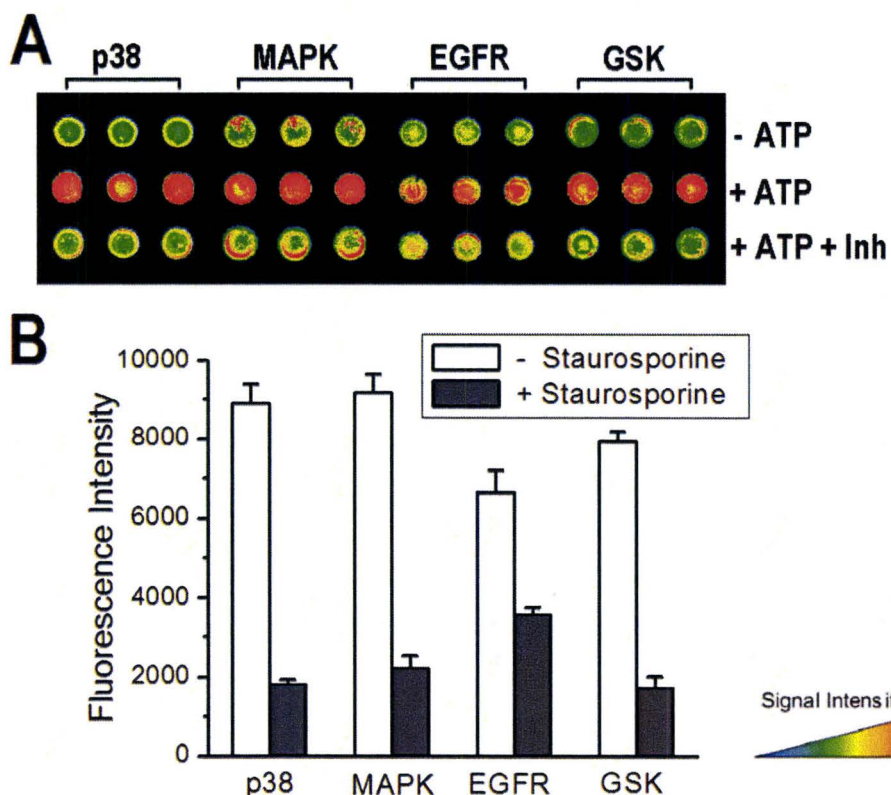


**Figure 3.7** Assays of 4 kinases preformed on a sol-gel based microarray in 1.5SS/1PVA printed on an amine-derivatized slide. (A) slide scanning image of the microarray. Mixtures of substrate/kinase were pin-printed, followed by overprinted with reaction buffer without ATP (negative control, top row), with ATP (middle row), with ATP containing the inhibitor staurosporine (bottom row); (B) Plot of signal intensity after subtracting the background signal of the negative control (2200 cps).

*IC<sub>50</sub> Measurements.* To assess the ability of the microarray to provide quantitative inhibition data, p38 $\alpha$  kinase was co-entrapped with MBP in 1.5SS/1PVA as the test system to evaluate the use of over-spotting of solution onto arrays for generating inhibition data. In this method, several identical microarrays were fabricated in different locations on the microscope slide and each sub-array was incubated with an ATP/inhibitor solution containing varying levels of inhibitor to generate a concentration dependent inhibition curve. This format is essential if the microarray technology is to be

integrated into a conventional high-throughput screening facility, where conventional liquid handling systems are designed to dispense microlitre volumes of reagents into microwell plates. For this assay, ATP concentration was held constant at 100 mM while staurosporine concentrations varied from 1 nM to 100  $\mu$ M. Images of arrays are shown in Figure 6A, while the  $IC_{50}$  curve generated from the array images is shown in Figure 6B. Analysis of the response indicated an  $IC_{50}$  value of 1.0  $\mu$ M. These results demonstrate that over-spotting of reagents onto microarrays can be used to provide data on inhibitor efficacy.

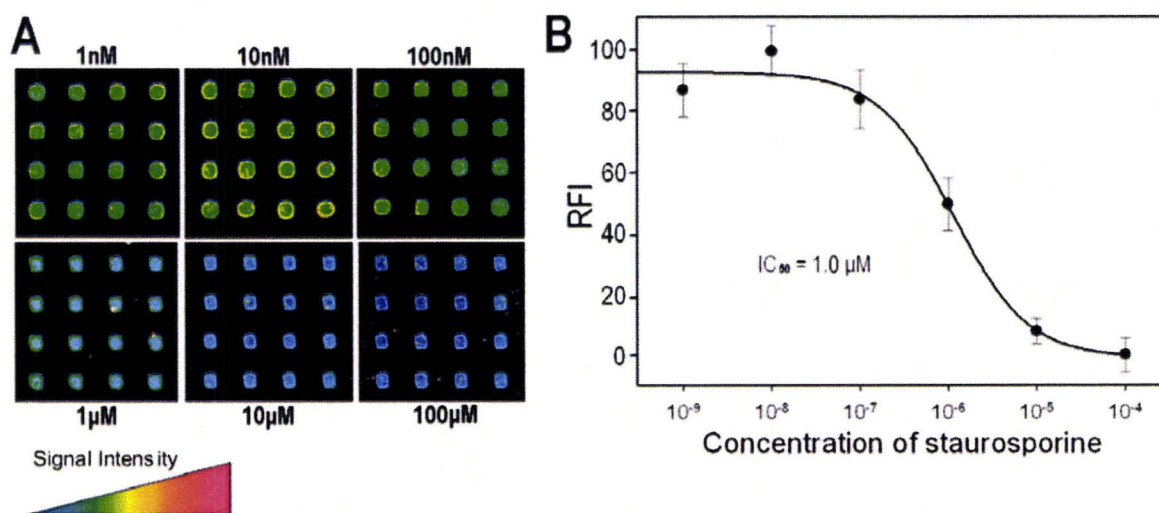


**Figure 3.8**  $IC_{50}$  assay performed on a p38a/MBP microarray over-spotted with several concentrations of staurosporine at a constant ATP concentration. (A) Images of arrays obtained by a single scan of the same slide; a composite image is shown for clarity. (B)  $IC_{50}$  curve generated from the array images. The intensity obtained at 100  $\mu$ M was subtracted from all images to produce a zero level; all other intensities were normalized by setting the intensity of the highest intensity image (10 nM) to a value of 100 % activity.

### 3.4 Conclusion

The present study has demonstrated the use of a directed screening methodology to identify sol-gel compositions that can be used for fabrication of high-density kinase microarrays. By assessing the variables in a stepwise fashion, the number of possible formulations requiring screening is drastically reduced from ~20,000 to 540. Sol-gel formulations were assessed for their ability to print high-density, robust microarrays by assessing criteria in the following order: i) gel time, ii) printability and iii) stain compatibility. Two silica precursors at two concentrations, three polymers at two concentrations, six silanes, five small molecules and four slide surface chemistries were screened against these criteria. In total, 69 formulations were identified for fabrication of high-density microarrays. By testing a selection of these materials for kinase activity in monoliths, two compositions were identified as potential formulations for the fabrication of high-density sol-gel-derived kinase microarrays.

### 3.5 References

1. Hunter, T. Protein kinases and phosphatases: the yin and yang of protein phosphorylation and signaling. *Cell*. **1995**, *80*, 225-236.
2. Manning, G.; Whyte, D.B.; Martinez, R.; Hunter, T.; Sudarsnam, S. 2002. The protein kinase complement of the human genome. *Science*. **298**: 1912-1934.
3. Dancey, J.; Sausville, E.A. Issues and progress with protein kinase inhibitors for cancer treatment. *Nature Reviews Drug Discovery*. **2003**, *2*, 296-313.
4. Kumar, S.; Boehm, J.; Lee, J.C. p38 MAP kinases: key signaling molecules as therapeutic targets for inflammatory diseases. *Nature Reviews Drug Discovery*. **2003**, *2*, 717-726.
5. Ishii, H.; Koya, D.; King, G.L. Protein kinase C activation and its role in the development of vascular complications in diabetes mellitus. *Journal of Molecular Medicine*. **1998**, *76*, 21-31.
6. Hopkins, A.L.; Groom, C.R. The druggable genome. *Nature Reviews Drug Discovery*. **2002**, *1*, 727-730.
7. Von Ahsen, O.; Bomer, U. High-throughput screening for kinase inhibitors. *ChemBioChem*. **2005**, *6*, 481-490.
8. Templin, M.F.; Stoll, D.; Schrenk, M.; Traub, P.C.; Vohringer, C.F.; Joos, T.O. Protein microarray technology. *Trends in Biotechnology*. **2002**, *20*, 160-166.
9. Johnson, S.A.; Hunter, T. Kinomics: methods for deciphering the kinome. *Nature Methods*. **2005**, *2*, 17-25.
10. Rychlewski, L.; Kschicho, M.; Dong, L.; Schutkowski, M.; Reimer, U. Target specificity analysis of the Abl kinase using peptide microarray data. *Journal Molecular Biology*. **2004**, *336*, 307-311.
11. Panse, S.; Dong, L.; Burian, A.; Carus, R.; Schutkowski, M.; Reimer, U.; Schneider-Mergener, J. Profiling of generic anti-phosphopeptide antibodies and kinases with peptide microarrays using radioactive and fluorescence-based assays. *Molecular Diversity*, **2004**, *8*, 291-299.
12. Zhu, H.; Klemic, J.F.; Chang, S.; Bertone, P.; Casamayor, A.; Klemic, K.G.; Smith, D.; Gerstein, M.; Reed, M.A.; Snyder, M. Analysis of yeast protein kinases using protein chips. *Nature Genetics*. **2000**, *26*, 283-289.

13. Reimer, U.; Schneider-Mergener, Peptide arrays: from macro to micro. *Current Opinion Biotechnology*. **2002**, *13*, 315-320.
14. Houseman, B.T.; Huh, J.H.; Kron, S.J.; Mrksich, M. Peptide chips for the quantitative evaluation of protein kinase activity. *Nature Biotechnology*. **2002**, *20*, 270-274.
15. Schutkowski, M.; Reimer, U.; Panse, S.; Dong, L.; Lizcano, J.M.; Alessi, D.R.; Schneider-Mergener, J. High-content peptide microarrays for deciphering kinase specificity and biology. *Angewandte Chemie International Edition*. **2004**, *43*, 2671–2674.
16. Min, D.H.; Su, J.; Mrksich, M. Profiling kinase activities by using a peptide chip and mass spectrometry. *Angewandte Chemie International Edition*. **2004**, *43*, 5973-5977.
17. Rupcich, N.; Green, J.R.A.; Brennan, J.D. Nanovolume kinase inhibition assay using a sol-gel-derived multicomponent microarray. *Analytical Chemistry*. **2005**, *77*, 8013-8019.
18. Jin, W.; Brennan, J.D. Properties and applications of proteins encapsulated within sol-gel-derived materials. *Analytical Chemistry*. **2001**, *461*, 1-36.
19. Pierre, A.C. The sol-gel encapsulation of enzymes. *Biocatalysis and Biotransformation*. **2004**, *22*, 145-170.
20. Avnir, D.; Coradin, T.; Livage, J. Recent bio-applications of sol-gel materials. *Journal of Materials Chemistry*. **2006**, *16*, 1013-1030.
21. Gill, I.; Ballesteros, A. Encapsulation of biologicals within silicate, siloxane, and hybrid sol-gel polymers: an efficient and generic approach. *Journal of the American Chemical Society*. **1998**, *120*, 8587-8598.
22. Rupcich, N.; Brennan, J.D. Optimization of sol-gel formulations and surface treatments for the development of pin-printed protein microarrays. *Chemistry of Materials*. **2003**, *15*, 1803-1811.
23. Rupcich, N.; Brennan, J.D. Coupled enzyme reaction microarrays based on pin-printing of sol-gel derived biomaterials. *Analytica Chimica Acta*. **2003**, *500*, 3–12

24. Lee, M-Y.; Park, C.B.; Dordick, J.S.; Clark, D.S. Metabolizing enzyme toxicology assay chip (MetaChip) for high-throughput microscale toxicity analyses. *Proceedings of the National Academy of Sciences*. **2005**, *102*, 983-987.
25. Pro-Q® Diamond phosphoprotein gel stain (P-33301). *Invitrogen*. <<www.invitrogen.com>>.
26. Kim, S.; Kim, Y.; Kin, P.; Ha, J.; Kim, K.; Sohn, M.; Yoo, J-S.; Lee, J.; Kwon, J-a.; Lee, K.N. Improved sensitivity and physical properties of sol-gel protein chips using large-scale material screening and selection. *Analytical Chemistry*. **2006**, *78*, 7392-7396.
27. Brook, M.A.; Chen, Y.; Guo, K.; Zhang, Z.; Brennan, J.D. Sugar-modified silanes: precursors for silica monoliths. *Journal of Materials Chemistry*. **2004**, *14*, 1469-1479.
28. Kiiianitsa, K.; Solinger, J.A.; Heyer, W-D. NADH-coupled microplate photometric assay for kinetics studies of AT-hydrolyzing enzymes with low and high specific activities. *Analytical Biochemistry*. **2003**, *321*, 266-271.
29. Besanger, T.R.; Easwaramoorthy, B.; Brennan, J.D. Entrapment of highly active membrane-bound receptors in macroporous sol-gel derived silica. *Analytical Chemistry*. **2004**, *76*, 6470-6475.
30. Herskovits, T.T.; Gadegbeku, B.; Jaillet, H. On the structural stability and solvent denaturation of proteins. I: Denaturation by the alcohols and glycols. *The Journal of Biological Chemistry*. **1970**, *245*, 2588-2598.
31. Cruz-Aguado, J.A.; Chen, Y.; Zhang, Z.; Brook, M.A.; Brennan, J.D. Entrapment of Src protein tyrosine kinase in sugar-modified silica. *Analytical Chemistry*. **2004**, *76*, 4182-4188.
32. Arakawa, T.; Timasheff, S.N. Stabilization of protein structure by sugars. *Biochemistry*. **1982**, *21*, 6536-6544.
33. Brennan, J.D; Benjamin, D.; DiBattistia, E.; Gulcev, M.D. Using sugar and amino acid additives to stabilize enzymes within sol-gel derived silica. *Chemistry of Materials*. **2003**, *15*, 737-745.
34. Xie, G.; Timasheff, S.N. The thermodynamic mechanism of protein stabilization by trehalose. *Biophysical Chemistry*. **1997**, *64*, 25-43.

35. Brinker, C.J.; Scherer, G.W. *Sol-Gel Science: The Physics and Chemistry of Sol-Gel Processing*. Academic Press, San Diego, CA. **1990**.
36. Olson, J.M.; Hallahan, A.R. p38 MAP kinase: a convergence point in cancer therapy. *Trends in Molecular Medicine*. **2004**, *10*, 125-129.
37. Sebolt-Leopold, J.S. Development of anticancer drugs targeting the MAP kinase pathway. *Oncogene*. **2000**, *19*, 6594-6599.
38. Mendelsohn, J.; Baselga, J. The EGF receptor family as targets for cancer therapy. *Oncogene*. **2000**, *19*, 6550-6565.
39. Cohen, P.; Frame, S. The renaissance of GSK3. *Nature Review Molecular Cell Biology*. **2001**, *2*, 769-776.

### 3.6 Supplementary Information

**Table 3.2** A summary of the sol-gel formulations screened and the results. \* indicates the criteria not met by the corresponding material. Formulations in red are those, which have passed all criteria for high-density microarray fabrication.

Silica Precursor	[Silica]	Buffer	[Buffer]	pH of Buffer	Final pH	Polymer	Silanes	Small Molecule	Surface	Gel Time	# of Spot	Uniformity	Adhesion	Cracking (Pre)	Cracking (Post)	S/N Ratio	Other
SS	3	Tris	100	7.5	6.0	-	-	-		*							
SS	3	HEPES	100	7.5	7.0	-	-	-									
SS	3	HEPES	50	7.5	6.2	-	-	-									
SS	3	HEPES	50	7.0	6.0	-	-	-									
SS	3	HEPES	50	7.2	6.2	-	-	-									
SS	3	HEPES	50	7.4	6.4	-	-	-									
SS	3	HEPES	50	7.6	6.6	-	-	-									
SS	3	HEPES	50	7.8	6.8	-	-	-									
SS	3	HEPES	50	8.0	7.0	-	-	-									
SS	3	HEPES	50	8.2	7.9	-	-	-									
SS	1.5	HEPES	50	7.0	6.2	-	-	-									
SS	1.5	HEPES	50	7.2	6.4	-	-	-									
SS	1.5	HEPES	50	7.4	6.5	-	-	-									
SS	1.5	HEPES	50	7.6	6.6	-	-	-									
SS	1.5	HEPES	50	7.8	6.8	-	-	-									
SS	1.5	HEPES	50	8.0	7.0	-	-	-									
SS	1.5	HEPES	50	8.2	7.2	-	-	-									
SS	3	HEPES	50	8.0	7.0	-	-	-	Amine		*						*
SS	3	HEPES	50	8.0	7.0	-	-	-	Aldehyde		*						*
SS	3	HEPES	50	8.0	7.0	-	-	-	Epoxy		*						*
SS	3	HEPES	50	8.0	7.0	-	-	-	PMMA		*	*					
SS	3	HEPES	50	8.0	7.0	0.5PVA			Amine								*
SS	3	HEPES	50	8.0	7.0	0.5PVA			Aldehyde								*
SS	3	HEPES	50	8.0	7.0	0.5PVA			Epoxy								*
SS	3	HEPES	50	8.0	7.0	0.5PVA			PMMA		*						
SS	3	HEPES	50	8.0	7.0	1PVA			Amine			*					
SS	3	HEPES	50	8.0	7.0	1PVA			Aldehyde								*
SS	3	HEPES	50	8.0	7.0	1PVA			Epoxy		*						*
SS	3	HEPES	50	8.0	7.0	1PVA			PMMA		*						
SS	3	HEPES	50	8.0	7.2	3.75PEG			Amine						*		
SS	3	HEPES	50	8.0	7.2	3.75PEG			Aldehyde						*		
SS	3	HEPES	50	8.0	7.2	3.75PEG			Epoxy				*		*		*
SS	3	HEPES	50	8.0	7.2	3.75PEG			PMMA			*					
SS	3	HEPES	50	8.0	7.2	7.5PEG			Amine						*		
SS	3	HEPES	50	8.0	7.2	7.5PEG			Aldehyde						*		*
SS	3	HEPES	50	8.0	7.2	7.5PEG			Epoxy				*		*		*
SS	3	HEPES	50	8.0	7.2	7.5PEG			PMMA			*					
SS	3	HEPES	50	8.0	7.6	0.5PEI				*							
SS	3	HEPES	50	8.0	>8	1PEI				*							
SS	1.5	HEPES	50	8.0	7.0	-	-	-	Amine								*
SS	1.5	HEPES	50	8.0	7.0	-	-	-	Aldehyde								*
SS	1.5	HEPES	50	8.0	7.0	-	-	-	Epoxy				*				*
SS	1.5	HEPES	50	8.0	7.0	-	-	-	PMMA			*					
SS	1.5	HEPES	50	8.0	8.0	-	SI-COOH		Amine				*	*			
SS	1.5	HEPES	50	8.0	8.0	-	SI-COOH		Aldehyde				*	*			
SS	1.5	HEPES	50	8.0	8.0	-	SI-COOH		Epoxy			*		*			*
SS	1.5	HEPES	50	8.0	7.0	-	GLS		Amine								*
SS	1.5	HEPES	50	8.0	7.0	-	GLS		Aldehyde								*
SS	1.5	HEPES	50	8.0	7.0	-	GLS		Epoxy								*

continued . . .

Table 3.2 continued.

Silica Precursor	[Silica]	Buffer	[Buffer]	pH of Buffer	Final pH	Polymer	Silanes	Small Molecule	Surface	Gel Time	# of Spot	Uniformity	Adhesion	Cracking (Pre)	Cracking (Post)	S/N Ratio	Other
SS	1.5	HEPES	50	8.0	7	-	Bis-TEOS										*
SS	1.5	HEPES	50	8.0	>8	-	APTES			*							
SS	1.5	HEPES	50	8.0	7	-	PhDMS										*
SS	1.5	HEPES	50	8.0	7.0	0.5PVA			Amine								
SS	1.5	HEPES	50	8.0	7.0	0.5PVA			Aldehyde							*	*
SS	1.5	HEPES	50	8.0	7.0	0.5PVA			Epoxy								
SS	1.5	HEPES	50	8.0	7.0	0.5PVA			PMMA			*					*
SS	1.5	HEPES	50	8.0	8.0	0.5PVA	Si-COOH		Amine				*				*
SS	1.5	HEPES	50	8.0	8.0	0.5PVA	Si-COOH		Epoxy				*				*
SS	1.5	HEPES	50	8.0	7.0	0.5PVA	GLS		Amine								
SS	1.5	HEPES	50	8.0	7.0	0.5PVA	GLS		Epoxy								*
SS	1.5	HEPES	50	8.0	7	0.5PVA	GLS	Sorb	Amine			*			*		*
SS	1.5	HEPES	50	8.0	7	0.5PVA	GLS	Trehalose	Amine			*			*		*
SS	1.5	HEPES	50	8.0	7	0.5PVA	GLS	Ac-Lysine	Amine			*		*	*	*	*
SS	1.5	HEPES	50	8.0	7	0.5PVA	GLS	Glycerol	Amine						*		*
SS	1.5	HEPES	50	8.0	7	0.5PVA	GLS	Triton	Amine			*					*
SS	1.5	HEPES	50	8.0	7	0.5PVA	Bis-TEOS										*
SS	1.5	HEPES	50	8.0	>8	0.5PVA	APTES			*							
SS	1.5	HEPES	50	8.0	7	0.5PVA	PhDMS										*
SS	1.5	HEPES	50	8.0	7.0	1PVA			Amine								
SS	1.5	HEPES	50	8.0	7.0	1PVA			Aldehyde								
SS	1.5	HEPES	50	8.0	7.0	1PVA			Epoxy								
SS	1.5	HEPES	50	8.0	7.0	1PVA			PMMA		*	*					
SS	1.5	HEPES	50	8.0	7	1PVA	-	Sorb	Amine								
SS	1.5	HEPES	50	8.0	7	1PVA	-	Sorb	Aldehyde								
SS	1.5	HEPES	50	8.0	7	1PVA	-	Sorb	Epoxy							*	
SS	1.5	HEPES	50	8.0	7	1PVA	-	Trehalose	Amine								*
SS	1.5	HEPES	50	8.0	7	1PVA	-	Trehalose	Aldehyde								*
SS	1.5	HEPES	50	8.0	7	1PVA	-	Trehalose	Epoxy							*	*
SS	1.5	HEPES	50	8.0	7	1PVA	-	Ac-Lysine	Amine			*		*			*
SS	1.5	HEPES	50	8.0	7	1PVA	-	Ac-Lysine	Aldehyde				*	*			*
SS	1.5	HEPES	50	8.0	7	1PVA	-	Ac-Lysine	Epoxy				*	*			*
SS	1.5	HEPES	50	8.0	7	1PVA	-	Glycerol	Amine								
SS	1.5	HEPES	50	8.0	7	1PVA	-	Glycerol	Aldehyde								
SS	1.5	HEPES	50	8.0	7	1PVA	-	Glycerol	Epoxy								
SS	1.5	HEPES	50	8.0	7	1PVA	-	Triton	Amine								
SS	1.5	HEPES	50	8.0	7	1PVA	-	Triton	Aldehyde								
SS	1.5	HEPES	50	8.0	7	1PVA	-	Triton	Epoxy								
SS	1.5	HEPES	50	8.0	8.0	1PVA	Si-COOH		Amine				*				*
SS	1.5	HEPES	50	8.0	8.0	1PVA	Si-COOH		Aldehyde				*				*
SS	1.5	HEPES	50	8.0	8.0	1PVA	Si-COOH		Epoxy				*				*
SS	1.5	HEPES	50	8.0	7.0	1PVA	GLS		Amine								
SS	1.5	HEPES	50	8.0	7.0	1PVA	GLS		Aldehyde			*					*
SS	1.5	HEPES	50	8.0	7.0	1PVA	GLS		Epoxy								*
SS	1.5	HEPES	50	8.0	7	1PVA	GLS	Sorb	Amine								*
SS	1.5	HEPES	50	8.0	7	1PVA	GLS	Tre	Amine								*
SS	1.5	HEPES	50	8.0	7	1PVA	GLS	Ac-Lysine	Amine			*		*			*
SS	1.5	HEPES	50	8.0	7	1PVA	GLS	Glycerol	Amine				*		*		*
SS	1.5	HEPES	50	8.0	7	1PVA	GLS	Triton	Amine								*

continued ...

Table 3.2 continued

Silica Precursor	[Silica]	Buffer	[Buffer]	pH of Buffer	Final pH	Polymer	Silanes	Small Molecule	Surface	Gel Time	# of Spot	Uniformity	Adhesion	Cracking (Pre)	Cracking (Post)	S/N Ratio	Other
SS	1.5	HEPES	50	8.0	7	1PVA	Bis-TEOS										*
SS	1.5	HEPES	50	8.0	>8	1PVA	APTES			*							
SS	1.5	HEPES	50	8.0	7	1PVA	PhDMS										*
SS	1.5	HEPES	50	8.0	7.2	3.75PEG			Amine						*		
SS	1.5	HEPES	50	8.0	7.2	3.75PEG			Aldehyde							*	
SS	1.5	HEPES	50	8.0	7.2	3.75PEG			Epoxy						*		
SS	1.5	HEPES	50	8.0	7.2	3.75PEG			PMMA		*						*
SS	1.5	HEPES	50	8.0	7.2	7.5PEG			Amine						*	*	
SS	1.5	HEPES	50	8.0	7.2	7.5PEG			Aldehyde						*	*	
SS	1.5	HEPES	50	8.0	7.2	7.5PEG			Epoxy						*	*	*
SS	1.5	HEPES	50	8.0	7.2	7.5PEG			PMMA			*					*
SS	1.5	HEPES	50	8.0	7.6	0.5PEI				*							
SS	1.5	HEPES	50	8.0	>8	1PEI				*							
DGS	0.5	Tris	100	7.5	6.2	-	-	-			*						
DGS	0.5	HEPES	100	7.5	6.6	-	-	-			*						
DGS	0.5	HEPES	50	7.5	6.4	-	-	-			*						
DGS	0.5	HEPES	50	7.0	6	-	-	-			*						
DGS	0.5	HEPES	50	7.2	6	-	-	-			*						
DGS	0.5	HEPES	50	7.4	6.2	-	-	-			*						
DGS	0.5	HEPES	50	7.6	6.2	-	-	-			*						
DGS	0.5	HEPES	50	7.8	6.4	-	-	-			*						
DGS	0.5	HEPES	50	8.0	6.6	-	-	-			*						
DGS	0.5	HEPES	50	8.2	6.6	-	-	-			*						
DGS	0.5	HEPES	50	8.2	6.6	0.5PVA	-	-		*							
DGS	0.5	HEPES	50	8.2	6.6	1PVA	-	-		*							
DGS	0.5	HEPES	50	8.2	6.8	3.75PEG	-	-		*							
DGS	0.5	HEPES	50	8.2	6.8	7.5PEG	-	-		*							
DGS	0.5	HEPES	50	8.2	7.4	0.5PEI	-	-		*							
DGS	0.5	HEPES	50	8.2	7.6	1PEI	-	-		*							
DGS	0.25	HEPES	50	7.0	6.1	-	-	-									
DGS	0.25	HEPES	50	7.2	6.2	-	-	-									
DGS	0.25	HEPES	50	7.4	6.4	-	-	-									
DGS	0.25	HEPES	50	7.6	6.5	-	-	-									
DGS	0.25	HEPES	50	7.8	6.6	-	-	-									
DGS	0.25	HEPES	50	8.0	6.8	-	-	-									
DGS	0.25	HEPES	50	8.2	6.8	-	-	-									
DGS	0.25	HEPES	50	8.0	6.8	-	-	-	Amine								
DGS	0.25	HEPES	50	8.0	6.8	-	-	-	Aldehyde								
DGS	0.25	HEPES	50	8.0	6.8	-	-	-	Epoxy								
DGS	0.25	HEPES	50	8.0	6.8	-	-	-	PMMA		*						
DGS	0.25	HEPES	50	8.0	6.8	-	-	-	Sorb								
DGS	0.25	HEPES	50	8.0	6.8	-	-	-	Aldehyde							*	
DGS	0.25	HEPES	50	8.0	6.8	-	-	-	Sorb								
DGS	0.25	HEPES	50	8.0	6.8	-	-	-	Epoxy								
DGS	0.25	HEPES	50	8.0	6.8	-	-	-	Trehalose							*	*
DGS	0.25	HEPES	50	8.0	6.8	-	-	-	Aldehyde						*	*	*
DGS	0.25	HEPES	50	8.0	6.8	-	-	-	Trehalose						*	*	*
DGS	0.25	HEPES	50	8.0	6.8	-	-	-	Epoxy								
DGS	0.25	HEPES	50	8.0	6.8	-	-	-	Ac-Lysine								
DGS	0.25	HEPES	50	8.0	6.8	-	-	-	Aldehyde						*	*	
DGS	0.25	HEPES	50	8.0	6.8	-	-	-	Epoxy						*	*	

continued . . .

Table 3.2 continued

Silica Precursor	[Silica]	Buffer	[Buffer]	pH of Buffer	Final pH	Polymer	Silanes	Small Molecule	Surface	Gel Time	# of Spot	Uniformity	Adhesion	Cracking (Pre)	Cracking (Post)	S/N Ratio	Other
DGS	0.25	HEPES	50	8.0	6.8	-	-	Glycerol	Amine						*		
DGS	0.25	HEPES	50	8.0	6.8	-	-	Glycerol	Aldehyde								
DGS	0.25	HEPES	50	8.0	6.8	-	-	Glycerol	Epoxy							*	
DGS	0.25	HEPES	50	8.0	6.8	-	-	Triton	Amine								*
DGS	0.25	HEPES	50	8.0	6.8	-	-	Triton	Aldehyde							*	
DGS	0.25	HEPES	50	8.0	6.8	-	-	Triton	Epoxy							*	
DGS	0.25	HEPES	50	8.0	8.0	-	Si-COOH		Amine								
DGS	0.25	HEPES	50	8.0	8.0	-	Si-COOH		Aldehyde				*				
DGS	0.25	HEPES	50	8.0	8.0	-	Si-COOH		Epoxy				*				
DGS	0.25	HEPES	50	8.0	8.0	-	SiCOOH	Sorb	Amine				*				
DGS	0.25	HEPES	50	8.0	8.0	-	SiCOOH	Trehalose	Amine				*				
DGS	0.25	HEPES	50	8.0	8.0	-	SiCOOH	Ac-Lysine	Amine							*	
DGS	0.25	HEPES	50	8.0	8.0	-	SiCOOH	Glycerol	Amine				*				
DGS	0.25	HEPES	50	8.0	8.0	-	SiCOOH	Triton	Amine							*	
DGS	0.25	HEPES	50	8.0	6.8	-	GLS		Amine								
DGS	0.25	HEPES	50	8.0	6.8	-	GLS		Aldehyde								
DGS	0.25	HEPES	50	8.0	6.8	-	GLS		Epoxy								
DGS	0.25	HEPES	50	8.0	6.8	-	GLS	Sorb	Amine								
DGS	0.25	HEPES	50	8.0	6.8	-	GLS	Sorb	Aldehyde						*		
DGS	0.25	HEPES	50	8.0	6.8	-	GLS	Sorb	Epoxy								
DGS	0.25	HEPES	50	8.0	6.8	-	GLS	Trehalose	Amine								
DGS	0.25	HEPES	50	8.0	6.8	-	GLS	Trehalose	Aldehyde						*		
DGS	0.25	HEPES	50	8.0	6.8	-	GLS	Trehalose	Epoxy								
DGS	0.25	HEPES	50	8.0	6.8	-	GLS	Ac-Lysine	Amine								
DGS	0.25	HEPES	50	8.0	6.8	-	GLS	Ac-Lysine	Aldehyde						*		
DGS	0.25	HEPES	50	8.0	6.8	-	GLS	Ac-Lysine	Epoxy						*		
DGS	0.25	HEPES	50	8.0	6.8	-	GLS	Glycerol	Amine								
DGS	0.25	HEPES	50	8.0	6.8	-	GLS	Glycerol	Aldehyde						*		
DGS	0.25	HEPES	50	8.0	6.8	-	GLS	Glycerol	Epoxy						*		
DGS	0.25	HEPES	50	8.0	6.8	-	GLS	Triton	Amine						*		
DGS	0.25	HEPES	50	8.0	6.8	-	GLS	Triton	Aldehyde						*		
DGS	0.25	HEPES	50	8.0	6.8	-	GLS	Triton	Epoxy								
SS	1.5	HEPES	50	8.0	6.8		Bis-TEOS										*
SS	1.5	HEPES	50	8.0	>8		APTES			*							
SS	1.5	HEPES	50	8.0	6.8		PhDMS										*
DGS	0.25	HEPES	50	8.0	6.8	0.5PVA	-	-	Amine						*		
DGS	0.25	HEPES	50	8.0	6.8	0.5PVA	-	-	Aldehyde								
DGS	0.25	HEPES	50	8.0	6.8	0.5PVA	-	-	Epoxy								
DGS	0.25	HEPES	50	8.0	6.8	0.5PVA	-	-	PMMA		*						
DGS	0.25	HEPES	50	8.0	6.8	0.5PVA	-	Sorb	Aldehyde								
DGS	0.25	HEPES	50	8.0	6.8	0.5PVA	-	Sorb	Epoxy						*		
DGS	0.25	HEPES	50	8.0	6.8	0.5PVA	-	Trehalose	Aldehyde								
DGS	0.25	HEPES	50	8.0	6.8	0.5PVA	-	Trehalose	Epoxy						*	*	
DGS	0.25	HEPES	50	8.0	6.8	0.5PVA	-	Ac-Lysine	Aldehyde							*	
DGS	0.25	HEPES	50	8.0	6.8	0.5PVA	-	Ac-Lysine	Epoxy							*	
DGS	0.25	HEPES	50	8.0	6.8	0.5PVA	-	Glycerol	Aldehyde								
DGS	0.25	HEPES	50	8.0	6.8	0.5PVA	-	Glycerol	Epoxy							*	
DGS	0.25	HEPES	50	8.0	6.8	0.5PVA	-	Triton	Aldehyde						*		
DGS	0.25	HEPES	50	8.0	6.8	0.5PVA	-	Triton	Epoxy								

continued . . .

Table 3.2 continued

Silica Precursor	[Silica]	Buffer	[Buffer]	pH of Buffer	Final pH	Polymer	Silanes	Small Molecule	Surface	Get Time	# of Spot	Uniformity	Adhesion	Cracking (Pre)	Cracking (Post)	S/N Ratio	Other
DGS	0.25	HEPES	50	8.0	8.0	0.5PVA	Si-COOH		Aldehyde							*	
DGS	0.25	HEPES	50	8.0	8.0	0.5PVA	Si-COOH		Epoxy				*			*	
DGS	0.25	HEPES	50	8.0	6.8	0.5PVA	GLS		Aldehyde						*		
DGS	0.25	HEPES	50	8.0	6.8	0.5PVA	GLS		Epoxy						*		
SS	1.5	HEPES	50	8.0	6.8	0.5PVA	Bis-TEOS										*
SS	1.5	HEPES	50	8.0	>8	0.5PVA	APTES			*							
SS	1.5	HEPES	50	8.0	6.8	0.5PVA	PhDMS										*
DGS	0.25	HEPES	50	8.0	6.8	1PVA	-	-	Amine								
DGS	0.25	HEPES	50	8.0	6.8	1PVA	-	-	Aldehyde								
DGS	0.25	HEPES	50	8.0	6.8	1PVA	-	-	Epoxy								
DGS	0.25	HEPES	50	8.0	6.8	1PVA	-	-	PMMA		*					*	
DGS	0.25	HEPES	50	8.0	6.8	1PVA	-	Sorb	Amine								
DGS	0.25	HEPES	50	8.0	6.8	1PVA	-	Sorb	Aldehyde								
DGS	0.25	HEPES	50	8.0	6.8	1PVA	-	Sorb	Epoxy								
DGS	0.25	HEPES	50	8.0	6.8	1PVA	-	Trehalose	Amine								
DGS	0.25	HEPES	50	8.0	6.8	1PVA	-	Trehalose	Aldehyde								
DGS	0.25	HEPES	50	8.0	6.8	1PVA	-	Trehalose	Epoxy								
DGS	0.25	HEPES	50	8.0	6.8	1PVA	-	Ac-Lysine	Amine								
DGS	0.25	HEPES	50	8.0	6.8	1PVA	-	Ac-Lysine	Aldehyde								
DGS	0.25	HEPES	50	8.0	6.8	1PVA	-	Ac-Lysine	Epoxy								
DGS	0.25	HEPES	50	8.0	6.8	1PVA	-	Glycerol	Amine								
DGS	0.25	HEPES	50	8.0	6.8	1PVA	-	Glycerol	Aldehyde								
DGS	0.25	HEPES	50	8.0	6.8	1PVA	-	Glycerol	Epoxy								
DGS	0.25	HEPES	50	8.0	6.8	1PVA	-	Triton	Amine								
DGS	0.25	HEPES	50	8.0	6.8	1PVA	-	Triton	Aldehyde								
DGS	0.25	HEPES	50	8.0	6.8	1PVA	-	Triton	Epoxy								
DGS	0.25	HEPES	50	8.0	8.0	1PVA	Si-COOH		Amine								
DGS	0.25	HEPES	50	8.0	8.0	1PVA	Si-COOH		Aldehyde							*	
DGS	0.25	HEPES	50	8.0	8.0	1PVA	Si-COOH		Epoxy				*			*	
DGS	0.25	HEPES	50	8.0	6.8	1PVA	GLS		Amine								
DGS	0.25	HEPES	50	8.0	6.8	1PVA	GLS		Aldehyde								
DGS	0.25	HEPES	50	8.0	6.8	1PVA	GLS		Epoxy						*		
DGS	0.25	HEPES	50	8.0	6.8	1PVA	GLS	Sorb	Amine						*		
DGS	0.25	HEPES	50	8.0	6.8	1PVA	GLS	Sorb	Aldehyde								
DGS	0.25	HEPES	50	8.0	6.8	1PVA	GLS	Sorb	Epoxy								
DGS	0.25	HEPES	50	8.0	6.8	1PVA	GLS	Trehalose	Amine						*		
DGS	0.25	HEPES	50	8.0	6.8	1PVA	GLS	Trehalose	Aldehyde								
DGS	0.25	HEPES	50	8.0	6.8	1PVA	GLS	Trehalose	Epoxy								
DGS	0.25	HEPES	50	8.0	6.8	1PVA	GLS	Ac-Lysine	Amine						*		
DGS	0.25	HEPES	50	8.0	6.8	1PVA	GLS	Ac-Lysine	Aldehyde							*	
DGS	0.25	HEPES	50	8.0	6.8	1PVA	GLS	Ac-Lysine	Epoxy						*		
DGS	0.25	HEPES	50	8.0	6.8	1PVA	GLS	Glycerol	Amine						*		
DGS	0.25	HEPES	50	8.0	6.8	1PVA	GLS	Glycerol	Aldehyde								
DGS	0.25	HEPES	50	8.0	6.8	1PVA	GLS	Glycerol	Epoxy								
DGS	0.25	HEPES	50	8.0	6.8	1PVA	GLS	Triton	Amine								
DGS	0.25	HEPES	50	8.0	6.8	1PVA	GLS	Triton	Aldehyde								
DGS	0.25	HEPES	50	8.0	6.8	1PVA	GLS	Triton	Epoxy						*		
SS	1.5	HEPES	50	8.0	6.8	1PVA	Bis-TEOS										*
SS	1.5	HEPES	50	8.0	>8	1PVA	APTES			*							

continued . . .

Table 3.2 continued

Silica Precursor	[Silica]	Buffer	[Buffer]	pH of Buffer	Final pH	Polymer	Silanes	Small Molecule	Surface	Gel Time	# of Spot	Uniformity	Adhesion	Cracking (Pre)	Cracking (Post)	S/N Ratio	Other
SS	1.5	HEPES	50	8.0	6.8	1PVA	PhDMS										*
DGS	0.25	HEPES	50	8.0	7	3.75PEG	-	-	Amine						*	*	
DGS	0.25	HEPES	50	8.0	7	3.75PEG	-	-	Aldehyde						*		
DGS	0.25	HEPES	50	8.0	7	3.75PEG	-	-	Epoxy						*		
DGS	0.25	HEPES	50	8.0	7	3.75PEG	-	-	PMMA		*					*	
DGS	0.25	HEPES	50	8.0	7	7.5PEG	-	-	Amine						*	*	
DGS	0.25	HEPES	50	8.0	7	7.5PEG	-	-	Aldehyde						*	*	
DGS	0.25	HEPES	50	8.0	7	7.5PEG	-	-	Epoxy						*		
DGS	0.25	HEPES	50	8.0	7	7.5PEG	-	-	PMMA		*					*	
DGS	0.25	HEPES	50	8.0	7.6	0.5PEI	-	-			*						
DGS	0.25	HEPES	50	8.0	8	1PEI	-	-			*						

Silane bis(3-methylidimethoxysilyl)-propyl polypropylene oxide did not dissolve in water to create the stock solution.

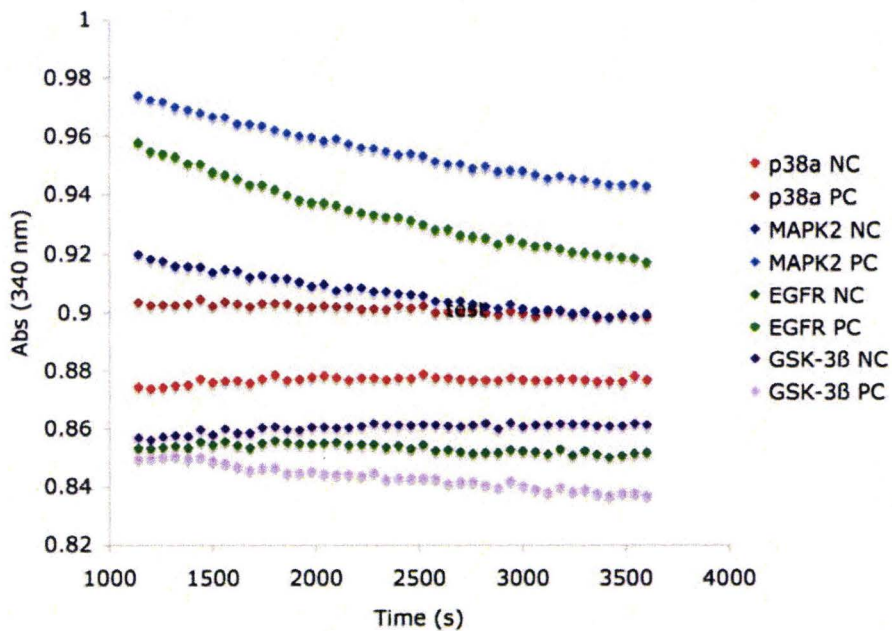


Figure 3.9 Kinase activity in 1.5SS/1PVA/Glycerol monoliths. A coupled NADH assay was used to detect kinase activity by monitoring signal decrease at 340 nm.

## **Chapter 4**

# **Acetylcholinesterase Assay Using a Fluorogenic Thiol-Reactive Dye Compatible with Standard Microarray Scanner Technology**

I was responsible for the experiment design, analysis and interpretation presented in this Chapter 4. Jessamyn Little was a summer student under my direct supervision and assisted me in experimental execution and data collection for Figures 4.3 – 4.5. Dr. Brennan provided editorial input to generate the final draft of this chapter.

## **Chapter 4: Acetylcholinesterase Assay Using a Fluorogenic Thiol-Reactive Dye Compatible with Standard Microarray Scanner Technology**

### **Abstract**

A fluorogenic acetylcholinesterase (AChE) assay that is compatible with standard DNA microarray scanners (543nm/554nm) was developed and characterized in solution and for AChE entrapped in sol-gel-derived silica. A thiol-reactive fluorogenic dye was used to monitor thiocholine generation by AChE catalyzed hydrolysis of acetylthiocholine (ATCh) in both kinetic and end point assays. Using this fluorogenic assay,  $K_M$  values for acetylthiocholine were determined both in solution and in silica and were found to be comparable to literature. Functional AChE microarrays were fabricated using silica sol-gel immobilization and contact pin-printing. By overprinting nanolitre volumes of ATCh solutions with and without inhibitor, the retention of AChE activity on array was demonstrated and inhibition of the enzyme could be detected.

### **4.1 Introduction**

Acetylcholinesterase (AChE) plays an important role in acetylcholine (ACh) mediated neurotransmission, catalyzing the hydrolysis of the neurotransmitter acetylcholine to inactive choline thereby releasing acetate.<sup>1</sup> Functioning in the synaptic cleft, AChE is one of the fastest known enzymes with rates approaching diffusion limited turnover.<sup>2</sup> While the role of AChE in neurotransmission was discovered almost a century

ago,<sup>3</sup> it has recently regained attention due to its association with Alzheimer's disease (AD)<sup>4</sup> as well as other neurological diseases.<sup>5</sup> Several drugs are now available on the market to treat AD via inhibition of AChE, including galantamine,<sup>6</sup> donepezil,<sup>7</sup> and rivastigmine.<sup>8</sup> Additionally, various toxins in the environment that inhibit AChE have also been of concern over the past decade. Examples of such toxins include organophosphate esters (OPs),<sup>9, 10</sup> aflatoxin B<sub>1</sub><sup>11</sup> and certain metal ions.<sup>12</sup> This makes AChE a particularly interesting target for high throughput screening to discover novel drug leads as well as for biosensing applications. Of particular interest is adapting AChE assay technology to a miniaturized microarray format, which allows for nanovolume assays<sup>13</sup> and highly parallel screening.<sup>14</sup>

Acetylcholinesterase is typically assayed using the well-known colorimetric Ellman assay.<sup>15</sup> The Ellman assay monitors the hydrolysis of acetylthiocholine (ATCh) via the reaction of ATCh with 5,5'-dithiobis(2-nitrobenzoic acid) (DTNB), generating 5-thio-2-nitrobenzoic acid (TNB), which absorbs highly at 412 nm. While the Ellman assay is time-tested and robust, solution-based assays are limited in the degree of miniaturization due to path length issues and thus are not easily adapted to the microarray format. By employing fluorescence as a detection mode, assays become compatible with microarray scanner instruments and thus can be run on the nanovolume scale.

There are a number of fluorogenic AChE assays available, which rely on either direct monitoring of AChE activity using a fluorogenic substrate or indirect monitoring using coupled assay or pH-sensitive dyes. Examples of fluorogenic substrates for AChE include 1-naphthylacetate<sup>16</sup> and 1-methyl-7-acetoxy-quinolinium iodide.<sup>17</sup> These assays,

however, the fluorescence product requires excitation in the near UV range or blue-violet visible region. Excitation in this wavelength region can result in higher levels of interferences due to compound absorbance or fluorescence.<sup>18</sup> Additionally, in order to adapt these fluorogenic AChE assays to a microarray format, it is desirable to have the wavelength compatible with typical DNA microarray scanners using 532 nm laser excitation.

A coupled AChE assay compatible with microarray scanners is the Amplex<sup>®</sup> Red Acetylcholine/Acetylcholinesterase Assay from Invitrogen<sup>19</sup>. The Amplex<sup>®</sup> Red assay relies on the coupling of choline generation to H<sub>2</sub>O<sub>2</sub> production using choline oxidase. In turn, H<sub>2</sub>O<sub>2</sub> with horseradish peroxidase reacts with the Amplex Red reagent to generate a fluorescent signal (570/585 ex/em maxima). Difficulties arise when using coupled assays for screening, however, as secondary screens are required to eliminate off-target hits.<sup>20</sup>

In 2005, Tsai and Doong reported on the fabrication of functional AChE microarrays using sol-gel immobilization and a pH sensitive dye.<sup>21</sup> Utilizing the pH shift due to acetate generation from the hydrolysis reaction, they were able to monitor AChE activity on array. While this method provides a novel miniaturized method for screening AChE activity, inhibitor screening using pH as a readout is not ideal because such assays are sensitive to environmental changes and require careful control of initial pH and buffer capacity. By using a non-pH sensitive fluorogenic dye to develop functional sol-gel-derived AChE microarrays, these obstacles can be overcome. For this purpose, the thiol-reactive BODIPY<sup>®</sup> FL L-Cystine dye was explored.<sup>22</sup> In a similar manner to the Ellman assay, the AChE-catalyzed generation of thiocholine from acetylthiocholine can be

monitored by the thiol-reactive reagent, fluorogenic BODIPY® FL L-cystine. A sulphur exchange reaction can occur between TCh and this dimeric dye to relieve the fluorescent quenching between the two BODIPY FL fluorophores and generate two fluorescent products (Figure 4.1). While this dye has been used previously to monitor thioreductase activity;<sup>23</sup> its use with AChE has not been reported. Herein, we report on the adaptation of this reagent for monitoring AChE activity both in solution and in silica and the extension of the assay to a microarray format.

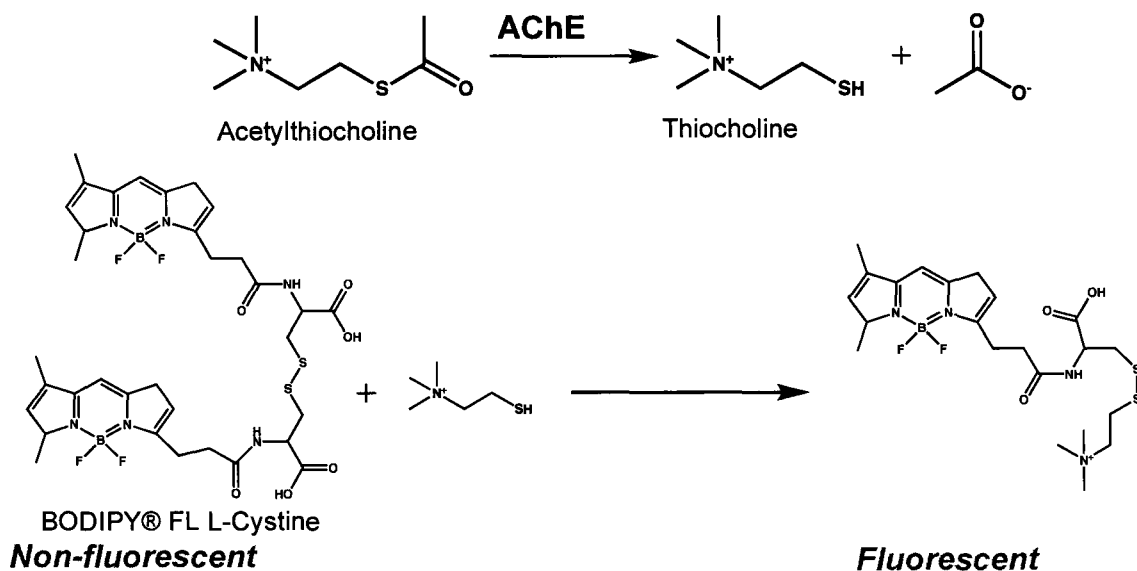


**Figure 4.1** Assay scheme for AChE activity detection using BODIPY® FL L-Cystine.

## 4.2 Experimental

**4.2.1 Materials.** Acetylcholinesterase from *Electrophorus electricus*, HEPES, Tris, Dowex 50X8-100 cation exchange resin, and acetylthiocholine were purchased from Sigma (Oakville, ON). Bodipy® FL L-Cystine was obtained from Invitrogen (Burlington,

ON). Sodium silicate was purchased from Fischer Scientific (Ottawa, ON). SuperAmine and SuperEpoxy derivatized slides were obtained from ArrayIt<sup>®</sup> (Sunnyvale, CA). Galanthamine was a gift from Dr. Jim McNulty. Water was filtered through a Milli-Q Synthesis A10 water purification system (ddH<sub>2</sub>O). All other chemical and solvents were of analytical grade and used without further purification. All reagents were prepared in ddH<sub>2</sub>O unless otherwise specified.

#### **4.2.2 Procedures.**

*Sodium silicate preparation.* Sodium silicate (SS) spotting solution was prepared by stirring 2.59 g of sodium silicate solution with 10 mL ddH<sub>2</sub>O and 5.5 g Dowex 50W80 cation exchange resin for 1 minute. The mixture was filtered with a Buchner funnel and then through a 0.2 µm syringe filter. This solution was used directly or diluted 1:1 with ddH<sub>2</sub>O (1/2SS). The solutions were kept on ice until use.

*Platereader settings.* All experiments were run in black 96-well plates with transparent bottoms, excluding those conducted with microarrays. Microwell plates were analyzed using a Tecan Sapphire with 532 nm excitation and 554 nm emission. The excitation bandwidth was at 2.5 nm and the emission bandwidth was at 12 nm, unless otherwise stated. The instrument gain was set between 140-150 and 10-20 flashes with a 500 µs integration time was used unless otherwise stated. Assays monitored over time were carried out at 25 °C.

*Microarray fabrication, imaging and analysis.* The microarray printing was performed with a Virtek Chipwriter Pro (Virtek Engineering Sciences Inc., Toronto, ON, Canada) robotic contact microarray printer using 10 mm/s printhead speed with a SMP3 stealth

microspotting pin with 250 nL uptake 0.7 nL delivery to produce spots of approximately 100  $\mu\text{m}$  diameter. Humidity of the chamber was  $>80\%$ . The slides were imaged using a ScanArray Express (Perkin Elmer) microarray scanner with the Alexa 532 settings, 70% gain and 90% laser power. The resulting images were analyzed using ArrayPro Analyzer software. Signal values were calculated by subtracting local background from each spot. The signal average of the replicates is reported with error bars representing 1 standard deviation.

*Characterization of thiol-reactive dye.* Emission spectra (excitation 505 nm) of BODIPY<sup>®</sup> FL L-Cystine were obtained for the dimerized and free form. In a 96-well plate, 200  $\mu\text{L}$  of BODIPY<sup>®</sup> FL L-cystine (12.5  $\mu\text{M}$ ) in 50 mM Tris pH 7.0 was examined in the presence and absence of  $\beta$ -mercaptoethanol (1  $\mu\text{L}$ , absolute). Emission spectra were scanned from 510-650 nm (505 nm excitation) using a Tecan Sapphire with 2.5 nm bandwidth, 1 nm steps, 100 gain setting and 500  $\mu\text{s}$  integration time. Background fluorescence from the plate was negligible.

*pH-Dependence of ATCh autohydrolysis.* Initial efforts to study the kinetics of the assay in solution and in silica were hindered by background fluorescence. To study the effect of pH on the background levels, ATCh (18.75 mM) was incubated with BODIPY<sup>®</sup> FL L-cystine (10  $\mu\text{M}$ ) in 50 mM Tris buffer at various pH levels. This study was repeated with 1 mM DTNB in place of BODIPY<sup>®</sup> FL L-cystine with absorbance being monitored at 412 nm to confirm the source of the background fluorescence was due to autohydrolysis of ATCh.

*Assay Proof of concept.* For solution-based assays, AChE (0.25 U/mL) in 25 mM Tris, pH 7.0 (200  $\mu$ L), was incubated with either 1  $\mu$ L DMSO (PC) or 1  $\mu$ L galanthamine (3.484 mM, DMSO) for 30 min. Negative controls with either thermally denatured AChE or no addition of ATCh were treating in the same way as the positive control (PC). AChE was thermally denatured by heating in a water bath for 30 min at 60 °C. Following incubation of AChE with the galanthamine, BODIPY<sup>®</sup> FL L-cystine and ATCh were added to final concentrations of 12.5  $\mu$ M and 250  $\mu$ M, respectively, immediately before acquiring data. The final assay volume was 200  $\mu$ L. For the 'in silica' assays, a 50  $\mu$ L solution containing 0.5 U/mL AChE (or denatured AChE), 25  $\mu$ M BODIPY<sup>®</sup> FL L-Cystine, and 25 mM Tris Buffer pH 8.0 was mixed 1:1 (v:v) with SS. Following gelation, the resulting hydrogel (100  $\mu$ L) was aged for 3 hours at 4 °C. Similar to the solution assays, the various controls were incubated with either 1  $\mu$ L DMSO (PC, NC – AChE, NC – No ATCh) or 1  $\mu$ L galanthamine (3.484 mM, DMSO) (NC – Galanthamine) in 94  $\mu$ L of buffer (50 mM Tris, pH 7.0) for 30 min prior to the addition ATCh to a final concentration of 250  $\mu$ M immediately before analysis. Negative controls were performed with thermally denatured AChE in place of active AChE and with no substrate added. Using the Tecan platereader, the reactions were monitored for ~1 hour with shaking between each read. This set of experiments was repeated under identical conditions with the Ellman assay, where 1 mM DTNB was used in place of the BODIPY<sup>®</sup> FL L-cystine and absorbance at 412 nm was monitored.

*K<sub>M</sub> Determination in solution and in silica.* The Michaelis-Menten constant, K<sub>M</sub>, of ATCh was determined both in solution and in silica. In solution, the following conditions

were used to generation the Michaelis-Menten curve: 0.25 U/mL AChE, 25 mM Tris, pH 7.0, 12.5  $\mu\text{M}$  BODIPY<sup>®</sup> FL L-cystine, and ATCh (0 - 937.5  $\mu\text{M}$ ). Both the dye and the substrate were added immediately prior to analysis. For the 'in silica'  $K_M$  determination, AChE was first entrapped in sodium silicate (SS) using the sol-gel process described above; the sample solution containing 0.5 U/mL AChE, 25 mM Tris, pH 8.0, 25  $\mu\text{M}$  BODIPY<sup>®</sup> FL L-cystine was mixed 1:1 with SS to produce a 100  $\mu\text{L}$  hydrogel. Note that Tris buffer at pH 8.0 was used for the entrapment step in order to achieve neutral pH in the final hydrogel. After gelation and aging at 4 °C for 2-3 hours, the monoliths were incubated with 100  $\mu\text{L}$  of various concentrations of ATCh (0 - 937.5  $\mu\text{M}$ ) in 25 mM Tris, pH 7.0. Both in solution and in silica assays used shaking between each measurements and were monitored for ~1 hour. Using the linear slope ( $\Delta\text{RFU}/\text{min}$ ) for each concentration of ATCh, Lineweaver-Burke plots were generated to determine  $K_M$  and  $V_{\text{max}}$  values using the following equation [1]:

$$\frac{1}{V} = \frac{K_M}{V_{\text{max}}} \frac{1}{[S]} + \frac{1}{V_{\text{max}}} \quad [1]$$

This experiment was repeated with the Ellman assay using 1mM DTNB in place o BODIPY<sup>®</sup> FL L-cystine and monitoring of absorbance at 412 nm.

*AChE activity on array.* Spotting samples (100  $\mu\text{L}$ ) contained 1.25 U/mL AChE, 25  $\mu\text{M}$  BODIPY<sup>®</sup> FL L-cystine in 25 mM Tris, pH 8.0. Samples were mixed with 100  $\mu\text{L}$  1/2SS then immediately pin-printed onto an epoxy-derivatized slide. The microarray was aged for 1 hour in the microarrayer humidity chamber (>80% humidity) at room temperature. Samples were then over-printed with nanoliter volumes of solutions containing 20% (v/v)

glycerol in 25 mM Tris buffer, pH 7.0 with 1% (v/v) DMSO or 34.8  $\mu\text{M}$  galanthamine in DMSO. Arrays were incubated with the DMSO or inhibitor solution for 30 min, after which they were over-printed again with identical solutions except containing 250  $\mu\text{M}$  ATCh. For the negative control where no ATCh was added, ddH<sub>2</sub>O was substituted in the spotting solutions.

### 4.3 Results and Discussion

*Characterization of Fluorogenic Dye.* The fluorogenic properties of BODIPY<sup>®</sup> FL L-Cystine were examined using  $\beta$ -mercaptoethanol to reduce the disulfide bond. The emission properties of the dimerized and free forms of the dye with excitation at 505 nm (absorbance  $\lambda_{\text{max}}$ ) are shown in Figure 4.2. At the emission  $\lambda_{\text{max}}$  (514 nm) a 32-fold increase in fluorescence intensity was observed between the disulphide coupled dye and its free form. The initial rate of reaction between thiocholine and the dye was also examined to demonstrate that in this coupled assay, the reaction of thiocholine with the dye is not the rate-limiting step. It was found to be approximately 1700  $\Delta\text{RFU}/\text{min}$ , which is 5-times greater than the rate observed for the AChE-catalyzed reaction in solution (see Table 4.1) suggesting that this dye reacts sufficiently rapidly to be used as a reporter for the AChE assay.

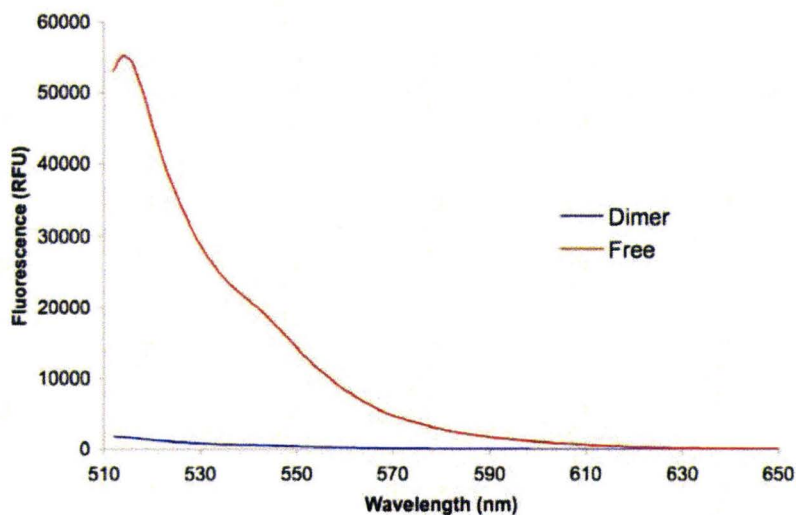


**Figure 4.2** Fluorescence spectra (excitation 505 nm) of BODIPY<sup>®</sup> FL L-Cystine in dimer and free forms.

*pH-Dependence of Autohydrolysis.* While phosphate buffer is most frequently used in AChE assays, Tris buffer was used to allow the assay conditions to be compatible with microarray fabrication using sol-gel materials. HEPES buffer was also considered for the assay, however higher fluorescence levels for the negative controls were observed for this buffer. In order to determine the optimal pH for this experiment, the substrate, ATCh, and the dye were mixed at seven pH levels (pH 7.0-8.2) and assessed for background fluorescence over time (Figure 4.3). The background fluorescence over time increased with increasing pH, with little background fluorescence observed for neutral pH (7.0). While the optimum pH is 7.6 for this enzyme,<sup>24</sup> the subsequent experiments were run at pH 7.0 to minimize background levels. To determine if the background fluorescence was due to autohydrolysis of ATCh or pH-sensitivity of the dye, this series of

experiments was repeated with DTNB (Ellman reagent) and a similar trend was observed (Figure 4.3 panel), suggesting that the background source is autohydrolysis of ATCh.

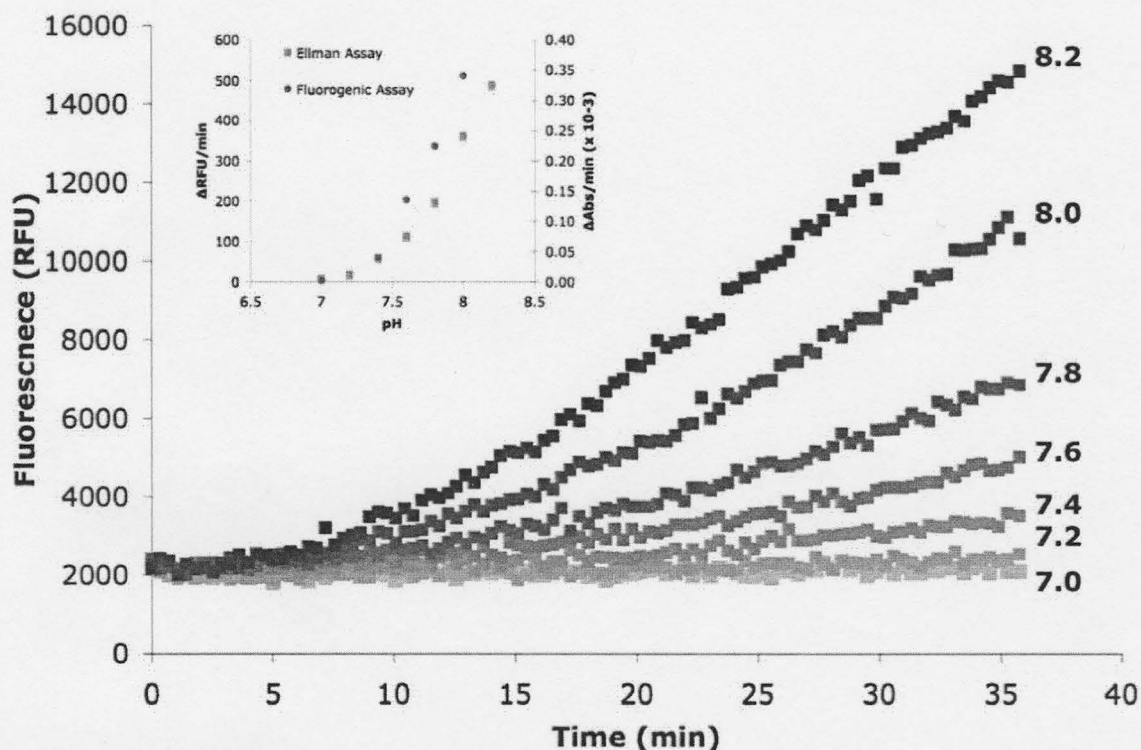


**Figure 4.3** pH-dependence of background fluorescence. Background fluorescence monitored over for ATCh and BODIPY<sup>®</sup> FL L-cystine incubated at various pH levels (indicated on graph). Panel shows the rate of fluorescence and absorbance increase over time from incubating ATCh with the Ellman or fluorogenic reagent at various pH levels.

*Assay Proof of Concept.* BODIPY<sup>®</sup> FL L-cystine reacts in a similar manner to DNTB, whereby it can undergo a thiol exchange reaction with thiocholine produced from the AChE-catalyzed hydrolysis of ATCh. The amenability of this dye to monitor AChE activity was determined by measuring the fluorescence signal increase of the positive control assay, along with negative control assays containing denatured AChE or no ATCh or AChE inhibitor galanthamine. Studies were conducted both in solution and in

silica to establish the compatibility of this dye with silica sol-gel-derived microarrays silica-based assays and the results were compared with identical assays run using the Ellman assay (Figure 4.4, Tables 4.1 and 4.2).

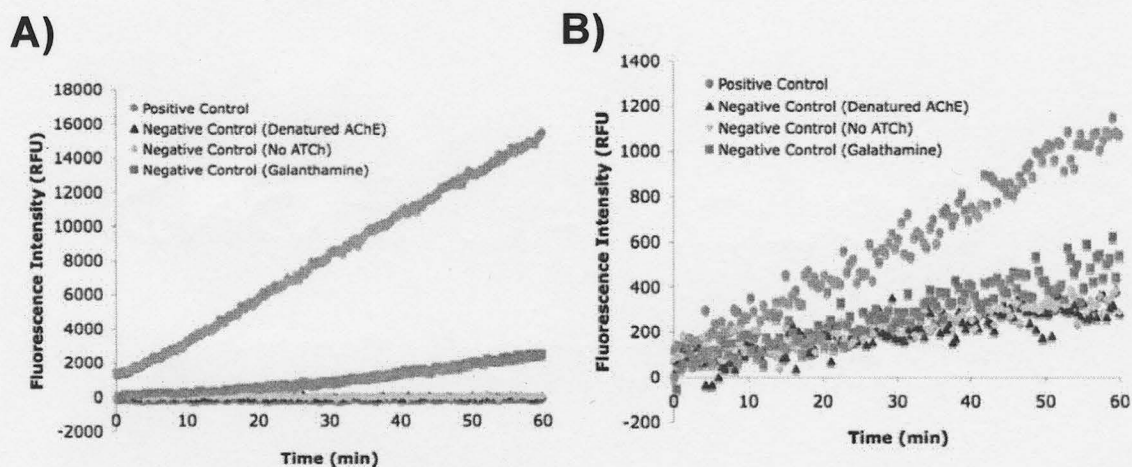


**Figure 4.4** Activity of AChE A) in solution and B) entrapped in silica monitored using BODIPY<sup>®</sup> FL L-Cystine. Negative controls were run under the condition indicated in brackets. A galanthamine concentration of 17.5  $\mu\text{M}$  was used for the negative control assay run in the presence of inhibitor. Fluorescence intensities shown are after background subtraction of initial fluorescence from the negative control (No ATCh).

**Table 4.1** Activity of AChE in solution and entrapped in silica using thiol-reactive fluorogenic dye. PC = positive control, NC - dAChE = negative control assay run with denatured AChE, NC - ATCh = negative control assay run without ATCh, NC - galanthamine = assay run in presence of inhibitor galanthamine (17.5  $\mu\text{M}$ ).

	<i>In Solution</i>		<i>In Silica</i>	
	Slope ( $\Delta\text{RFU}/\text{min}$ )	Standard Error	Slope ( $\Delta\text{RFU}/\text{min}$ )	Standard Error
PC	241.7	0.7	16.9	0.2
NC - dAChE	0.5	0.3	4.5	0.2
NC - No ATCh	0.3	0.3	4.3	0.2
NC - galanthamine	42.5	0.7	7.7	0.3

**Table 4.2** Activity of AChE in solution and entrapped in silica using the Ellman assay. PC = positive control, NC = negative control, dAChE = denatured AChE, PC+IN = assay inhibited by galanthamine (35  $\mu$ M).

	<i>In Solution</i>		<i>In Silica</i>	
	Slope ( $\Delta$ Abs/min)	Standard Error	Slope ( $\Delta$ Abs/min)	Standard Error
PC	0.1215	0.0016	0.01777	0.00009
NC - dAChE	-0.0008	0.0002	0.00144	0.00003
NC - No ATCh	-0.0006	0.0001	0.00014	0.00001
NC - galanthamine	0.0120	0.0004	0.00255	0.00006

In solution studies with the fluorogenic dye, it was found that the fluorescence response was linear over time and negative controls resulted in little autohydrolysis (<1% of the positive control) (Figure 4.4A, Table 4.1). Additionally, the inhibited reaction showed a ~6-fold decrease in activity over the positive control. Similar observations were made for the Ellman assay under identical conditions (Table 4.2). While the 'in silica' Ellman and fluorogenic assays followed similar trends to the solution-based assays, the rate of reaction for the positive controls were both roughly 10-fold lower compared to the respective solution-based assays (Figure 4.4B, Tables 4.1 and 4.2). This is most likely due to mass transfer issues; however for the fluorogenic assay, the slow formation of non-emissive BODIPY dimers in silica has previously been reported and could also be a source of the lower signal intensities.<sup>25</sup>

The background fluorescence increased over time for both the solution and silica-based fluorogenic assays, although the rate was found to be much higher for the silica-based assay, especially for the fluorogenic assay. When compared to the results from the Ellman assay in silica, the background from the negative controls for the fluorogenic assay are more significant. The background from the negative controls (denatured AChE and no ATCI controls) for the Ellman assay was less than 10% of the positive control.

However, for the fluorogenic assay in silica, the background from the negative control with denatured AChE was ~25% of the positive control signal. This suggests that the fluorogenic dye may be interacting with the silica to cause higher background levels.

*Measurement of  $K_M$  in solution and in silica.* To validate the assay both in solution and in silica, the  $K_M$  of AChE/ATCh was determined for each (Figure 4.5). Lineweaver-Burke plots were used to determine the  $K_M$  and  $V_{max}$  values for both the solution and in silica assays. The calculated solution  $K_M$  value of  $78 \pm 9 \mu\text{M}$  compared well with the literature value of  $140 \mu\text{M}$ .<sup>15</sup> The  $V_{max}$  for this assay was determined to be  $1300 \pm 100 \Delta\text{RFU}/\text{min}$ . The apparent  $K_M^{\text{app}}$  found for AChE in silica,  $250 \pm 30 \mu\text{M}$ , was higher than that for the solution assay. This increase in  $K_M^{\text{app}}$  has been observed for a number of assay systems,<sup>26</sup> and was also observed when this experiment was performed in silica with the Ellman assay ( $K_M \sim 300 \mu\text{M}$ , data not shown). The  $V_{max}^{\text{app}}$  was 5-fold lower for the silica-based assay at  $50 \pm 9 \Delta\text{RFU}/\text{min}$ . Similarly with the Ellman assay, a 8-fold decrease in  $V_{max}$  was observed between the solution and silica-based assays.

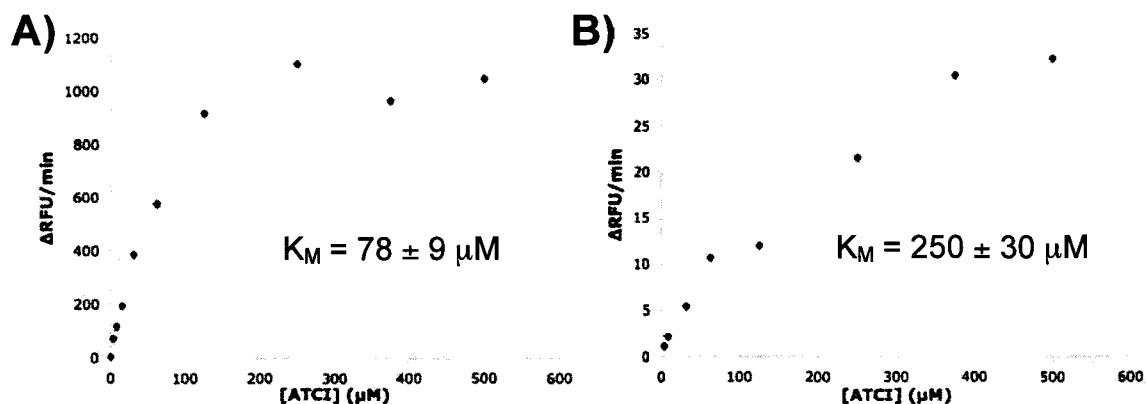


**Figure 4.5** Michaelis-Menten curves for AChE in A) solution and B) silica.  $K_M^{\text{app}}$  values were determined using Lineweaver-Burke plots with the standard error calculated from linear regression analysis.

*AChE Activity on Array.* Functional sol-gel-derived AChE microarrays were prepared by entrapping AChE and BODIPY<sup>®</sup> FL L-Cystine in SS in array format. By depositing microspots of reagents directly over the AChE-containing array elements, assays could be run in nanovolume scale. The results show that AChE activity is retained on array and inhibition of the reaction can be detected with a ~2-fold reduction in signal compared to the positive control (Figure 4.6). In order to obtain a larger signal differences between the positive and inhibited controls and thus obtain a  $z'$  value  $>0.5$ , which is needed for adaptation of this assay to small molecule screening, it will be necessary to further optimize the assay. The AChE concentration within the elements will be increased to improved signals as previous work by our group suggests higher concentrations of AChE in silica are optimal.<sup>27</sup> Additionally, the robustness of the microarray assay and long-term stability of the fabricated microarrays still require optimization and assessment.

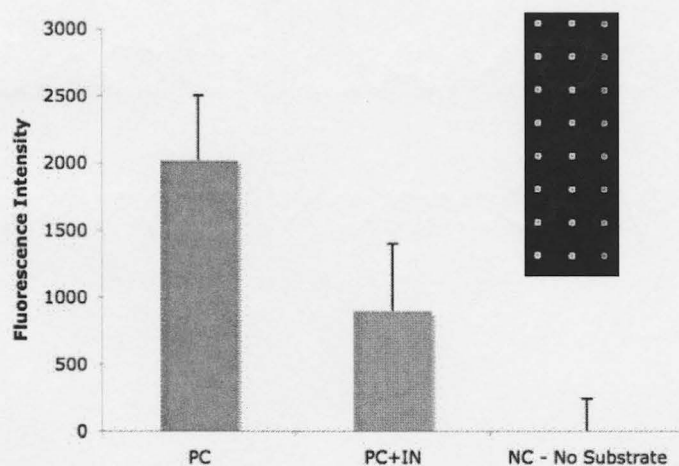


**Figure 4.6** Fabrication of sol-gel-derived AChE microarray with retention of AChE activity on array. PC = positive control, PC+IN = assay run in presence of inhibitor galanthamine (35  $\mu$ M), NC – No substrate = negative control assay run without ATCh. Fluorescence intensity values shown are after background subtraction of fluorescence intensity from the negative control (NC – No Substrate). Microarray image columns correspond to PC, PC+IN and NC- No Substrate, from left to right.

## 4.4 Conclusion

AChE is an interesting target for high throughput screening due to its involvement in various neurological diseases. Current assay methods are not easily amenable to the microarray format using standard microarray scanning technology. We have reported on the development of a novel AChE assay utilizing a thiol-reactive fluorogenic dye that is compatible with standard DNA microarray scanners and with sol-gel-based bio-immobilization for microarray fabrication.  $K_M$  values were determined both in solution and in silica and found to be comparable with the values determined using the Ellman assay. By entrapping AChE in sol-gel-derived silica in microarray format and overprinting substrate and inhibitor solutions, both activity and inhibition could be detected on array.

## 4.5 References

1. Quinn, D.W. Acetylcholinesterase: enzyme structure, reaction dynamics, and virtual transition states. *Chemical Reviews*. **1987**, *87*, 955-979.
2. Bazelyansky, M.; Robey, E.; Kirsch, J.F. Fractional diffusion-limited component of reactions catalyzed by acetylcholinesterase. *Biochemistry*. **1986**, *25*, 125-130.
3. Augustinsson, K-B.; Nachmansohn, D. Distinction between acetylcholine-esterase and other choline ester-splitting enzymes. *Science*. **1949**, *110*, 98-99.
4. Talesa, V.N. Acetylcholinesterase in Alzheimer's disease. *Mechanisms of Ageing and Development*. **2001**, *112*, 1961-1969.
5. Soreq, H.; Seidman, S. Acetylcholinesterase – new roles for an old actor. *Nature Reviews Neuroscience*. **2001**, *2*, 294-302.
6. Scott, L.J.; Goa, K.L. Galantamine: A review of its use in Alzheimer's disease. *Drugs*. **2000**, *60*, 1095-1122.
7. Rogers, S.L.; Farlow, M.R.; Doody, R.S.; Moh, R.; Friedhoff, L.T. A 24-week, double-blind, placebo-controlled trial of donepezil in patients with Alzheimer's disease. *Neurology*. **1998**, *50*, 136-145.
8. Rosler, M.; Anand, R.; Cicin-Sain, A.; et al. Efficacy and safety of revistigmine in patients with Alzheimer's disease: international randomized controlled trial. *BMJ*. **1999**, *318*, 633-639.
9. Marrs, T.C. Organophosphate poisoning. *Pharmacology & Therapeutics*. **1993**, *58*, 51-66.
10. Hsieh, B.H.; Deng, J.F.; Tsai, W.J. Acetylcholinesterase inhibition and the extrapyramidal syndrome: a review of the neurotoxicity of organophosphate. *NeuroToxicology*. **2001**, *22*, 423-427.
11. Cometa, M.F.; Lorenzini, P.; Fortuna, S.; Volpe, M.T.; Menegruz, A.; Palmery, M. In vitro inhibitory effect of aflatoxin B<sub>1</sub> on acetylcholinesterase activity in mouse brain. *Toxicology*. **2005**, *206*, 125-135.
12. Stoytcheva, M.; Sharkova, V.; Panayotova, M. Electrochemical approach in studying the inhibition of acetylcholinesterase by arsenate(III): analytical characterization and application for arsenic determination. *Analytica Chimica Acta*. **1998**, *364*, 195-201.

13. Rupcich, N.; Green, J.R.A.; Brennan, J.D. Nanovolume kinase inhibition assay using a sol-gel-derived multicomponent microarray. *Analytical Chemistry*. **2005**, *77*, 8013-8019.
14. MacBeath, G.; Schreiber, S.L. Printing proteins as microarrays for high-throughput function determination. *Science*. **2000**, *289*, 1760-1763.
15. Ellman, G.L.; Courtney, K.D.; Andres, V.; Featherstone, R.M. A new and rapid colorimetric determination of acetylcholinesterase activity. *Biochemical Pharmacology*. **1961**, *7*, 88-95.
16. Siegel, G.J.; Lehrer, G.M.; Silides, D. The kinetics of cholinesterases measured fluorometrically. *The Journal of Histochemistry and Cytochemistry*. **1966**, *14*(6), 473-478.
17. Prince, A.K. Spectrophotometric study of the acetylcholinesterase-catalyzed hydrolysis of 1-methyl-acetoxyquinolinium iodides. *Archives of Biochemistry and Biophysics*. **1966**, *113*, 195-204.
18. Comley, J. Assay interference, a limiting factor in HTS? *Drug Discovery World*, **2003**, *4*, 91-98.
19. Amplex® Red Acetylcholine/Acetylcholinesterase Assay Kit (A12217). *Invitrogen*. <<<http://probes.invitrogen.com/media/pis/mp12217.pdf>>>.
20. Kruger, N.J. Errors and artifacts in coupled spectrophotometric assays of enzyme activity. *Phytochemistry*. **1995**, *38*, 1065-1071.
21. Tsai, H-C.; Doong, R-A. Simultaneous determination of pH, urea, acetylcholine and heavy metals using array-based enzymatic optical biosensor. *Biosensors and Bioelectronics*. **2005**, *20*, 1796-1804.
22. BODIPY® FL L-cystine (B20340). *Invitrogen*. <<[www.invitrogen.com](http://www.invitrogen.com)>>.
23. Lackman, R.L.; Jamieson, A.M.; Griffith, J.M.; Geuze, H.; Cresswell, P. Innate immune recognition triggers secretion of lysosomal enzymes by macrophages. *Traffic*. **2007**, *8*, 1179-1189.
24. Acetylcholinesterase from *Electrophorus electricus* (electric eel) (C2888). *Sigma*. <<[www.sigmaaldrich.com](http://www.sigmaaldrich.com)>>.

25. Tleugabulova, D.; Zhang, Z.; Brennan, J.D. Characterization of bodipy dimmers formed in a molecularly confined environment. *Journal of Physical Chemistry B*. **2002**, *106*, 13133-13138.
26. Besanger, T.R.; Chen, Y.; Desisingh, A.K.; Hodgson, R.; Jin, W.; Mayer, S.; Brook, M.W.; Brennan, J.D. Screening of inhibition using enzymes entrapped in sol-gel-derived materials. *Analytical Chemistry*. **2003**, *75*, 2382-2391.
27. Hossain, S.M.Z.; Luckham, R.E.; Smith, A.M.; Lebert, J.M.; Davies, L.M.; Pelton, R.H.; Filipe, C.D.M.; Brennan, J.D. Development of a bioactive paper sensor for detection of neurotoxins using piezoelectric inkjet printing of sol-gel-derived bioinks. *Analytical Chemistry*. **2009**, *81*, 5464-5483.

## Chapter 5: Conclusions and Outlook

Miniaturized assays using functional protein microarrays are an attractive means to increase the throughput and cost effectiveness of small molecule screening efforts. Sol-gel immobilization as an approach to protein microarray fabrication has shown potential to become a leading methodology in this field. While this technology has been applied to sensitive proteins such as kinases<sup>1</sup> and cytochrome p450s<sup>2</sup>, there remain a number of issues when employing this technique. Foremost, there are few reports discussing adaptations of assay systems to this format. Thus in order to demonstrate the utility of such a method, it is necessary to increase the number of assays compatible with the technique. Furthermore, sol-gel compositions have been limited in scope of specific proteins and applications. There has yet to be described an example of a widely applicable material. For instance, we have found that, while functional PKA microarrays can be fabricated using SS, this material is not amenable to all kinases. Additionally, typical sol-gel formulations have gel times <30 minutes, limiting their application to formats such as the pin-printing of high-density microarrays. Given the potential of sol-gel derived microarrays, this thesis focused on evaluating new assay systems amenable to this technology and the development of methods to fabricate high-density sol-gel-derived microarrays.

In Chapter 2, a novel GSK-3 $\beta$  assay was described where sol-gel-derived microarrays were employed as a solid phase platform to assess kinase activity. By conducting assays in solution and subsequently printing the assay solutions as sol-gel

derived microarrays, a fluorescent phosphospecific stain could be used to assess the degree of phosphorylation within each microarray element. The linear response of the dye and quantitative nature of this assay was demonstrated through analysis of a gradient of GSM, a phosphopeptide substrate of GSK-3 $\beta$ , and generation of an IC<sub>50</sub> curve for a known GSK-3 $\beta$  inhibitor. Compatibility of this assay with high throughput screening efforts shows promise ( $Z' = 0.5$ ), however further optimization is required before this method can be implemented in single point screening. This assay format was also successfully used with another GSK-3 $\beta$  substrate, tau protein, indicating applicability to both peptide and protein substrates and the potential to simultaneously assay multiple substrates of GSK-3 $\beta$  to assess substrate-specificity of inhibitors.

In Chapter 3, the results of a materials screen used to identify optimal sol-gel compositions for fabrication of high-density kinase microarrays were presented. Initial investigations revealed that the method previously reported by our group was not amenable to all kinases and, due to short gelation times, was also not applicable for fabrication high-density microarrays. As such, it was necessary to screen a variety of sol-gel compositions to identify optimal materials for maximal retention of kinase activity. Using a directed, criteria-based approach, the following variables were screened in a rapid and cost-effective manner: silica precursor types (2) and concentration (2), polymer additives (3) and concentration (2), silane additives (6), small molecule additives (5) and surface chemistry of slides (4). In total, 69 sol-gel/surface combinations were identified that were amenable to fabrication of high-density microarrays and were compatible with the staining assay. Preliminary studies showed retention of kinase activity on array.

In Chapter 4, we reported on the development of functional sol-gel-derived acetylcholinesterase microarrays using a commercially available fluorogenic thiol-reactive dye. This fluorogenic dye, BODIPY® FL L-Cystine, was able to successfully monitor AChE activity both in solution and in silica using micro-well plate assays. Michaelis-Menton curves were generated in both solution and silica to compare  $K_M$  and  $V_{max}$  values. It was found that the  $K_M$  was greater in silica than in solution, while the  $V_{max}$  observed was lower in silica. This trend has previously been observed with other assay systems.<sup>3</sup> Finally, retention of AChE activity in microarray format was demonstrated using nanovolume assays on array.

Future work will firstly focus on using the presented assay systems to screen small molecule libraries. In each case, a 1000-compound library will be screened against the target in efforts to identify novel inhibitors. Additionally, in the longer term, other assay systems will be explored for use with sol-gel-derived microarrays. In particular, efforts will concentrate on development of G-protein coupled receptor (GPCR) functional microarrays, as they are the most targeted protein family by pharmaceutical companies for drug development.<sup>4</sup>

## 5.1 References

1. Rupcich, N.; Green, J.R.A.; Brennan, J.D. Nanovolume kinase inhibition assay using a sol-gel-derived multicomponent microarray. *Analytical Chemistry*. **2005**, *77*, 8013-8019.
2. Lee, M-Y.; Park, C.B.; dordick, J.S.; Clark, D.S. Metabolizing enzyme toxicology assay chip (MetaChip) for high-throughput microscale toxicity analyses. *Proceedings of the National Academy for Science*. **2005**, *102*, 983-987.
3. Besanger, T.R.; Chen, Y.; Desisingh, A.K.; Hodgson, R.; Jin, W.; Mayer, S.; Brook, M.W.; Brennan, J.D. Screening of inhibition using enzymes entrapped in sol-gel-derived materials. *Analytical Chemistry*. **2003**, *75*, 2382-2391.
4. Hopkins, A.L.; Groom, C.R. The druggable genome. *Nature Reviews Drug Discovery*. **2002**, *1*, 727-730.